# A New Approach to the Study of Middle Cerebral Artery Occlusion in the Rat Using Magnetic Resonance Techniques

*by*

*Asta Håberg*

Thesis submitted in partial fulfillment
of the degree of doctor medicinae

**Department of Clinical Neuroscience**
**Medical Faculty**
**Norwegian University of Science and Technology**
**2001**

dn 1634

ISBN 82-471-5082-4

**Acknowledgment**

The study was supported by the Norwegian Council on Cardiovascular Disease, the Norwegian Research Council, the SINTEF Foundation, Yamanouchi Pharmaceuticals and Inger R. Haldorsen's Grant.

This thesis presents results of experimental work carried out at the MR-center at RiT over three years and three months from January 1995.

I would like to thank Professor Ursula Sonnewald, Professor Olav Haralseth and Professor Geirmund Unsgård for giving me the opportunity to enter the exciting field of cerebral research. The present work would not have been compiled without Professor Ursula Sonnewald introducing me to the world of cerebral metabolism and compartmentation, or without Can. sci. Hong Qu's excellent technical assistance and help. I am also grateful for their continued support and encouragement throughout the years, and for our fruitful discussions. I would like to thank Dr. med. Tomm B. Müller for showing me the MCAO model. Dr. ing. Mari H. Hjellstuen, Dr. ing. Inger Johanne Bakken, Siv. ing. Oddbjørn Sæther are acknowledged for their skills and assistance. I am very grateful to Trond Singstand and David Axelson for their help with the new Biospec. In addition, I appreciated all help and encouragement from my other co-workers at the MR-center.

Finally, I would like to thank my family for their love and support.

**Table of Contents**

**List of Papers**

This thesis is based on the following papers:

I. Håberg A, Qu H, Haraldseth O, Unsgård G, Sonnewald U (1998) In vivo injection of [1-$^{13}$C]glucose and [1,2-$^{13}$C]acetate combined with ex vivo $^{13}$C NMR spectroscopy: A novel approach to the study of MCA occlusion in rat. *J Cereb Blood Flow Metab* 18: 1223-1232

II. Håberg A, Qu H, Bakken IJ, Sande LM, White L, Haraldseth O, Unsgård G, Aasly J, Sonnewald U (1998) In vitro and ex vivo $^{13}$C NMR spectroscopy studies of pyruvate recycling in brain. *Dev Neurosci* 20: 289-398

III. Håberg A, Qu H, Haraldseth O, Unsgård G, Sonnewald U (2000) In vivo effects of adenosine $A_1$ receptor agonist and antagonist on neuronal and astrocytic intermediary metabolism studied with ex vivo $^{13}$C NMR spectroscopy. *J Neurochem* 74: 327-333

IV. Qu H, Håberg A, Haraldseth O, Unsgård G, Sonnewald U (2000) $^{13}$C MR spectroscopy study of lactate as substrate for rat brain. *Dev Neurosci* 22: 429-436

V. Håberg A, Qu H, Sæther O, Haraldseth O, Unsgård G, Sonnewald U (2001) Differences in neurotransmitter synthesis and intermediary metabolism between glutamatergic and GABAergic neurons during 4 hours of MCAO in the rat. The role of astrocytes in neuronal survival. In press *J Cereb Blood Flow Metab*

VI. Håberg A, Takahashi M, Yamaguchi T, Hjelstuen M Haraldseth O (1998) Neuroprotective effect of the novel glutamate AMPA receptor antagonist YM872 assessed with in vivo MR imaging of rat MCA occlusion. *Brain Res* 811: 63-70

The papers are referred to by their roman numeral in the text.

**Abbreviations**

ADC, apparent diffusion coefficient

AMPA, α-amino-3-hydroxy-5-mehtyl-4-isoxazole-propionic acid

ALAT, alanine aminotransferase

ASAT, aspartate aminotransferase

BBB, blood brain barrier

CBF, cerebral blood flow

DWI, diffusion weighted imaging

FID, free induction decay

GABA, γ-aminobutyric acid

GABA-T, GABA aminotransferase

GAD, glutamate decarboxylase

GS, glutamine synthetase

HPLC, high performance liquid chromatography

iv, intravenous

KA, kainate

MCAO, middle cerebral artery occlusion

MR, magnetic resonance

MRI, magnetic resonance imaging

MRS, magnetic resonance spectroscopy

NMDA, N-methyl-D-aspartate

nOe, nuclear Overhauser effects

PAG, phosphate activated glutaminase

PC, pyruvate carboxylase

PDH, pyruvate dehydrogenase

ppm, parts per million

RF, radio frequency

TCA, tricarboxylic acid

# 1. Introduction

## 1.1 *Brain structure and metabolism*

### 1.1.1 The cellular elements in the brain

The brain parenchyma is made up of neurons and glia. The neuron is the critical cellular element in the brain as all neurological processes are dependent on complex cell-cell interactions between single neurons and/or groups of related neurons. The glial cell is the other cell type in the brain and was originally considered to keep neurons in their proper orientation, acting as scaffolding or glue (glia = glue). Glial cells include astrocytes, oligodendrocytes, microglia and ependymal cells. In short oligodendrocytes provide the myelin sheath of the axons, microglia are the resident macrophage of the brain and ependymal cells line the brain ventricles and the spinal cord central canal. The role of the astrocytes remains incompletely understood, but is related to maintenance and support of neuronal physiology. As the name suggests astrocytes are star shaped, process-bearing cells which isolate neurons, ensheathing synapses and dendrites. Usually the membranes of astrocytes and neurons are separated only by narrow extracellular clefts, of the order of 15 nm wide. Astrocytes are connected to each other by gap junctions, forming a syncytium that allows ions, second messenger molecules and metabolites to diffuse across the brain parenchyma (Cornell-Bell et al., 1989; Dermietzel and Spray, 1993; Giaume and McCarthy, 1996). A number of functions necessary for normal brain development and performance has been ascribed to astrocytes. Some examples are induction and maintenance of the blood brain barrier (BBB) (Janzer and Raff, 1987; Raub et al., 1992) and production of a variety of extracellular adhesion molecules, cytokines and growth factors (Liesi and Risteli, 1989; Lin et al., 1993). The extracellular concentrations of $K^+$ and $H^+$ are regulated by astrocytes, and thus neurotransmission can be modified (Verkhratsky and Steinhauser, 2000; Walz, 2000). Furthermore, astrocytes efficiently remove certain neurotransmitters from the synaptic cleft (Tanaka, 2000; Schousboe, 2000) thereby participating in the termination of neurotransmission. Astrocytes also provide precursors for neuronal neurotransmitter synthesis (Hertz, 1979; Hertz et al., 1999), and recent data imply that astrocytes supply energy substrates to neurons during neurotransmission (Pellerin and Magisteretti, 1994; Magisteretti et al., 1999a). The positioning of astrocytes between the

brain capillaries and the neurons is considered to make the astrocytes ideally suited to sense local neuronal activity and couple it with energy metabolism and cerebral blood flow (CBF).

### **1.1.2** Substrates for cerebral metabolism

The adult brain depends almost entirely upon oxidative metabolism of glucose to support its metabolic needs (Lund-Andersen, 1979; Clarke and Sokoloff, 1999). In the brain glucose is as good as completely oxidized to $CO_2$ and water through the sequential processing by glycolysis, the tricarboxylic acid (TCA) cycle and oxidative phosphorylation. Together these processes yield between 31 and 38 mol ATP per mol glucose (Clarke and Sokoloff, 1999; Magistretti, 1999b). Glucose is also used in glycogen synthesis, but this pathway makes up only 2% of the normal glycolytic flux in the brain. Glycogen is mainly localized to astrocytes (Cataldo and Broadwell, 1986). Moreover, glucose is a precursor for neurotransmitters such as glutamate, GABA and acetylcholine, and the important amino acid glutamine. Finally, glucose is a constituent of some macromolecules, i.e. glycolipids and glycoproteins.

In the brain ketone bodies (acetoacetate and D-3-hydroxybutyrate) and free fatty acids (butyrate, proprionate and acetate) can also enter the TCA cycle, but these substrates cannot fully replace glucose in the adult brain, as illustrated by hypoglycemic coma. Neurons predominantly metabolize glucose, but can also use ketone bodies (Künnecke et al., 1993; Clarke and Sokoloff, 1999). The free fatty acids are, however, only utilized by astrocytes (Auestad et al., 1991; Waniewski and Martin, 1998). Plasma lactate has traditionally not been considered an energy substrate for the adult brain, due to poor BBB penetrance (Pardridge, 1983; Clarke and Sokoloff, 1999). Recent data do, however, indicate that during neuronal activation astrocytes metabolize glucose glycolytically to lactate which is released to the extracellular space and taken up by neurons for use mainly as energy substrate (Pellerin and Magistretti, 1994; Magistretti et al., 1999a). Pyruvate recycling is another controversial metabolic pathway in the brain. This pathway involves synthesis of pyruvate from malate and/or oxaloacetate from the TCA cycle, thus making brain cells able to produce pyruvate from amino acids and other metabolic intermediates connected to the TCA cycle. Evidence of pyruvate

recycling has been detected by some groups (Cerdan et al., 1990; Künneck et al., 1993; Hassel and Sonnewald, 1995; Sonnewald et al., 1996a; Bakken et al., 1997), whereas other find no evidence of such activity (Lapidot and Gopher, 1994; Lee et al., 1996).

### **1.1.3** Neurotransmitters

The major route of signal transmission from one neuron to another is chemically mediated transmission achieved by the release of neurotransmitters. The neurotransmitters are divided into classical and non-classical neurotransmitters (see f. ex., Deutch and Roth, 1999; Holz and Fisher, 1999). The classical neurotransmitters include acetylcholine, the catecholamines (dopamine, noreinephrine, epinephrine), serotonine, and the amino acids (glutamate and γ-aminobutyric acid, GABA). These neurotransmitters are synthesized in the synaptic terminal and stored in vesicles there until release which is elicited by depolarization and depends on $Ca^{2+}$. Once released, the classical neurotransmitters are either taken up by specific reuptake mechanisms on neurons and astrocytes, and/or inactivated enzymatically in the synaptic cleft. Non-classical neurotransmitters include peptides (for instance substance P and vasopressin) and unconventional transmitters such as NO, CO and growth factors.

### **1.1.4** Synthesis and breakdown of amino acid neurotransmitters

Glutamate and GABA are respectively the major excitatory and inhibitory neurotransmitters in the brain. Both neurotransmitters are derived from the TCA cycle and thus have a dual role as participant in the intermediary metabolism as well as in cellular communication. The part of glutamate or GABA stored in synaptic vesicles and in rapid exchange with these vesicles is considered to belong to the neurotransmitter pool of glutamate or GABA, whereas the remaining glutamate or GABA is designated the metabolic pool.

*Glutamate synthesis*

In the neuron the carbon backbone of glutamate is synthesized from glucose via the TCA cycle and subsequent transamination of α-ketoglutarate to glutamate by aspartate aminotransferase (ASAT, EC 2.6.1.1) or alanine aminotransferase (ALAT, EC 2.6.1.2). Glutamate *de novo* synthesis in neurons is considered not to take place (Hertz et al.,

1999). Only in astrocytes is glutamate synthesized *de novo*. However, also in astrocytes is transamination of α-ketoglutarate the main metabolic pathway in glutamate formation. α-Ketoglutarate comes from glucose or other acetyl CoA precursors via the TCA cycle, and the amino group required for net glutamate synthesis is obtained from the systemic circulation (Yudkoff et al., 1992; Yudkoff, 1997). In the astrocyte glutamate is converted to glutamine by the action of glutamine synthetase (GS, EC 6.3.1.2), which is found only in astrocytes and oligodendrocytes (Norenberg and Martinez-Hernandez, 1979; Tansey et al., 1991). Glutamine is released from astrocytes and subsequently taken up by high affinity glutamine transporters present on neurons (Varoqui et al., 2000). In the neuron glutamine is converted to glutamate by phosphate activated glutaminase (PAG, EC 3.4.1.2; Hogstad et al., 1988; Kvamme et al., 2000) which is located to the inner mitochondrial membrane. Alanine and α-ketoglutarate released from astrocytes have also been proposed to be a source of neuronal glutamate via transamination by ALAT (Peng et al., 1991; Westergaard et al., 1994 and 1995a). Neurons depend on transfer of metabolites from astrocytes (Hertz, 1979; Yudkoff et al., 1992; Hertz et al., 1999) because of their inability of *de novo* glutamate synthesis and the fact that a substantial amount of the neurotransmitters released is taken up by high affinity uptake carriers on astrocytes. The latter is particularly notable in glutamate neurotransmission (Erecinska, 1987; Tanaki, 2000). Furthermore, the neurons lack an anaplerotic pathway as the brain's principal anaplerotic enzyme pyruvate carboxylase (PC, EC 6.4.1.1, Patel, 1974), is found only in astrocytes (Yu et al., 1983; Shank et al., 1985). Neuronal pyruvate carboxylation via mitochondrial malic enzyme (EC 1.1.1.39) has been demonstrated in mice *in vivo* (Hassel and Bråthe, 2000), but the physiological importance of this reaction is uncertain.

Neurotransmitter glutamate taken up by astrocytes is either converted directly to glutamine by GS or enters the astrocytic TCA cycle via transamination by ASAT or NAD-requiring oxidative deamination by glutamate dehydrogenase (EC 1.4.1.2) (Yudkoff et al., 1986; Farinelli and Nicklas, 1992; Westergaard et al., 1996). The close metabolic co-operation between neurons and astrocytes in synthesis and disposal of glutamate is termed the glutamate-glutamine cycle (Hertz, 1979; Westergaard et al., 1995a; Daikhin and Yudkoff, 2000).

*GABA synthesis*

Glutamate is the immediate precursor for GABA, and is converted to GABA by the cytosolic enzyme glutamate decarboxylase (GAD; EC 4.1.1.15). GAD has been regarded as a marker for GABAergic neurons, but is also been found in a subpopulation of excitatory neurons (Sloviter et al., 1996). GAD exists in two isoforms: $GAD_{65}$ and $GAD_{67}$. $GAD_{65}$ is predominantly localized to nerve terminals, and may be anchored to the GABA neurotransmitter vesicle, whereas $GAD_{67}$ is a cytosolic enzyme distributed throughout the GABAergic cell body (Kaufmann et al., 1991). The regulation of GAD is complex. About 50% of GAD is present as an apoenzyme of which $GAD_{65}$ is the major contributor. The interconversion between apo- and holoenzyme is regulated by ATP and $P_i$ (Martin and Rimvall, 1993; Bao et al., 1995; Hsu et al., 1999).

The relative contribution from astrocytic intermediates to GABA synthesis is controversial. Since GABA is taken up primarily by GABAergic neurons, and only to a lesser extent by astrocytes (Hertz and Schousboe, 1987; Borden, 1996; Schousboe, 2000), it has been proposed that astrocytic glutamine plays a minor role in GABA synthesis (Hertz and Schousboe, 1987; Hertz et al., 1992; Westergaard et al., 1995b). *In vivo* data on glutamine's importance in GABA synthesis have been conflicting (Ward et al., 1983; Paulsen et al, 1988; Cerdan et al., 1990; Hertz et al., 1992; Preece and Cerdan, 1996). The pathway from glutamine to GABA is also a subject of controversy. Some *in vitro* data point to glutamine first entering the TCA cycle in GABAergic neurons before incorporation into GABA (Westergaard et al., 1995b, Waagepetersen et al., 1999a), but *in vivo* experiments have demonstrated significant direct conversion of glutamine to glutamate and subsequently to GABA (Hassel et al., 1995a and 1998; Sonnewald et al., 1996b).

GABA is metabolized by GABA aminotransferase (GABA-T; EC 2.6.1.19) in the so-called GABA-shunt (Balázs et al., 1970) which allows four of the five C-atoms from α-ketoglutarate to re-enter the TCA cycle as succinate. Flux through the GABA-shunt compared to TCA cycle activity has been calculated to be between 1-17% (Balázs et al., 1970; Martin and Rimvall, 1993, Hassel et al., 1998). The GABA-shunt bypasses one substrate-level phosphorylation catalyzed by succinyl-CoA synthetase and is therefore slightly less energy efficient than the TCA cycle. GABA-T activity is predominantly

found in neurons, but is also present in astrocytes, making astrocytes and neurons equally capable of metabolizing GABA (Baxter, 1976).

### **1.1.5** Cellular compartmentation

Compartmentation refers to the presence of more than one pool of a metabolite/compound in the tissue. By definition each compartment of a metabolite/compound has its own metabolic rate which distinguishes it from the same metabolite/compound in another compartment. The differences in metabolism observed between each compartment are founded on the expression of specific enzymes and transporter mechanisms in distinct cellular subtypes. The original observations of metabolic compartments in the brain were made in 1953 and 1957, but these findings were first later explained on the basis of compartmentation (Lajtha et al., 1959; Berl et al., 1961). A large glutamate pool with slow turnover and a small glutamate pool which was precursor for glutamine were demonstrated by this group. The large glutamate pool was considered to represent neuronal metabolism, and the small glutamate pool astrocytic metabolism. This two compartment model is naturally an oversimplification as the neuronal population is heterogeneous, consisting of a variety of cells using different neurotransmitters. Furthermore, glutamatergic and GABAergic neurons exist as both interneurons and projectory neurons, which possibly give rise to differences in metabolic characteristics. In glutamatergic neurons for instance, PAG has been shown to be distributed unevenly (Laake et al., 1999), and in synaptosomes from different neuronal subpopulations heterogeneous metabolic pathways have been described (Gorini et al., 1999). Also metabolic differences between astrocytes from different brain regions have been demonstrated *in vitro* (Schousboe and Divac, 1979; Hassel et al., 1995b). In cell cultures evidence of compartmentation within a relative homogenous cell population has been found, suggesting the existence of intraneuronal and intraastrocytic compartmentation, which is believed to be caused by mitochondrial heterogeneity (Sonnewald et al., 1993a and 1998; McKenna et al., 1996; Waagepetersen, 2000).

### *1.2 The pathophysiology of cerebral ischemia*

The brain depends on continuos supply of glucose and oxygen since neither is stored in appreciable amounts. The glycogen reserve in the brain has been estimated to maintain normal glycolytic flux for about 5 min if glycogen were the sole supply (Clarke and Sokoloff, 1999). There are two manners in which the normal supply of oxygen and glucose to the brain can be interrupted thereby causing immediate loss of brain function. The first is global ischemia which refers to complete loss of CBF, as in cardiac arrest. The second is focal ischemia resulting from thromboembolic occlusion of an intracranial artery. Focal cerebral ischemia together with intracerebral hemorrhage and subarachnoid hemorrhage are classified as stroke. Stroke is a clinically defined syndrome of rapidly developing symptoms or signs of focal loss of cerebral function with no apparent cause other than that of vascular origin, but the loss of function can at times also be global, i.e. coma. The symptoms last for more than 24 hours or lead to death. Stroke is the most common life-threatening neurological disorder and has an adjusted annual incidence rate for first-ever stroke of 2.21 per 1 000 at the age of 15 or older in Norway (Ellekjær et al., 1997). Furthermore, stroke is a major source of disability, dependency and reduced quality of life (Thommessen et al., 1997).

#### **1.2.1** The concept of the ischemic core and penumbra

Occlusion of an intracranial artery by a thrombus or an embolus results in CBF decline which initiats a complex series of events transforming the ischemic tissue into infarction. The ultimate area of infarction depends mainly on the residual CBF, the duration of ischemia and selective neuronal vulnerability. The tissue damage spreads circumferentially from a central ischemic core where CBF is severely impaired and the brain tissue rapidly becomes irreversibly damaged (Symon et al., 1974; Heiss et al., 1994; Touzani et al., 1995). Surrounding and probably also intermixed in this core are zones of less severely reduced CBF. With declining CBF the normal biochemical processes in the cells are affected in a sequential manner (Astrup et al., 1977 and 1981; Mies et al., 1991; Hossmann, 1994). Animal studies have demonstrated that there are two important threshold values for CBF in cerebral ischemia. At CBF values between 5-15 ml/100g/min anoxic depolarization occurs (Branston et al., 1977; Astrup et al., 1977;

Morawetz et al., 1978; Hossmann, 1994). Anoxic depolarization leads to irreversible cell damage due to failure of the $Na^+/K^+$ATPase disrupting the cell membrane potential. Tissue with CBF values in this range has been termed the ischemic core. Surrounding the ischemic core is brain tissue with CBF values between 12-25 ml/100g/min where spontaneous electrical activity is abolished, but ion homeostasis and membrane potentials remain intact. Several studies have shown that this tissue is potentially viable (Astrup et al., 1977; Morawetz et al., 1978; Jones et al., 1981; Ginsberg and Pulsinelli, 1994). In analogy to the partly lighted area surrounding the center of a complete solar eclipse this region has been termed the penumbra (Astrup et al., 1981). Since the electrophysiological definition of penumbra is of little clinical value, various operational definitions have emerged. The penumbra has been defined as the ischemic tissue salvageable by reperfusion (Memezawa et al., 1992a and b), or by pharmacological agents (Siesjö, 1992). Using magnetic resonance imaging (MRI), the penumbra has been described as the area with reduced perfusion but no changes in diffusion characteristics (Warach et al., 1993; Sorensen et al., 1996; Barber et al., 1998). A metabolic penumbra has been described in which increased metabolism and $O_2$ extraction are coupled to decreased CBF (Baron et al., 1989; Heiss et al., 1994), or alternatively as tissue with acidosis, but no ATP depletion (Hossmann, 1994). The presence of central benzodiazepine receptors as a marker of neuronal integrity has also been used to identify the penumbra (Heiss et al., 2000). Independent of the definitions used to conceptualize this region, it is the possibility of reversing the failure in the neuronal activity which is quintessential to the concept of the ischemic penumbra. The potential for recovery of function is determined not only by the level of residual CBF, but also by the duration of the flow disturbance as the CBF thresholds for electrical and membrane failure increase with increasing duration of ischemia (Mies et al., 1991; Kohno et al., 1995; Zhao et al., 1997). In addition, reduced CBF has been demonstrated to initiate detrimental biochemical processes amplifying the harmful CBF reduction and increasing the final infarct volume. Some of the mechanisms identified today as important mediators of ischemic cell death are glutamate excitotoxicity, intracellular $Ca^{2+}$ accumulation, $Zn^{2+}$ neurotoxicity, induction of apoptosis, and generation of oxygen free radicals and NO

(for reviews see, Bredt, 1999; Lee et al., 1999; Meldrum, 2000; Zipfel et al., 2000; Fiskum, 2000; Mattson et al., 2000).

### **1.2.2** Glutamate excitotoxicity

In cerebral ischemia increased extracellular glutamate concentrations leading to excessive stimulation of glutamate receptors are considered a major contributor to neuronal death (Rothman and Olney, 1986; Benveniste et al., 1991; Choi, 1992; Meldrum, 2000). This phenomenon was termed glutamate excitotoxicity by Olney in 1974. When CBF values are reduced to 20-40% of preischemic values, substantial elevation of extracellular glutamate content has been demonstrated using microdialysis in the ischemic core and penumbra (Shimada et al., 1989; Butcher et al., 1990; Takagi et al., 1993; Uchiyama-Tsuyuki et al., 1994). In the ischemic core several mechanisms for glutamate release are probably involved (Wahl et al., 1994). The early component of glutamate release is considered to be of neurotransmitter origin, using ATP at the expense of phosphocreatine whose depletion precedes that of ATP (Drejer et al., 1985; Wahl et al., 1994). However, the majority of glutamate released in this region is considered to belong to the metabolic pool, released by reversal of the glutamate transporter system owing to ATP decline and/or increased extracellular $K^+$ concentrations (Sanchez-Pietro and Gonzalez, 1988; Kauppinen et al., 1988; Szatkowski et al., 1990; Rossi et al., 2000). In the ischemic penumbra glutamate release is considered to be mainly from the neurotransmitter pool (Obrenovitch, 1996; Zhao et al., 1998).

The contribution from astrocytes to glutamate release during ischemia is controversial. Some studies have demonstrated glutamate release from astrocytes under ischemia-like conditions (Kimmelberg et al., 1990; Ogata et al., 1992; Phillis et al., 2000; Dawson et al., 2000), but other data indicate that reversal of astrocytic glutamate uptake contributes minimally (Mitani et al., 1994; Obrenovitch, 1996; Ottersen et al., 1996). There is substantial evidence for continued astrocytic glutamate uptake during ischemia (Aas et al., 1993; Takagi et al., 1993; Swanson, 1992; Torp et al., 1991 and 1993), and inhibition of the glial glutamate transporter GLT-1 results in increased infarct volume and mortality after transient focal ischemia (Rao et al., 2001).

Increased extracellular glutamate concentrations lead to prolonged and excessive stimulation of glutamate receptors. Glutamate activates four major classes of ionophore-linked receptors: N-methyl-D-aspartate (NMDA), α-amino-3-hydroxy-5-mehtyl-4-isoxazole-propionic acid (AMPA), kainate (KA) and quisqualate. The AMPA and KA receptors are often referred totogether as AMPA/KA receptors. The NMDA and AMPA/KA receptors gate ion channels permeable to both $Na^+$ and $K^+$. In addition, all NMDA receptors and a small subset of AMPA/KA receptors gate $Ca^{2+}$ channels (Hume et al., 1991; Wollmuth et al., 1996). Quisqualate receptors have the capacity to activate both ionotropic and metabotropic glutamate receptor subtypes and are thus unique within this group (Hollmann and Heinemann, 1994). Glutamate also activates three classes of metabotropic glutamate receptors. How these are involved in excitotoxic injury is still uncertain, but they appear to modify events in the excitotoxic cascade (Maiese, 1998; Pizzi et al., 1999).

Antagonist studies in cell cultures have suggested that NMDA receptors mediate most of the neuronal death associated with brief (minutes) intense glutamate exposure. AMPA/KA receptor activation induces neuronal death only when persisting for an extended time period (hours), but will then do so even at low agonist concentrations (Choi, 1992 and 1997). Intense and prolonged stimulation of NMDA and AMPA/KA receptors results in massive influx of $Na^+$ and $Ca^{2+}$, which is neurotoxic to the cell. $Na^+$ influx activates voltage gated $Ca^{2+}$ channels, and also leads to cell swelling due to entry of concomitant water. The $Ca^{2+}$ influx results in increased free intracellular $Ca^{2+}$ concentrations which trigger a cascade of unfavorable biochemical processes. The increased free cytosolic $Ca^{2+}$ levels will activate $Ca^{2+}$-dependent proteolytic enzymes such as lipases, proteases and endonucleases, resulting in protein phosporylation. Protein phosphorylation in turn causes sustained changes in the activity of ion channels and receptors, leads to generation of free radicals, enhances proteolysis and microtubular disassembly, interrupts the axoplasmic transport, and alters gene transcription and translation (Siesjö and Bengtson, 1989; Siesjö, 1992; Morley et al., 1994; Abe et al., 1995; Choi, 1995; Zipfel et al., 2000). Furthermore, increased cytosolic $Ca^{2+}$ results in accumulation of large amounts of $Ca^{2+}$ in the mitochondria which precipitates activation of mitochondrial phospolipases, generation of free radicals and

decreased ATP synthesis (Richter et al., 1995; Kristian and Siesjö, 1998; Fiskum, 2000). Finally the mitochondrial membrane potential collapses and the mitochondria depolarize (Kristian and Siesjö, 1998; Nicholls and Budd, 1998). Sustained depolarization will damage the mitochondria irreversibly. It is suggested that the mitochondrion is the sensor that converts the elevation of intracellular $Ca^{2+}$ from a physiological modulator into a trigger for cell death (Kristan and Siesjö, 1998; Nicholls and Budd, 1998).

The significance of NMDA versus AMPA/KA receptor activation to neuronal death *in vivo* is yet undetermined. There are several factors operating in the ischemic brain considered to attenuate NMDA receptor function such as acidosis, extracellular buildup of $Zn^{2+}$, receptor dephosphorylation owing to lowered cellular ATP levels and inhibition by $Ca^{2+}$/calmodulin (Dingledine and McBain, 1999; Lee et al., 1999). In addition, NMDA receptor antagonists have been shown to have adverse psycomimetic effects and possibly to be neurotoxic in clinical studies (Olney, 1994; Lees, 1999; Davis et al., 2000). AMPA/KA receptor antagonists appear not to share these unfavorable properties with the NMDA receptor antagonists (Kapus et al., 2000). Moreover, the importance of AMPA/KA receptor activation may be increased in ischemia as the expression of $Ca^{2+}$ permeable AMPA receptors increases (Pellegrini-Giampietro et al., 1992 and 1997) and receptor function is enhanced by acidosis (McDonald et al., 1998). Thus neuroprotection by AMPA/KA receptor antagonists has gained increasing attention.

The strongest evidence today implicating excitotoxicity with attendant neuronal $Ca^{2+}$ overload in the pathogenesis of ischemic neuronal death is data obtained in cell cultures and animal studies demonstrating decreased neuronal death with the administration of antagonist contracting the action of one or several of these mechanisms (Scatton, 1994; Choi, 1997; Kobayashi and Mori, 1998; Lee et al., 1999). However, all neuroprotective drugs have failed so far in clinical trials (European Ad Hoc Consensus Group, 1998; Davies et al., 2000; DeGraba and Pettigrew, 2000; Horn and Limburg, 2001). Whether this discrepancy is caused by the set up of the clinical trials, or the lack of applicability of results from *in vitro* and animal experiments to human stroke pathology is yet to be discovered.

### **1.2.3** Brain edema

Brain edema is classified as cytotoxic or vasogenic depending upon whether the BBB is intact or not (Klatzo, 1967). The cytotoxic edema is primarily found in gray matter and appears almost instantaneously after onset of ischemia (Matsuoka and Hossmann, 1982a and b). In cytotoxic edema, cell volume is increased owing to uptake of extracellular fluid into the cells while the BBB remains intact. Maintenance of normal cell volume involves the double-Donnan-equilibrium, thus disruption of cell membrane $Na^+$-permeability, leading to $Na^+$ influx exceeding $Na^+$ extrusion will cause cytotoxic edema. All processes that result in a net increase of intracellular $Na^+$ which by osmosis increases cell water, can cause cytotoxic edema. Thus swelling of astrocytes associated with accumulation of glutamate, $H^+$, $K^+$ and $Na^+$ is not necessarily pathological, but a mere compensatory response aimed at restoring cellular and/or extracellular homeostasis (Baethman and Staub, 1997). This is in line with the observation that the flow threshold for development of cytotoxic edema is higher than for anoxic depolarization (Matsuoka and Hossmann, 1982b).

Vasogenic edema is associated with increased vascular permeability resulting from breakdown of the BBB. Increased BBB permeability leads to leakage of protein-rich fluid from plasma into the extracellular space. The ensuing edema is especially prominent in white matter where enlargement of the extracellular space is noted. In focal cerebral ischemia the BBB remains intact the initial 3-6 h after ictus (Olsson et al., 1971; Løberg et al., 1994).

### **1.2.4** Astrocytes in ischemia

The role of astrocytes in ischemia is controversial, as is the susceptibility of astrocytes to ischemia. On one hand, astrocytes are considered to die as a secondary consequence of neuronal death (Lee et al., 1999), and their presence has been regarded as a mere impediment to neuronal regeneration after CNS injury (Aguayo et al., 1981; Reier et al., 1983). On the other hand, astrocytes have been shown to promote neuronal survival after brain damage *in vitro* and *in vivo* through synthesis and release of glial cell-line derived neurotrophic factor (Ridet et al., 1997; Kitagawa et al.,1998; Louw et al., 1998), and mice deficient for glial fibrillary acidic protein (an astrocytic marker) suffer

significantly bigger cortical infarcts after focal cerebral ischemia than do normal mice (Nawashiro et al., 2000).

Since astrocytes are intimately involved in glutamate neurotransmission, astrocytes may also play an important role in glutamate excitotoxicity. Continued astrocytic glutamate uptake is considered to protect neurons during ischemia/excitotoxicity (Rosenberg and Aizenman, 1989; Rosenberg et al., 1991). However, glutamate release from astrocytes is believed to contribute significantly to glutamate excitotoxicity (see section 1.2.3). Furthermore, astrocytic glutamine has been demonstrated to both increase and decrease neuronal survival *in vitro* (Goldberg et al., 1988; Simantov, 1989; Driscoll et al., 1993).

Astrocytes are considered to be more resistant to ischemia than neurons, partly due to the more flexible astrocytic metabolism. Astrocytes can obtain sufficient energy through glycolysis, whereas neurons depend on mitochondrial function and have a high degree of mitochondrial coupling (Almeida and Medina, 1997). However, some *in vitro* data has demonstrated increased sensitivity of astrocytes compared to neurons to hypoxia/ischemia/excitotoxicity (Tholey and Ledig, 1990; Simantov, 1989; Sonnewald et al., 1994a and b). Moreover, certain astrocytic sub-populations have been shown to be more vulnerable to hypoxic-hypoglycemic conditions than other (Zhao and Flavin., 2000).

## 2. Methods

### *2.1 Experimental procedures*

**2.1.1** Middle cerebral artery occlusion (MCAO)

Middle cerebral artery occlusion (MCAO) was induced with the intraluminal filament technique first developed by Koizumi and co-workers in 1986, and later made internationally known by Longa et al. (1989). Since then the model has been modified by various groups (Memezawa et al., 1992a; Müller et al., 1994; Kawamura et al., 1994).

Male Wistar rats (Møllegaard Breeding Center, Copenhagen, Denmark) weighing 320-340 g were fasted over night with free access to water. Anesthesia was introduced in a closed chamber with 3.5% isoflurane in 70/30% $N_2/O_2$. During surgery the animals were placed on a feedback controlled heating blanket connected to a rectal temperature probe,

and the body temperature was maintained at 37°C. Anesthesia was continued with 2% isoflurane in 70/30% $N_2/O_2$ delivered through a close fitting snout mask. Through a mid-line incision in the neck the right common carotid artery was exposed. Aneurysm clips were placed on the common carotid artery and the internal carotid artery. A small incision was made in the proximal part of the external carotid artery through which a nylon filament with a diameter of 0.27 mm and a rounded tip was introduced and secured with a silk suture. The external carotid artery was ligated distally for the incision. The proximal end of the external carotid artery was mobilized, and the aneurysm clips removed from the common and internal carotid arteries. Next the filament was pushed into the internal carotid artery and advanced 19-20 mm, thereby blocking the origin of the middle cerebral artery. In this position the filament was tightly secured with the silk suture. Anesthesia was turned off at time of MCAO. All incisions were sprayed with lidocaine (10 mg/ doses) before closure.

Permanent MCAO induced with the intraluminal filament technique results in infarction of the caudoputamen and the overlaying cortex (Longa et al., 1986; Memezawa et al., 1992a and b; Müller et al.,1995). The most severe reduction in flow is found in the lateral caudoputamen and lower part of the somatosensory area in the frontoparietal cortex. In the upper somatosensory and motor areas of the frontoparietal cortex blood flow is moderately reduced (Müller et al., 1994 and 1995; Belayev et al., 1997). The former region is considered to represent the ischemic core, the latter the penumbra in this MCAO model.

**2.1.2** Experimental procedures using $^{13}C$ labeled compounds in vivo

The $^{13}C$ labeled compounds, [1-$^{13}C$]glucose, [1,2-$^{13}C$]acetate and [U-$^{13}C$]lactate (Cambridge Isotope Laboratories, Woburn, Mass., USA), were given as an intravenous (iv.) bolus injection over two min or administered intraperitoneally or subcutanously. The rats were decapitated into liquid $N_2$ 15 or 30 min after administration of the $^{13}C$ labeled compound had started. Blood was collected from the severed neck vessels, immediately centrifuged, and plasma retained and frozen at -80°C.

The frozen brains were subsequently removed and either the entire cerebrum or selected regions were sampled. In rats subjected to MCAO, a 3 or 5 mm coronal slice extending

caudally from the chiasma opticum was cut from the frozen brains using a brain tissue matrix (RBM-40000, Activational Systems Inc., USA). The lateral caudoputamen and lower parietal cortex, and the upper frontoparietal cortex from both hemispheres were sampled (Fig.1), thus aiming to obtain severely and moderately ischemic tissue. Identical samples were also taken from sham operated rats.

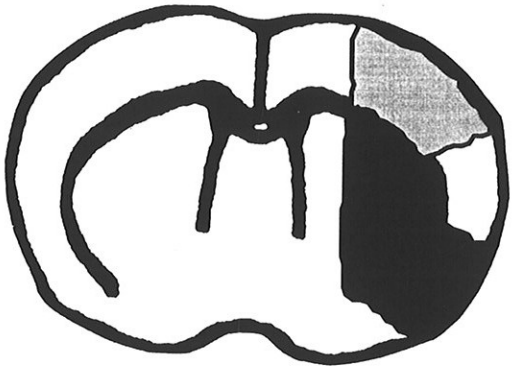

**Fig. 1.** Coronal section of the rat brain

Lateral caudoputamen and lower parietal cortex

Upper frontoparietal cortex

As discussed above, cerebral ischemia is a dynamic process and there is a gradual progression from reversible ischemia towards infarction. The time-frame within which penumbral deterioration occurs is still controversial. In order to avoid misunderstandings anatomical designations are used.

The frozen brain samples were homogenized in 1 ml 70% ethanol (v/v) and centrifuged at 4 000 to 10 000 *g* for 5 to 30 min. To the frozen plasma samples 7% PCA (w/v) was added before centrifugation at 4 000 *g* for 10 min. Supernatants from both brain and plasma samples were retained and neutralized with KOH to pH 6.5-7.5 before lyophilization. The brain and plasma samples were redissolved in 0.5 ml $D_2O$ containing 0.1% dioxane or 0.15% ethyleneglycol as a chemical shift and quantification standard before $^{1}H$ and $^{13}C$ magnetic resonance spectroscopy (MRS). The pH in all samples were adjusted to 6.5- 7.5 before MRS acquired on a Bruker DRX-500 spectrometer (Bruker AG, Fällanden, Switzerland).

### **2.1.3** Magnetic resonance imaging (MRI)

During MRI the rats were placed in a plexiglass cradle heated with circulating fluorocarbons in order to maintain body temperature, which was monitored with a rectal

temperature probe. The rat head was fixed inside a specially designed rat-head coil using a small bar underneath the front teeth. To the rats assigned to recover after MRI, isoflurane anesthesia was delivered through a close fitting snout mask during image acquisition. The rats undergoing MRI directly before termination of the experimental period were intubated and connected to a respirator. Full muscle relaxation was induced with pancuronium bromide (2 mg/kg rat). MRI was performed on a 2.35 T Bruker Biospec (Bruker AG, Fällanden, Switzerland).

**2.1.4** Preparation for histopathological evaluation

The rats were transcardially perfusion fixed with 4% formaldehyde while under continued isoflurane anesthesia and connected to the respirator. The heads were stored in 4% formaldehyde for 24 h before the brains were removed. From each brain eight coronal sections were cut, aiming at representing the middle of each of the eight slices visualized with MRI. The slices were stained with hematoxylin and eosin. Neuronal damage was based on the following morphological characteristics: microvacuolation, shrinkage of the neuropil and the presence of dark and eosinophilic neurons. The infarct area was calculated using a computer-aided image analyzer system (Luzek III, Nireco, Tokyo, Japan).

**2.1.5** High performance liquid chromatography (HPLC)

HPLC was used for quantitative analysis of the amino acids glutamate, glutamine, GABA, aspartate and alanine in the rat brain samples. After $^{13}C$ MRS, 50 µL of the brain extracts were retained, lyophilized, redissolved and diluted (1:1000) in sterile water prior to HPLC analysis using either Merck-Hitachi LaChrom HPLC system (Merck KGaA, Darmstadt, Germany) or Specta Physics P2000 system (Specta System, Freemont, CA, USA), and fluorescence detection (Shimadzu RF 530, Tokyo, Japan) after derivatization with σ-phthaldialdehyde (Sigma Chemical Co., St. Louis, MO, USA). L-amino-butyric acid was used as the internal standard.

## 2.2 Magnetic resonance (MR)

### 2.2.1 General introduction

MRS and MRI are based on the same physiochemical principles which will be described briefly in the following section (for further details see Bachelard and Badar-Goffer, 1993; Bachelard, 1998; Friebolin 1998; Westbrook and Kaut, 1993; Baird and Warach, 1999).

Atoms with uneven mass numbers and/or atomic numbers have nuclear spin. There are several such nuclei, but to date only $^{1}H$, $^{13}C$, $^{31}P$ and to some extent $^{23}Na$ have proven useful in MR research. MRI is restricted to $^{1}H$ owing to the superior sensitivity and high natural abundance (99.98%) of this nucleus, whereas in MRS all of the above nuclei can be observed. The MR signal obtained from the nucleus under investigation depends on the sensitivity of that nucleus, its natural abundance, its chemical environment and the concentration of the specific nuclei in the tissue of interest. The MR active nuclei, $^{1}H$ and $^{13}C$ for example, possess a spin quantum number of $I=1/2$, and can therefore adopt two different orientations relative to an arbitrary axis. The spins are randomly oriented, but when placed along the Z axis in an external magnetic field ($B_0$), the spins will align themselves either with or against the direction of $B_0$. Each orientation is associated with an energy state, and more spins will align themselves with the magnetic field since this is the lower energy state. The energy difference between the two states is: $\Delta E= \gamma h B_0/2\pi$, $\gamma$ is the gyromagnetic ratio. The distribution of the spins between the two energy states can be described by Bolzman statistics: $N_\beta/N_\alpha=e^{-\Delta E/K_B T}$. $N_\beta$ is the number of spins in the higher energy state, $N_\alpha$ is the number of spins in the lower energy state, $K_B$ is the Bolzman's constant and T is the absolute temperature. At normal temperatures the excess in the lower energy level is very small. However, this small difference in populations of precessing nuclei leads to a net magnetization which can be represented as a vector *M* aligned along Z. To detect these spins it is necessary to perturb the system which is at equilibrium. This is done by the application of a second magnetic field ($B_1$) in the form of a radio frequency (RF) pulse. The system will only absorb the energy from the RF pulse if the resonance condition is fulfilled: $\Delta E=h\nu$, which gives: $\nu= \gamma B_0/2\pi$. This frequency is called the Larmor frequency. When a RF pulse at the Larmor frequency is applied at a right angle to $B_0$, via a tuned coil, it has the effect of tilting the

net magnetization $M_z$ towards the $M_{xy}$ plane. It is the duration of the RF pulse which determines how far M will tilt. If the duration is set to tilt M completely to $M_{xy}$, i.e., $M_z$=0, it is referred to as a 90° pulse. When $B_1$ is removed, i.e. RF pulse is off, the spins in $M_{xy}$ return to $M_z$ in a precessing manner at their Larmor frequency. During this process they induce a current in the coil that decays as the equilibrium is reestablished. The current induced in the coil is recorded as the MR signal known as the free induction decay (FID). The FID is usually a superposition of several signals with slightly different precessing frequencies. These different components can be resolved using the mathematical method known as a Fourier transformation, which converts amplitude against time to amplitude against frequency. In MRS the field strength is constant, and it is the amplitude of the frequencies of individual nuclei which is recorded. In MRI the spatial resolution is obtained by a gradient of the applied B over the brain, so that frequencies of the FDIs vary according to the field strength at the position in space throughout the brain.

One cycle of pulsing and data acquisition is called a scan. The signal to noise ratio increases with the square root of the number of scans, and usually averaging is performed from several scans.

### 2.2.2 $^{13}$C MRS

$^{13}$C MRS has been used to study cerebral metabolism *in vivo* and *in vitro* from the middle of the 1980s (Behar et al., 1985; Rothman et al., 1985; Morris et al., 1986). *In vivo* $^{13}$C MRS studies in humans and animals have mainly focused on the pathways of glucose metabolism (Fitzpatrick et al., 1990; Shank et al., 1993; Gruetter et al., 1994 and 1998; Rothman et al., 1999). However, other $^{13}$C labeled compounds have been used in cell cultures (Sonnewald et al., 1993a+b and 1996a; Bakken et al., 1998; Waagepetersen et al., 1999b), brain slices (Badar-Goffer et al., 1990 and 1992) and in animals *in vivo* (Cerdan et al., 1990; Künnecke et al., 1993; Hassel et al., 1995a).

The natural abundance of $^{13}$C is only 1.1% and the sensitivity is 0.02, which makes studies of endogenous $^{13}$C containing metabolites very difficult, unless they occur in large amounts. These features do, however, make the $^{13}$C nucleus perfectly suited for experiments using $^{13}$C labeled precursors to study metabolic pathways with little

background interference from endogenous metabolites. Using $^{13}C$ MRS it is possible to identify the position of the $^{13}C$ atom within a molecule. This property results from the fact that different $^{13}C$ atoms within a molecule experience small perturbations in the local magnetic field around the nucleus depending on the immediate physiochemical environment (due to the electrons surrounding the nucleus) therefore each nucleus will resonate at an unique Larmor frequency. The frequency scale at which the nuclei are measured is called the chemical shift and is given in units of parts per million (ppm) of the applied magnetic field (B), and has the advantage of being independent of magnet strength. In the present studies the chemical shift range was 200 ppm. Often in $^{13}C$ MRS an exogenous or endogenous reference compound is used. Furthermore, unlabelled substances in high concentrations can be added to the solution and a $^{13}C$ MR spectrum obtained utilizing the naturally occurring $^{13}C$ for confirmation of peak assignments. Identification of the different peaks in the $^{13}C$ spectra are usually based on previous reports (see f.ex. Fan, 1996).

The sensitivity of $^{13}C$ MRS is so low that considerable acquisition time is usually required to produce useful spectra. The low sensitivity of $^{13}C$ MRS is further reduced by splitting of some resonances into several peaks due to coupling between neighboring $^{1}H$ and $^{13}C$ atoms. This is called heteronuclear spin-spin coupling, and makes the spectra very complex. To avoid this, $^{13}C$ MR spectra are usually proton decoupled (broad-band decoupled). In the proton decoupled spectra all carbon nuclei give single peaks, as long as they are not coupled to other MR active nuclei, such as another $^{13}C$ nucleus (see below). In addition, the signal will be amplified by the nuclear Overhauser effects (nOe) in proton decoupled spectra (for details see Chp. 10, Friebolin, 1998). nOe effects depend on conditions influencing relaxation such as the number of protons covalently bound, and will therefore vary from nucleus to nucleus, making it impossible to obtain the theoretically estimated maximum nOe value of 2.98 in $^{13}C$ MRS experiments with broad-band decoupling. The different nOe are together with different relaxation times the most important sources of error in $^{13}C$ MRS. nOe can be suppressed by implementing inverse gated decoupling, which is done by applying proton decoupling only during acquisition in order to avoid nOe to build up. This will, however, decrease the signal intensity, and a larger number of scans will be necessary. By combining

proton (broad-band) decoupling and inverse-gated decoupling measurements in a few samples it is possible to get correction factors for the nOe of different atoms relative to the reference compound added. The correction factors can then be applied to all spectra.

The occurrence of two adjacent $^{13}C$ atoms, leading to homonuclear spin-spin coupling, causes splitting and displacement of the resonance from the central single resonance that is present if the $^{13}C$ atom were alone. $^{13}C$-$^{13}C$ spin coupling patterns make the detection of label incorporation unambiguous since the probability of having two naturally occurring $^{13}C$ atoms adjacent in the same molecule is very small (0.01%).

The best spectral resolution in $^{13}C$ MRS is obtained using protein free extracts of brain tissue (Morris et al., 1986; Badar-Goffer et al., 1990; Cerdan et al., 1990; Shank et al., 1993), and thus the metabolic pathways in the brain can be studied in detail based on isotopomer analysis. An isotopomer is an isotope isomer, i.e. a compound enriched with $^{13}C$ atom(s) in one or more positions. In the $^{13}C$ MR spectra the position of $^{13}C$ atoms within a variety of compounds can be discerned. Because the labeling of various carbon positions within a compound (usually an amino acid) depends on different enzymatic pathways, some of which are purely neuronal or glial, the metabolic fate of the $^{13}C$ labeled compound can be followed in great detail. It has been demonstrated *in vitro* that neuronal and astrocytic metabolism can be studied simultaneously by superfusion of brain slices with $^{13}C$ labeled glucose and acetate (Badar-Goffer et al., 1992; McLean et al., 1993; Taylor et al., 1996). In the present work concurrent administration of [1,2-$^{13}C$]acetate and [1-$^{13}C$]glucose to rats *in vivo* followed by *ex vivo* $^{13}C$ MRS of deproteinized brain extracts was employed for the first time.

A model of the compartmentation of glucose and acetate metabolism in the brain is shown in Fig. 2, and the labeling patterns in glutamate, glutamine and GABA resulting from [1,2-$^{13}C$]acetate and [1 -$^{13}C$]glucose metabolism are shown in Fig. 3. For more details see also section 1.1.4.

[1,2-$^{13}C$]Acetate is metabolized by astrocytes (Van den Berg, 1973) due to the presence of a specific acetate carrier on these cells (Waniewski and Martin, 1998). In the astrocyte [1,2-$^{13}C$]acetate is converted by acetyl CoA synthetase (EC 6.2.1.1) to double labeled acetyl CoA which enters the TCA cycle, and finally [4,5-$^{13}C$]glutamate can be

formed (Fig. 2 and 3). [4,5-$^{13}$C]Glutamate is rapidly converted to [4,5-$^{13}$C]glutamine by the glia specific enzyme GS. Glutamate is present only in low concentrations in astrocytes (Ottersen, 1989; Ottersen et al., 1992). [4,5-$^{13}$C]Glutamine is released from astrocytes and taken up by neurons.

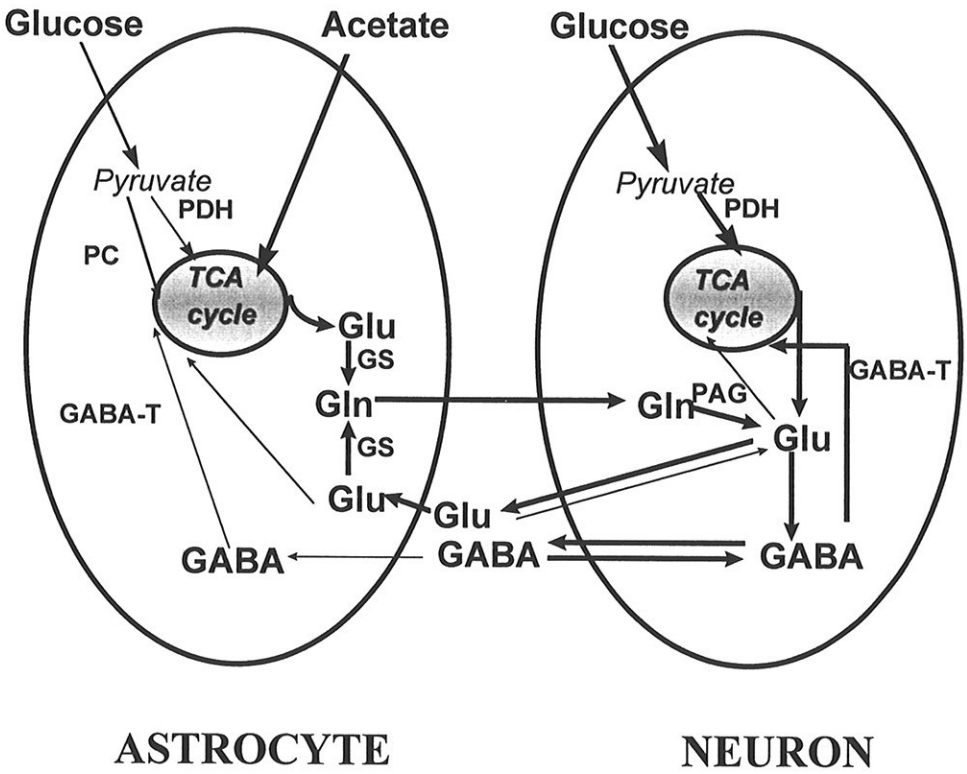


**Fig. 2.** Model of the astrocytic and neuronal compartments. Please note that the neuron depicted is a non-existing neuron using both glutamate and GABA as neurotransmitters. Furthermore, the enzymes have not been place in the correct subcellular location. For detailed explanation see also section 1.1.4.

In glutamatergic neurons direct conversion of [4,5-$^{13}$C]glutamine by PAG results in [4,5-$^{13}$C]glutamate formation. In GABAergic neurons [4,5-$^{13}$C]glutamate can be further directly metabolized by GAD to [1,2-$^{13}$C]GABA (Fig. 2 and 3). Astrocytes metabolize glucose to a lesser extent than neurons, but in these cells pyruvate from [1-$^{13}$C]glucose

can enter the TCA cycle via the astrocyte specific anaplerotic enzyme PC, and will then give rise to [2-$^{13}$C]glutamate and subsequently [2-$^{13}$C]glutamine (Fig. 3).

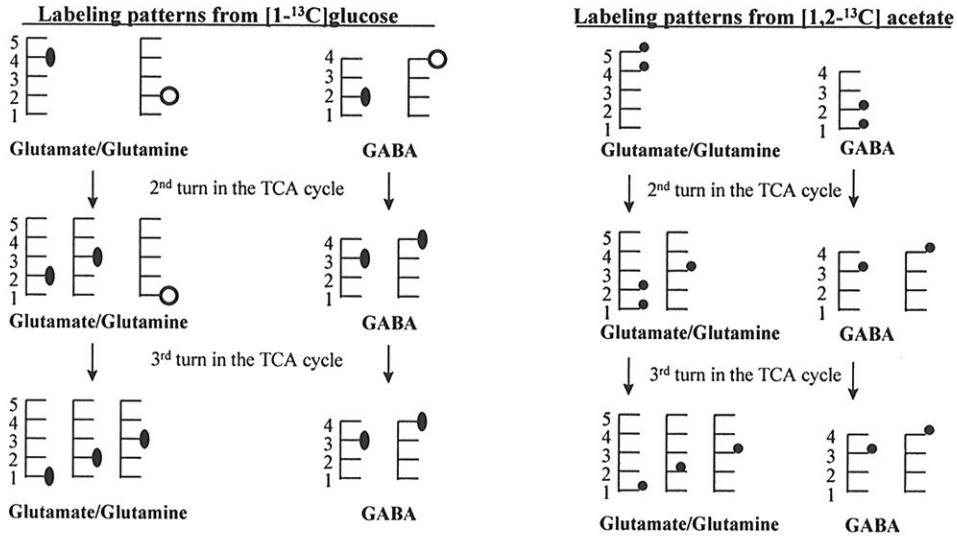


**Fig. 3.** The isotopomers arising from [1-$^{13}$C]glucose and [1,2-$^{13}$C]acetate metabolism. $^{13}$C labeling of glutamate, glutamine and GABA from [1-$^{13}$C]glucose via ● PDH or ○ PC activity, and • from [1,2-$^{13}$C]acetate.

Neurons metabolize primarily glucose (Van den Berg, 1973; Künnecke et al., 1993). [1-$^{13}$C]glucose enters the neuronal TCA cycle as single labeled acetyl CoA derived from pyruvate solely via the activity of pyruvate dehydrogenase (PDH; EC 1.2.4.1) and results in [4-$^{13}$C]glutamate formation (Fig. 2 and 3). The majority of glutamate is found in glutamatergic neurons (Ottersen, 1989; Ottersen et al., 1992). Astrocytes will take up [4-$^{13}$C]glutamate released from neurons and convert it to [4-$^{13}$C]glutamine. Alternatively, [4-$^{13}$C]glutamate enters the astrocytic TCA cycle. In GABAergic neurons [4-$^{13}$C]glutamate is rapidly converted to [2-$^{13}$C]GABA, and very little glutamate is present in these neurons (Ottersen, 1989; Ottersen et al, 1992; Martin and Rimvall, 1993). The relative contribution from the neuronal and the astrocytic compartment in glutamate, glutamine and GABA formation can be derived from analysis of the total amount and the distribution of label in the different isotopomers (Taylor et al., 1996).

### 2.2.3 Diffusion weighted MR imaging (DWI)

DWI has shown great promise in the evaluation of acute cerebral ischemia. In DWI it is the diffusion of water protons in the absence of any concentration gradient, i.e. random thermal motions, often called Brownian motion, which is mapped. The overall principle of DWI is that the spatial location of the water molecule is tagged so that any movement of the water molecule during the time of observation results in signal loss. This is achieved by applying very strong field gradients, called diffusion gradients, with increasing strength to a standard MR sequence, for instance a T2 weighted spin echo sequence. In the simplest type of DWI sequence two diffusion gradients are applied. The first of these diffusion gradients (the dephasing gradient) causes the spinning protons to fall out of phase with one another. The second diffusion gradient (the rephasing gradient) rephases the protons completely with one another only if there were no movement of the water molecules between the application of the two diffusion gradients. The further the water has moved, the more out of phase it will be, and the more signal attenuation will occur. As a result areas of high diffusion will appear dark, and areas with low diffusion bright. The amount of signal loss is related to the magnitude of the molecular translation, i.e. the net diffusion, and to the strength of the diffusion weighting. The strength of the diffusion gradient is expressed in b-values. Because of the restricted diffusion in biological tissue, self-diffusion of water is referred to as apparent diffusion and can be quantitatively described by the apparent diffusion coefficient (ADC). The ADC of water is calculated from the slope of the curve obtained by plotting signal intensity versus the b-value used. At least two b-values are required, one of which can be $b = 0$.

In acute cerebral ischemia diffusion is reduced. This was first demonstrated by Moseley and his group in the cat in 1990 and by Warach and co-workers in humans in 1992. Several theories have been proposed to explain the biophysical mechanisms causing restricted diffusion in ischemia, but only two have been commonly acclaimed. The leading theory suggests that the reduced diffusion observed in acute cerebral ischemia results from the formation of cytotoxic edema (Moseley et al., 1990a and b; Mintorovitch 1991; Benvensite et al., 1992). Cytotoxic edema results in an increased fraction of water protons in the intracellular space where diffusion is slower, and

correspondingly less water protons in the extracellular compartment with faster diffusion (Schuier and Hossmann, 1980). In the second theory developed by Norris et al. (1994), it has been suggested that cytotoxic edema causes entrapment of extracellular water in non-contiguous small pockets between the cells, which results in the extracellular water experiencing the same diffusion properties as intracellular water.

DWI hyperintensity has been observed as early as 2.5-6 min after arterial occlusion in cat and rat (Moseley et al., 1990a and b; Minematsu et al., 1992; Davis et al., 1994; Li et al., 1998), at which time there is no sign of histological damage (Benveniste et al., 1992; Knight et al., 1994). Ischemia induced ADC drop is observed at CBF values around 41 ml/100g/min at the beginning of the ischemic insult, but with increasing duration of ischemia ADC changes are detected at higher CBF values (Hoehn-Berlage et al., 1995; Kohno et al., 1995; Mancuso et al., 1995). ADC values continue to decrease for 24 hours after ictus to a level of about 50-60% of control values (Hoehn-Berlage et al., 1995). Regression of DWI hyperintesity has been reported to occur with reperfusion after 33-60 min of MCAO (Mintorovicht et al., 1991, Müller et al., 1995; Davis et al., 1994). However, the hyperintensity, which was first normalized after reperfusion, has been shown to reappear 24 hours later (Li et al., 2000). In cerebral ischemia the decrease in ADC precedes the changes on T2-weighted images by at least 2-3 hours (Mintorovitch et al., 1991; Moseley et al., 1990a and b; Lansberg et al., 2001) which coincides with the beginning formation of vasogenic edema.

## 3. Aim of study

Primary aims:

1. Development of a method for studying neuronal and astrocytic metabolism and trafficking of metabolites between these compartments simultaneously during MCAO by combining *in vivo* injection of [1-$^{13}$C]glucose and [1,2-$^{13}$C]acetate with *ex vivo* $^{13}$C MRS (Papers I-V).
2. Using the method to identify differences in neuronal and astrocytic metabolism and intercellular trafficking *in vivo* in two anatomical regions suffering severe and moderate ischemia respectively (Papers I and V).

Secondary aim:

1. Evaluate the effect of pharmacological neuroprotection in a rat model of middle cerebral artery occlusion using diffusion-weighted MRI (Paper VI).

## 4. Synopsis of Papers

**I.** *Håberg A, Qu H, Haraldseth O, Unsgård G, Sonnewald U (1998) In vivo injection of [1-$^{13}$C]glucose and [1,2-$^{13}$C]acetate combined with ex vivo $^{13}$C NMR spectroscopy: A novel approach to the study of MCA occlusion in rat. J Cereb Blood Flow Metab 18: 1223-1232*

Rats were subjected to permanent MCAO. At 75 min after on-set the fully awaken rats received an iv. bolus injection of [1-$^{13}$C]glucose and [1,2-$^{13}$C]acetate. The rats were decapitated 15 min later into liquid $N_2$. From the frozen brains 3 mm slices were cut, and from these the lateral caudoputamen plus lower parietal cortex, and the upper frontoparietal cortex from both hemispheres were sampled, aiming at representing severely and moderately ischemic tissue respectively. Then brain samples were extracted and analyzed with $^{13}$C MRS and HPLC. Distinct changes in glutamate and GABA metabolism, in astrocytic metabolism, as well as in neuro-astrocytic trafficking were identified in the regions suffering moderate and severe ischemia. The findings demonstrated that this approach can be used in the study of cerebral intermediary metabolism and intercellular trafficking during MCAO, and that the method is sensitive enough to reveal differences in metabolism within discreet regions suffering varying degrees of ischemia.

**II.** *Håberg A, Qu H, Bakken IJ, Sande LM, White L, Haraldseth O, Unsgård G, Aasly J, Sonnewald U (1998) In vitro and ex vivo $^{13}$C NMR spectroscopy studies of pyruvate recycling in brain. Dev Neurosci 20: 289-398*

Incubating astrocyte cultures with [U-$^{13}$C]glutamate and subsequently analyzing cell extracts and media with $^{13}$C MRS demonstrated that pyruvate recycling takes place in astrocytes *in vitro*. In the animal experiment, [1,2-$^{13}$C]acetate was administered to rats *in vivo* either subcutanously or intraperitoneally followed by *ex vivo* $^{13}$C MRS of the cerebral cortices and plasma. The results suggeste that pyruvate recycling is found in astrocytes also *in vivo*, but the activity of this pathway is very low.

**III.** *Håberg A, Qu H, Haraldseth O, Unsgård G, Sonnewald U (2000) In vivo effects of adenosine $A_1$ receptor agonist and antagonist on neuronal and astrocytic intermediary metabolism studied with ex vivo $^{13}C$ NMR spectroscopy. J Neurochem 74: 327-33*

Cerebral acetate metabolism has been suggested to induce adenosine formation and subsequent activation of $A_1$ receptors. Fasted rats received adenosine $A_1$ receptor agonist (CCPA), antagonist (DPCPX) or vehicle iv., followed 15 min later by either [1-$^{13}$C]glucose or [1,2-$^{13}$C]acetate intraperitoneally. DPCPX was shown to exert profound effects on both neuronal and astrocytic amino acid synthesis and degradation. CCPA only reduced the contribution from astrocytic anaplerotic activity in glutamate formation. Finally, no adenosine $A_1$ receptor effects arising from cerebral acetate metabolism were detected.

**IV**. *Qu H, Håberg A, Haraldseth O, Unsgård G, Sonnewald U (2000) $^{13}C$ MR spectroscopy study of lactate as substrate for rat brain. Dev Neurosci 22: 429-436*

Cerebral lactate metabolism was studied in fasted rats receiving either 0.3 M [U-$^{13}$C] lactate or 0.15 M [U-$^{13}$C] glucose iv. After 15 min the rats were decapitated into liquid $N_2$. Brain and plasma extracts were analyzed with $^{13}C$ MRS and HPLC. Neuronal metabolism of acetyl CoA from glucose was estimated to account for at least 2/3, and glia less than 1/3 of the total cerebral glucose consumption. Lactate crossed the BBB and was more avidly metabolized by neurons than astrocytes. Furthermore, the results suggest that lactate entered preferentially into glutamatergic neurons.

**V**. *Håberg A, Qu H, Sæther O, Unsgård G, Haraldseth O, Sonnewald U (2001) Differences in neurotransmitter synthesis and intermediary metabolism between glutamatergic and GABAergic neurons during 4 Hours of MCAO in the rat. The role of astrocytes in neuronal survival. Under revision for J Cereb Blood Flow Metab.*

Rats were subjected to permanent MCAO lasting 30, 60, 120 or 240 min, and the changes in neuronal and astrocytic metabolism during ischemia were analyzed using the method in Paper I. In the severely ischemic tissue both neurons and astrocytes had impaired metabolism from 30 min of MCAO. The normal equilibrium in the glutamate-glutamine cycle was greatly disturbed as indicated by mismatch between reduced

glutamate synthesis and re-uptake on one hand, and increased glutamate consumption and loss in to systemic circulation and CSF on the other hand. In GABAergic neurons astrocytic precursors were not used in GABA synthesis at any time after MCAO, and neuronal glucose metabolism and GABA-shunt activity declined with time. At 240 min of MCAO no flux through the tricarboxylic acid cycle was found in GABAergic neurons indicating neuronal death. In moderately ischemic tissue signs of decreased astrocytic metabolism were first seen at 120 min of MCAO. In glutamatergic neurons there was a progressive decline in glucose metabolism, but the neurotransmitter pool of glutamate coming from astrocytic glutamine was relatively preserved, implying that glutamine contributed significantly to glutamate excitotoxicity. In GABAergic neurons astrocytic precursors were used to a limited extent during the initial 120 min, and there was continued tricarboxylic acid cycle activity for 240 min. These results suggested that changes in the utilization of astrocytic precursors in neuronal metabolism during ischemia contribute significantly to neuronal death, although through different mechanisms in glutamatergic and GABAergic neurons.

**VI.** *Håberg A, Takahashi M, Yamaguchi T, Hjelstuen M, Haraldseth O (1998) Neuroprotective effect of the novel glutamate AMPA receptor antagonist YM872 assessed with in vivo MR imaging of rat MCA occlusion. Brain Res 811: 63-70*

The neuroprotective effect of 4 h versus 24 h of post-ischemic administration of the AMPA antagonist, YM872, was evaluated in permanent MCAO in rats. YM872 significantly reduced the volume of ischemic tissue measured with DWI 4 1/2 hour after MCAO as compared to control rats. After 24 h the infarct volume, based on T2 weighted MRI and histopathological assessment, was significantly smaller only in rats receiving YM872 treatment for 24 h compared to both the 4 h treatment group and the control group.

## 5. Discussion

The principal aim of this work was to establish a method for the study of neuronal and astrocytic metabolism *in vivo* during cerebral ischemia. This was done by combining *in vivo* injection of $^{13}C$ labeled glucose and acetate in rats subjected to MCAO with *ex vivo* $^{13}C$ MRS of brain and plasma extracts. There are several aspects of this methodology which need closer examination before this approach to the study of MCAO can be endorsed. Validation of the method, based on results obtained in the present work and by others, is thus discussed first before a brief recount of the major findings from the ischemic rat brains.

### 5.1 *Validation of method*

#### 5.1.1 Supply of labeled substrates

*5.1.1.1 Fasting and extracerebral substrate metabolism*

Extra cerebral formation of newly labeled substrates from the originally labeled glucose, acetate or lactate administered may be used in the cerebral metabolism and thus interfere with the interpretation of the isotopomer data. Plasma samples were analyzed in order to evaluate the extent of synthesis of labeled substrates from [1-$^{13}C$]- and [U-$^{13}C$]glucose, [1,2-$^{13}C$]acetate and [U-$^{13}C$]lactate.

All rats were fasted over night in order to control plasma glucose levels, thereby minimizing variability. However, fasting influences the rate of gluconeogenesis. Label from glucose and acetate (and lactate) can be incorporated into glucose via gluconeogenesis, resulting in new glucose isotopomers. Moreover, the Cori and alanine cycles as well as the presence of pyruvate recycling and futile cycling in the liver lead to non-symmetrical scrambling of label in glucose (Katz and Rognstad, 1976). The present studies demonstrated that label from [1-$^{13}C$]-, [U-$^{13}C$]glucose and [1,2-$^{13}C$]acetate was introduced into newly synthesized glucose within 15 min in fasted rats. [U-$^{13}C$]glucose gave rise to [1,2-$^{13}C$]glucose (Paper IV), and label from [1,2-$^{13}C$]acetate was detected in plasma glucose C-1$\alpha$ (Paper II) as well as in [2,3-$^{13}C$]- and [4,5-$^{13}C$]glucose (Paper I and V). [1-$^{13}C$]glucose was only about 1% enriched from [1,2-$^{13}C$]acetate, making the contribution from [1,2-$^{13}C$]acetate to [1-$^{13}C$]glucose minimal since [1-$^{13}C$]glucose was

around 50% enrichment (Paper I). No [1,2-$^{13}$C]- or [5,6-$^{13}$C]glucose were detected (Paper I, II and V). Such isotopomers would have labeled cerebral amino acids similarly to [1,2-$^{13}$C]acetate.

The presence of single labeled acetate may also interfere with label interpretation as [2-$^{13}$C]acetate gives rise to the same labeling patterns as [1-$^{13}$C]glucose. However, the amount of single labeled acetate was estimated to make up about 5% of total the acetate concentration which was less than 1/5 of the glucose concentration (Paper I), thus [2-$^{13}$C]acetate did not contribute significantly to amino acid labeling as compared [1-$^{13}$C]glucose.

Significant labeling of plasma lactate originating from labeled glucose was detected in fasted rats (Paper IV) in line with results from fasted mice (Hassel and Bråthe, 2000). Labeled lactate was also detected after simultaneous administration of [1-$^{13}$C]glucose and [1,2-$^{13}$C]acetate (Paper I and V). However, plasma lactate in rats receiving both glucose and acetate was less enriched than in rats receiving only glucose (Paper I, IV and V), perhaps owing to reduced glycolysis produced by the simultaneous fatty acid oxidation (Anderson and Bridges, 1984).

Label in amino acids in plasma was not quantifiable (Paper I, IV and V). This is in accordance with previous results (Gaitonde et al., 1965; Vrba, 1962) and is due to conversion of glucose into amino acids in the brain proceeding at a rate several times higher than in all other organs.

In conclusion, using the current set-up extracerebral metabolism of [1-$^{13}$C]glucose and [1,2-$^{13}$C]acetate does not result in significant amounts of newly labeled substrates for the cerebral metabolism.

*5.1.1.2 Cerebral uptake of labeled substrates*

The supply of the peripherally administered glucose, acetate and lactate to the brain tissue for further metabolism depends on BBB penetrance for each compound and CBF, as both critically influence the rate of exchange of substances between blood and brain tissue.

Glucose is avidly taken up by the brain via facilitated transport mediated by stereospecific, insulin-independent GLUT-1 transporters which are present in high

concentrations in brain capillary endothelial cells (Maher et al., 1994). Acetate and lactate are transported by separate stereospecific systems (Pardridge, 1983; Gerhart et al., 1997), and the entry rate of these substances is considered to be significantly lower than that of glucose. However, disagreement exists as to the permeability of the adult BBB to lactate and acetate (Oldendorf, 1973; Nemoto et al., 1974; Partridge, 1983; Harada et al., 1992, Clarke and Sokoloff, 1999). The results from the fasted rats receiving [U-$^{13}$C]lactate or [U-$^{13}$C]glucose confirmed that glucose is taken up more avidly by the brain, but also lactate crossed the BBB and was further metabolized there (Paper IV). Similar results were obtained in mice (Hassel and Bråthe, 2000). [1,2-$^{13}$C]Acetate was also rapidly taken up into the brain, but plasma concentrations appeared to seriously influence its availability as cerebral substrate (Paper II).

The presence of an intraluminal filament occluding the origin of the middle cerebral artery did not completely stop the supply of labeled substrates, as the total amount of [1-$^{13}$C]glucose was significantly increased in ischemic brain tissue at all times after MCAO, and the concentration of unmetabolized [1,2-$^{13}$C]acetate increased with time (Paper I and V). The existence of a rich network of end-to-end anastomoses connecting branches of the middle, anterior and posterior cerebral arteries at the surface of the rat brain (Coyle and Jokelainen, 1982) most likely played an important role in the continuos supply of labeled substrates to the ischemic brain tissue (Paper I and V). During neonatal life in rodents abundant collaterals between distal branches of the middle, anterior and posterior cerebral arteries do not undergo regression to the same extent as in primates (Coyle, 1975), but the gross vascular anatomy of rodents and primates is the same. Previous studies have also shown that glucose enters into both severely and mildly ischemic tissue after MCAO in the rat (Nowicki et al., 1988; Shiraishi et al., 1989; Belayev et al., 1997). Accumulation of unmetabolized acetate has been detected in ischemic brain tissue in a model of combined global and focal ischemia (Pascual et al., 1998). The current studies clearly showed that the peripherally administered [1-$^{13}$C]glucose and [1,2-$^{13}$C]acetate did reach the ischemic brain tissue in sufficient quantities. Moreover, the presence of markedly elevated [1-$^{13}$C]glucose and [1,2-

[13]C]acetate levels in the ischemic tissue demonstrated that reduced metabolism is an important consequence of reduced CBF.

### **5.1.2** Cerebral metabolism of labeled substrates

#### *5.1.2.1 Cerebral glucose and acetate metabolism*

The validity of systemic administration of labeled glucose and acetate for the study of neuronal and astrocytic metabolism relies on glucose being predominantly metabolized by neurons and acetate by astrocytes, which again depends on heterogeneous distribution of enzymes and transporter proteins between these two cellular subtypes. It is conceivable that some of these features may change during MCAO. As previously noted acetate is converted to acetyl CoA by acetyl CoA synthetase. This enzyme is found in both astrocytes and neurons, and actually has higher activity in synaptosomes than in astrocytes (Waniewski and Martin, 1998). The preferential utilization of acetate by astrocytes is attributed to the presence of a specific monocarboxylate transporter on astrocytes (Waniewski and Martin, 1998). Ischemia may alter the neuronal cell membrane, making it more permeable to acetate, causing acetate metabolism to take place in both cellular compartments. The total amount of [4,5-$^{13}$C]glutamine was invariably larger than the total amount of [4,5-$^{13}$C]glutamate during MCAO in both ischemic regions, and the acetate/glucose utilization ratio in glutamine was always greater than in glutamate (Paper I and V). Furthermore, labeling in [1,2-$^{13}$C]GABA was not detected in the ischemic lateral caudoputamen and lower parietal cortex (Paper V). These data indicate that acetate metabolism took place in the astrocytic compartment also during ischemia.

From hepatocytes and myocytes it is well known that cytosolic and mitochondrial enzymes leak out in response to cell injury and/or necrosis. During MCAO it is likely that neuronal and astrocytic enzymes enter into the extracellular space. The presence of active glial and neuronal specific enzymes outside the compartments of origin will make the isotopomer analysis used presently misleading. Fortunately, the astrocytic enzymes GS and PC are ATP dependent. In addition, acetyl CoA synthetase witch metabolizes acetate is also ATP dependent. Extracellular acetate metabolism, glutamine formation and anaplerosis thus appear unlikely. PAG activity in the extracellular space may cause

extracellular glutamate formation, but PAG is located to the inner mitochondrial membrane and since there is limited cell necrosis present until six hours after MCAO (Bartus et al.,1995; Garcia et al., 1995), the presence of significant amounts of PAG in the extracellular space during the first four hours of MCAO seems unlikely. GAD which is a cytosolic enzyme may, however, be relocated to the extracellular space. Extracellular GABA formation may ensue since this enzyme is stimulated by ischemic conditions (Turský, 1970; Erecinska et al., 1996).

In summary, acetate was metabolized by astrocytes also during MCAO, and the glial specific enzymes appeared to remain intracellularly, indicating that the astrocytic compartment can be described by the same metabolic pathways during four hours of MCAO as in the control situation. However, GAD which is a marker for the neuronal compartment may be active also extracellularly during MCAO.

*5.1.2.2 Alternative metabolic pathways*

5.1.2.2.1 Pyruvate recycling

Synthesis of pyruvate from part of the carbon skeleton of TCA cycle intermediates originating from labeled glucose, acetate or lactate, called pyruvate recycling (see section 1.1.2), will interfere with the interpretation of the labeling patterns (Paper I and II). Pyruvate recycling will result in [1-$^{13}$C]- and [2-$^{13}$C]acetyl CoA formation from [1,2-$^{13}$C]acetate, and thereby labeling coming from [1,2-$^{13}$C]acetate will appear as labeling from [1-$^{13}$C]glucose (Paper II). If pyruvate recycling were an important metabolic pathway in the brain, simultaneous injection of [1-$^{13}$C]glucose and [1,2-$^{13}$C]acetate cannot be used as a tool to differentiate between neuronal and astrocytic metabolism. The $^{13}$C enrichment in glutamate and glutamine C-4 singlet and in GABA C-2 singlet after [1,2-$^{13}$C]acetate administration demonstrated that pyruvate recycling took place in the rat brain, but that the activity of this pathway was very low (Paper II). Furthermore, the activity of pyruvate recycling has been shown to be reduced in acute ischemia in a model of combined focal and global ischemia (Pascual et al., 1998). Based on these results it appears unlikely that [1,2-$^{13}$C]acetate metabolism via pyruvate recycling contributes significantly to labeling of [4-$^{13}$C]glutamate/glutamine and [2-$^{13}$C]GABA in the brain during MCAO.

The results from cell cultures and animal experiments in our laboratory (Paper II; Sonnewald et al., 1996a; Bakken et al., 1997) and by others indicate that pyruvate recycling takes place in astrocytes (Hassel and Sonnewald, 1995), which is at variance with the results reported by Cerdan's group (Cerdan et al., 1990; Künnecke et al., 1993; Cruz and Cerdan, 1999).

5.1.2.2.2 Other pathways

In the brain metabolic pathways other than the TCA cycle exist where label from [1-$^{13}$C]glucose and/or [1,2-$^{13}$C]acetate may enter, and thus label can either be lost or scrambled into new positions in the amino acids under investigation.

The pentose phosphate pathway utilizes glucose, but by using [1-$^{13}$C]glucose label is almost quantitatively retained for 10 min after iv. injection in rats (Hawkins et al., 1985), and subsequently only a small proportion of label (<5%) enters this pathway. However, the activity of the pentose phosphate pathway has been suggested to increase in ischemia (Ben-Yoseph et al., 1995 and 1996), thus some label from [1-$^{13}$C]glucose may have been lost in this reaction during MCAO.

Cerebral lipid synthesis may also interfere with the interpretation of labeling patterns. Citrate produced from either [1-$^{13}$C]glucose or [1,2-$^{13}$C]acetate in the mitochondria is transferred to the cytosol and cleaved by ATP citrate lyase (EC 4.1.3.28) yielding oxaloacetate and acetyl CoA, which in turn can re-enter the TCA cycle. The activity of ATP citrate lyase is considered to be especially high in glia (Van den Berg and Ronda, 1976), but only about 2% of the glycolytic flux is directed towards lipid synthesis under control conditions (Sokoloff and Clark, 1999). Using the present experimental set-up, it is mainly label from [1,2-$^{13}$C]acetate entering into the initial step of free fatty acid synthesis for subsequently to re-enter the TCA cycle as single labeled acetyl CoA, which will interfere with isotopomer analysis. Increased activity of this pathway will for instance, lead to overestimation of PC/PDH activity. However, acetate metabolism via this pathway has been observed to a limited extent in mice *in vivo* 15 min after iv injection (Hassel et al., 1995a).

Backflow of TCA cycle intermediates, i.e. flow backward from oxaloacetate to fumarate, is also possible. This pathway would be thermodynamically favorable during

ischemia. If ischemia increased the backflow significantly, PC activity cannot be estimated reliably.

PC is considered the predominant anaplerotic pathway in the brain, and is located to the astrocytic compartment. However, neuronal anaplerotic activity has been described via mitochondrial malic enzyme in neurons in mice *in vivo* (Hassel and Bråthe, 2000). In rats there were no indications of neuronal anaplerosis *in vivo* (Paper IV). Thus the anaplerotic activity detected in the present studies may be regarded as derived from astrocytic PC activity alone.

From the above it is obvious that there are alternative metabolic pathways into which [1-$^{13}$C]glucose and [1,2-$^{13}$C]acetate may enter, leading to loss of label or the introduction of label into new positions in amino acids thereby complicating the isotopomer analysis. It is especially labeling of amino acids in the second and subsequent turns of the TCA cycle which has to be interpreted with the existence of these alternative pathways in mind, but also errors in the estimation of PC versus PDH activity is easily produced by changes in the activity of the pathways discussed above.

*1.2.3 Cerebral effects of acetate infusion*

The use of acetate for the study of cerebral metabolism depends on acetate being an inert probe not affecting cerebral processes. It has been suggested that cerebral acetate metabolism leads to increased adenosine formation (Carmichael et al., 1991 and 1993). Adenosine is considered to be a neuromodulator (Linden, 1999) which decreases the release of a broad range of neurotransmitters (Fredholm and Dunwiddie, 1988). These features of adenosine have lead to the assumption that adenosine is an endogenous neuroprotective substance (Rudolphi et al., 1992). However, in the present work no adenosine effects arising from acetate metabolism were observed (Paper III), concurring with results from other groups (Bundege and Dunwiddie, 1995; Fredholm and Wallman-Johansson, 1996). The tendency to lie down observed in rats receiving high doses of acetate (1.0 g/kg) was most likely connected to the depressed cardiac contractility and reduced blood pressure following bolus injections of acetate (Kirkendol et al., 1977). Furthermore, the administration of acetate has been reported to produce an array of adverse symptoms such as nausea, headache, confusion, dizziness and general weariness (Graefe et al., 1978; Diamond and Henrich, 1987). It should be noted that no behavioral

changes were observed in rats after iv. administration of 0.3 mM [1-$^{13}$C]glucose and [1,2-$^{13}$C]acetate, which corresponds to 0.25 g acetate per kg rat.

Acetate administration has also been shown to increase the content of glutamate and GABA in mice (Hassel et al., 1995a), but in the current work using rats no effect of acetate on amino acid levels was observed (Paper III).

Finally, acetate has been found to specifically reduce glucose incorporation into the TCA cycle via PDH activity in the heart (Randle et al, 1970). Whether acetate also inhibits PDH activity in the brain has to my knowledge not been studied. If such PDH inhibition were present in the brain, it is conceivable that co-administration of acetate and glucose leads to inhibition of glucose utilization via PDH in the astrocytic TCA cycle, thereby improving the specificity of glucose as a neuronal marker.

In conclusion, acetate can be regarded as an inert probe for the study of cerebral metabolism in rats.

*1.2.4 Cerebral effects of glucose infusion*

It is generally accepted that hyperglycemia aggravates cerebral injury in ischemia (Candelise et al., 1985; Bruno et al., 1999). In order to control plasma glucose levels all rats were fasted over night. Local cerebral glucose utilization has been shown not to be affect by fasting (Sokoloff et al., 1977). However, bolus injection of [1-$^{13}$C]glucose and [1,2-$^{13}$C]acetate led to a rapid increase in plasma glucose to approximately 18 mM at 15 min after infusion (Paper I and V). Acute hyperglycemia has previously been shown not to alter cerebral glucose metabolism (Duckrow and Bryan, 1987). In animal models of permanent focal cerebral ischemia, acute hyperglycemia occurring after onset of ischemia has been reported to be deleterious (Prado et al., 1988), beneficial (Ginsberg et al., 1987; Choi et al., 1994) and also to have no effect (Nedergaard and Diemer, 1987) on final infarct volume. Hyperglycemia may also alter glucose metabolism. Actually both increased and decreased glucose metabolism has been demonstrated surrounding the ischemic core in hyperglycemic rats (Nedergaard et al., 1988). Except for increased metabolism of glucose via PC activity at 60 min of MCAO in the ischemic lateral caudoputamen and lower parietal cortex, glucose metabolism via the TCA cycle was consistently reduced during MCAO (Paper I and V). The current infusion scheme, with 15 min from glucose administration to decapitation was chosen in an attempt to

minimize any adverse effects hyperglycemia may have on the evolution of ischemic tissue damage and on the cerebral metabolism.

*1.2.5 Effects of isoflurane anesthesia on cerebral metabolism*

Isoflurane decreases the cerebral metabolic rate while CBF increases, thereby uncoupling the tight relationship that normally exists between cerebral metabolic rate and CBF (Hoffman et al., 1991; Lenz et al., 1998). This observation has lead to the assumption that isoflurane is neuroprotective, which is supported by results from animal studies (Patel et al., 1995; Harada et al., 1999). In order to minimize possible effects of isoflurane on cerebral metabolism and CBF during MCAO, isoflurane administration was stopped at the time of MCAO in the present studies (Paper I,V and VI). However, isoflurane was shown to affect both neuronal and astrocytic metabolism *in vivo* 30, but not 60 min, after the anesthetic gas was turned off (Paper V). Furthermore, it was demonstrated that isoflurane reduced the metabolism in subcortical structures more than in pure cortical structures (Paper V), and that isoflurane reduced glutamate release in the former region (Paper V). The latter finding is line with the putative neuroprotective role of isoflurane.

These results underscore the importance of caution when interpreting data on cerebral metabolism obtained during anesthesia. Using the current experimental set-up more than 15 min should ideally pass from the anesthetic agent was turned off until administration of labeled glucose and acetate. It should, however, be noted that distinct changes induced by ischemia were detected in rats at 30 min of MCAO (Paper V).

*1.2.6 Effects of elevated body temperature*

Hyperthermia aggravates the extent of neuronal injury in cerebral ischemia, and increases morbidity and mortality (Ginsberg and Busto, 1998; Hajat et al., 2000). In the present work increased body temperature was detected in all rats subjected to MCAO (Paper VI). This is in line with results from other groups using the intraluminal filament technique for MCAO (Zhao et al. 1994; Li et al., 1999). The hyperthermia arises from ischemia in the medial hypothalamus (He et al., 1999). Elevated brain temperature is also present in all patients with severe MCA infarction (Schwab et al., 1998), and about 60% of patients with cerebral ischemia have fever during the first 72 h after ictus (Castillo et al., 1998). No effort was made to reduce body temperature to normal values

during MCAO in the present studies. This may have accelerated the neuronal injury, and had direct effects on the cerebral intermediary metabolism.

**5.1.3** Other factors

*1.3.1 Preservation of label and amino acid content during extract preparation*

The optimal method for preservation of cerebral metabolites *in situ* is considered to be funnel freezing (Pontén et al., 1973), which requires anesthesia and artificial ventilation. As discussed above isoflurane anesthesia influences both glucose and acetate metabolism. Decapitation and immediate immersion of the rat head in liquid $N_2$ was used instead. Previous studies have shown that there was no label incorporation from [1-$^{13}$C]glucose into glutamate and glutamine in rat brains when freezing was delayed with 2 min after death, but label was incorporated into GABA and aspartate (Shank et al., 1993). Furthermore, glutamate, glutamine and aspartate levels have been shown to remain constant for at least one hour after death in rat brains kept at 35°C, whereas alanine and GABA concentrations increase significantly with time (Perry et al., 1981). However, also aspartate synthesis has been shown to take place for several min postmortem (Shank and Aprison, 1971). Based on these data GABA, alanine and aspartate concentrations may have been increased, and label could be incorporated into these amino acids after decapitation. However, the concentrations of glutamate, glutamine, GABA, alanine and aspartate differed significantly between specific groups of rats, as seen in Paper I, III and V, which indicate that the technique preserves the original differences in amino acid content between the groups.

*1.3.2 Amount of tissue sampled for $^{13}$C MRS and choice of internal standard*

There are some discrepancies between the findings in Paper I and V that most likely arise from the modifications of the method used in Paper I compared to Paper V. In Paper I the size of the slice selected for $^{13}$C MRS was 3 mm thick, compared to 5 mm in Paper V. Furthermore, a shift in internal standard from dioxane (Paper I) to ethyleneglycol (Paper V) took place, making it possible to acquire spectra at half the delay time used previously owing to the shorter relaxation time for ethyleneglycol.

No PC activity was detected in glutamine or glutamate in the lateral caudoputamen and lower parietal cortex at 90 min of MCAO in Paper I. In Paper V, however, PC activity was found in glutamine and glutamate at 120 min of MCAO in the same region. There

are three possible explanation. 1. The low sensitivity of $^{13}C$ MRS may have interfered with the estimation of a small excess of label in the C-2 singlet position in glutamine/glutamate compared to in the C-3 singlet position. This phenomenon may be more prominent in smaller tissue samples. 2. The 5 mm thick slice in Paper V may have included more better perfused tissue where astrocytic PC activity was greater. 3. The use of ethyleneglycol as an internal standard in paper V resulted in improve spectral quality. In Paper I some samples from the upper frontoparietal cortex needed to be pooled in order to obtain useful $^{13}C$ MR spectra. This problem was not encountered in Paper V.

In conclusion, the spectral quality was greatly improved when sample size was increased from 3 to 5 mm and ethyleneglycol was used as the internal standard. It should, however, be noted that the 5 mm slice probably was more heterogeneous with regard to degree of ischemia, at least in the early phase of MCAO.

*1.3.3 Contralateral hemisphere or sham operated rats as control group*

In studies of MCAO both the contralateral hemisphere and brains from sham operated rats are used as controls. The contralateral hemispheres were used as control in Paper I, and brain tissue from sham operated were used in Paper V. The results from the current studies point to sham operated rats as the preferred control group. In Paper I [1,2-$^{13}C$]GABA was not present in quantifiable amounts in the samples taken from the hemisphere ipsilateral nor contralateral to the to MCAO. In sham operated rats, however, [1,2-$^{13}C$]GABA was present. Analysis of the hemispheres contralateral to the ischemic hemisphere in the rats in Paper V revealed that [1,2-$^{13}C$]GABA was not present in quantifiable amounts in this region before 120 min after MCAO (unpublished data). This observation shows that focal ischemia altered cerebral metabolism in the contralateral hemisphere, a phenomenon termed diaschisis (Andrews, 1991). The use of the contralateral hemispheres as controls in studies of cerebral metabolism during MCAO may thus lead to misinterpretation of the data obtained, thus making sham operated animals the preferred control group.

## 5.2 Major findings

**5.2.1** Changes in the glutamate-glutamine cycle during MCAO and its implications for glutamate exitotoxicity.

The glutamate-glutamine cycle underwent marked changes after on-set of MCAO (Paper I and V). In moderately ischemic tissue in the upper frontoparietal cortex, glutamate content was at control levels throughout 240 min of MCAO, despite evidence of increased glutamate oxidation and consumption of glutamate in glutamine, GABA and alanine formation. Furthermore, glutamate synthesis from neuronal precursors was markedly reduced from 30 min after MCAO. Direct conversion of glutamine to glutamate was also slightly reduced, to the same level throughout 240 min of MCAO. The contribution from astrocytic glutamine in glutamate formation was doubled at 240 min of MCAO. These results suggest that preservation of the glutamate content was largely due to continued utilization of astrocytic precursors in glutamate formation. It has previously been shown that astrocytic glutamine specifically replenish the neurotransmitter pool of glutamate (Laake et al., 1995), from which glutamate release is considered to originate in moderately ischemic tissue. The combination of continued replenishment of vesicular glutamate and gradually declining neuronal TCA cycle activity which was demonstrated currently, may render the neurons in the ischemic upper frontoparietal cortex extremely vulnerable to glutamate excitotoxicity. In addition, glutamate release further may have been accelerated further by the steadily increasing glutamine levels detected in this region (Thanki et al., 1983; Szerb and O'Regan, 1985). In conclusion, these results suggest that astrocytic glutamine contributes significantly to glutamate excitotoxicity, and that glutamate excitotoxicity is continued beyond 240 min after on-set of MCAO. This is supported by the findings in Paper VI, where administration of the AMPA receptor antagonist, YM872, for four hours did not reduce final infarct volume, whereas administration for 24 h did. Thus treatment with glutamate antagonists has to be continued for an extended period of time, which bears important implications for the use of such drugs in the clinical setting.

In the severely ischemic tissue in the lateral caudoputamen and lower parietal cortex, administration of the AMPA receptor antagonist, YM872, did not reduce the extent of infarction (Paper VI). This is in line with results from other groups (Gill and Lodge, 1994; Kawasaki-Yatsugi et al., 1998). The lack of efficacy of glutamate receptor antagonist in rescuing the severely ischemic region points to other mechanisms as more important in the development of cerebral infarction in this region. This notion is further

supported by the steadily declining glutamate levels in this region after MCAO, resulting from mismatch between glutamate synthesis and re-uptake on one hand, and consumption and loss into systemic circulation and CSF on the other hand. Furthermore, metabolism was reduced in both neurons and astrocytes from 30 min of MCAO, and at 240 min there was no TCA cycle flux in GABAergic neurons, giving additional evidence of severely impaired cellular function in this region.

### **5.2.2** The role of astrocytes in neuronal survival during MCAO

A complex picture of the involvement of astrocytes in neuronal survival in focal ischemia emerged from the present studies. Changes in the metabolic interactions between neurons and astrocytes during focal ischemia were identified, and neuronal utilization of astrocytic precursors and the metabolic activity of astrocytes appeared to be important determinants for neuronal survival.

Alterations in the utilization of astrocytic glutamine seemed to contribute significantly to neuronal death, although by different mechanisms in glutamatergic and GABAergic neurons. The results from Paper I, V and VI suggested that astrocytic glutamine contributed significantly to glutamate excitotoxicity in the moderately ischemic region in the upper frontoparietal cortex. Thus continued supply of glutamine to glutamatergic neurons, and the persistent conversion of glutamine to glutamate in these neurons contributed to neuronal death by excitotoxicity. In GABAergic neurons, on the other hand, there was complete stop in the use of glutamine in GABA formation. This was probably an important factor leading to stop in TCA cycle flux, and thus death of the GABAergic neurons in the lateral caudoputamen and lower parietal cortex at 240 min of MCAO. In summary, both continued supply and utilization of astrocytic precursors as well as cessation in the utilization of such precursors can be a major cause of neuronal death in focal ischemia. In previous studies the presence of astrocytes and supply of glutamine have been shown to both improve as well as reduce neuronal survival (see section 1.2.4). Two possible mechanisms behind these conflicting observations have been elucidated in the current work.

To further complicate the picture, normal astrocytic metabolism may be a prerequisite for neuronal survival. In severely ischemic tissue in the lateral caudoputamen and lower

parietal cortex, the first signs of reduced astrocytic metabolism was detected at 30 min of MCAO, whereas in moderately ischemic tissue in the upper frontoparietal cortex astrocytic metabolism was first reduced at 90-120 min of MCAO. Reperfusion within 30 min has been shown to rescue some of the lateral caudoputamen and lower parietal cortex, whereas the upper frontoparietal cortex can be saved by reperfusion within 90-120 min of MCAO (Memezawa et al., 1992b). These time points coincides with the beginning signs of reduced astrocytic metabolism, suggesting that successful reperfusion may depend on the presence of at least close to normal astrocytic metabolism.

In conclusion, the present work clearly demonstrated the paradoxical role of the astrocyte in neuronal survival in ischemia. On one hand, changes in the normal equilibrium between neuronal derived precursors and astrocytic derived precursors in neurotransmitter synthesis significantly contributed to neuronal death. On the other hand, neuronal survival may depend on the well-being of the astrocytic metabolism.

## 6. Conclusions

The present work demonstrated that neuronal and astrocytic metabolism, and trafficking of metabolites between these two compartments can be studied in detail in regions of severe and moderate ischemia using simultaneous administration of [1-$^{13}$C]glucose and [1,2-$^{13}$C]acetate *in vivo* combined with *ex vivo* $^{13}$C MRS and HPLC analysis. By applying this approach the role of the astrocyte in glutamate excitotoxicity and in neuronal survival in moderately and severely ischemic regions was further elucidated.

.

## References


Aas J-E, Berg-Johnsen J, Hegstad E, Laake JH, Langmoen IA, Ottersen OP (1993) Redistribution of glutamate and glutamine in slices of human neocortex exposed to combined hypoxia and glucose deprivation in vitro. *J Cereb Blood Flow Metab* 13: 503-515

Abe A, Aoki M, Kawagoe J, Yoshida T, Hattori A, Kogure K, Itoyama Y (1995) Ischemic delayed neuronal death: a mitochondrial hypothesis. *Stroke* 26: 1478-1489

Aguayo AJ, David S, Bray GM (1981) Influences of the glial environment on the elongation of axons after injury: transplantation studies in adult rodents. *J Exp Biol* 95: 231-240

Almeida A, Medina JM (1997) Isolation and characterization of tightly coupled mitochondria from neurons and astrocytes in primary culture. *Brain Res* 764: 167-172

Anderson JW, Bridges SR (1984) Short-chain fatty acids fermentation products of plant fiber affect glucose metabolism of isolated rat hepatocytes (41958) *PSEBM* 177: 373-376

Andrews RJ (1991) Transhemispheric diaschisis. A review and comment. *Stroke* 22: 943-949

Astrup J, Symon L, Branton NM, Lassen NA (1977) Cortical evoked potential and extracellular $K^+$ and $H^+$ at critical levels of brain ischemia. *Stroke* 8: 51-57

Astrup J, Symon L, Siesjö BK (1981) Thresholds in cerebral ischemia: the ischemic penumbra. *Stroke* 12: 723-725

Auestad N, Korsak RA, Morrow JW, Edmond F (1991) Fatty acid oxidation and ketogenesis by astrocytes in primary culture. *J Neurochem* 56: 1376-1386

Bachelard H (1998) Landmarks in the application of $^{13}C$-magnetic resonance spectroscopy to studies of neuronal/glial relationships. *Dev Neurosci* 20: 277-288

Bachelard H and Badar-Goffer R (1993) NMR spectroscopy in neurochemistry. *J Neurochem* 2: 412-429

Badar-Goffer RS, Bachelard HS, Morris PG (1990) Cerebral metabolism of acetate and glucose studied by $^{13}C$ NMR spectroscopy. A technique for investigating metabolic compartmentation in the brain. *Biochem J* 266: 133- 139

Badar-Goffer RS, Ben-Yoseph O, Bachelard HS, Morris PG (1992) Neuronal-glial metabolism under depolarizing conditions. A $^{13}C$ NMR study. *Biochem J* 282: 225-230

Baethmann A, Staub F (1997) Cellular edema. In: *Primer on Cerebrovascular Diseases* (Welch KMA, Caplan LR, Reis DJ, Siesjö BK, Weir B, eds.), pp.153-156. Academic Press, San Diego

Baird AE, Warach S (1999) Magnetic resonance imaging of acute stroke. *J Cereb Blood Flow Metab* 18: 583-609

Bakken IJ, Sonnewald U, Clark JB, Bates TE (1997) [U-$^{13}C$]Glutamate metabolism in rat brain mitochondria reveals malic enzyme activity. *NeuroReport* 8: 1567-1570

Bakken IJ, White LR, Aasly J, Unsgård G, Sonnewald U (1998) [U-$^{13}$C]Aspartate metabolism in cultured cortical astrocytes and cerebellar granule neurons studied by NMR spectroscopy. *Glia* 23: 271-277

Balázs R, Machiyama Y, Hammond BJ, Julian T, Richter D (1970) The operation of the gamma-aminobutyrate bypath of the tricarboxylic acid cycle in brain tissue in vitro. *Biochem J* 116: 445-461

Bao J, Cheung WY, Wu, JY (1995) Brain L-glutamate decarboxylase. Inhibition by phosphorylation and activation by dephosphorylation. *J Biol Chem* 270: 6464-6477

Barber PA, Darby DG, Desmond PM, Yang Q, Gerraty RP, Jolley D, Donnan GA, Tress BM, Davis SM (1998) Prediction of stroke outcome with echo-planar perfusion and diffusion-weighted magnetic resonance imaging. *Neurology* 51: 418-426

Baron JC, Frackowiak RSJ, Herholz K, Jones T, Lammertsma AA, Mazoyer B, Wienhard K (1989) Use of PET methods for measurement of cerebral energy metabolism and hemodynamics in cerebrovascular disease. *J Cereb Blood Flow Metab* 9: 723-742

Bartus RT, Dean RL, Cavanaugh K, Eveleth D, Carriero DL, Lynch G (1995) Time-related neuronal changes following middle cerebral artery occlusion: implications for the therapeutic intervention and the role of calpain. *J Cereb Blood Flow Metab* 15: 969-979

Baxter CF (1976) Some recent advances in studies of GABA metqbolism and compartmentation. In: *GABA in Nervous System Function* (Roberts E, Chase TN, Tower DB, eds.), pp. 61-87. Raven Press, New York

Behar KL, Petroff OAC, Prichard JW, Alger JR, Shulman RG (1985) Detection of metabolites in rabbit brain by $^{13}$C NMR spectroscopy following administration of [1-$^{13}$C]glucose. *Magn Res Med* 3: 911-920

Belayev L, Zhao W, Busto R, Ginsberg MD (1997) Transient middle cerebral artery occlusion by intraluminal suture: I. Three-dimensional autoradiographic image-analysis of local cerebral glucose metabolism - blood flow interrelationships during ischemia and early recirculation. *J Cerb Blood Flow Metab* 17: 1266-1280

Ben-Yoseph O, Camp DM, Robinson TE, Ross BD (1996) Dynamic measurement of cerebral pentose phosphate pathway activity in vivo using [1,6-$^{13}C_2$,6,6-$^{2}H_2$]glucose and microdialysis. *J Neurochem* 64: 1336-1342

Ben-Yoseph O, Boxer PA, Ross BD (1995) Assessment of the role of the gluthation and pentose phosphate pathways in the protection of primary cerebrocortical cultures from oxidative stress. *J Neurochem* 66: 2329-2337

Benveniste H (1991) The excitotoxin hypothesis in relation to cerebral ischemia. *Cerebrovasc Brain Metab Rev* 3: 213-245

Benveniste H, Hedlund LW, Johnson GA (1992) Mechanism of detection of acute cerebral ischemia in rats by diffusion-weighted magnetic resonance microscopy. *Stroke* 23: 746-754

Berl S, Lajtha A, Waelsch H (1961) Amino acid and protein metabolism-VI. Cerebral compartments of glutamic acid metabolism. *J Neurochem* 7: 186-197

Borden LA (1996) GABA transporter heterogeneity: pharmacology and cellular localization. *Neurochem Int* 29: 335-356

Branston NM, Strong AJ, Symon L (1977) Extracellular potassium activity, evoked potential and tissue blood flow. *J Neurol Sci* 32: 305-321

Bredt DS (1999) Endogenous nitric oxide synthesis: biological functions and pathophysiology. *Free Radic Res* 31: 577-596

Bruno A, Biller J, Adams HP Jr, Clarke WR, Woolson RF, Williams LS, Hansen MD (1999) Acute blood glucose level and outcome from ischemic stroke. Trial of ORG 10172 in Acute Stroke Treatment (TOAST) Investigators. *Neurology* 52: 280-284

Bundege JM, Dunwiddie TV (1995) The role of acetate as a potential mediator of the effects of ethanol on the brain. *Neurosci Lett* 186: 214-218

Butcher SP, Bullock R, Graham DI, McCulloch J (1990) Correlation between amino acid release and neuropathological outcome in rat brain following middle cerebral artery occlusion. *Stroke* 21: 1727-1733

Candelise L, Landi G, Orazio EN, Boccardi E (1985) Prognostic significance of hyperglycemia in acute stroke. *Arch Neurol* 42: 661-663

Carmichael FJ, Israel Y, Crawford M, Saldivia V, Sandrin S, Campisi P, Orrego H (1991) Central nervous system effects of acetate: contribution to the central effects of ethanol. *J Pharmacol Exp Ther* 259: 403- 408

Carmicael FJ, Orrego H, Israel Y (1993) Acetate-induced adenosine mediated effects of ethanol. *Alcohol (Alcohol suppl)* 2:411- 418

Castillo J, Dávalos A, Marrugat J, Noya M (1998) Timing for fever-related brain damage in acute ischemic stroke. *Stroke* 29: 2455-2460

Cataldo AM, Broadwell RD (1986) Cytochemical identification of cerebral glycogen and glucose-6-phospate activity under normal and experimental conditions. I. Neurons and glia. *J Electon Microsc Tech* 3: 413-437

Cerdan S, Künnecke B, Seelig J (1990) Cerebral metabolism of [1,2-$^{13}$C]acetate as detected by *in vivo* and *in vitro* $^{13}$C NMR. *J Biol Chem* 265: 12916-12926

Choi DW (1992) Excitotoxic cell death. *J Neurobiol* 23: 1261-1276

Choi DW (1995) Calcium: still center-stage in hypoxic-ischemic neuronal death. *Trends Neurosci* 18: 58-60

Choi DW (1997) The excitotoxic concept. In: *Primer on Cerebrovascular Diseases* (Welch KMA, Caplan LR, Reis DJ, Siesjö BK, Weir B, eds.), pp. 187-190. Academic Press, San Diego

Choi KT, Illievich UM, Zornow MH, Scheller MS, Strnat MAP (1994) Effect of hyperglycemia on per-ischemic neurotransmitter levels in the rabbit hippocampus. *Brain Res* 642: 104-110

Clarke DD, Sokoloff L (1999) Circulation and energy metabolism of the brain. In: *Basic Neurochemistry*, Sixth edition (Siegel GJ, Agranoff BW, Albers RW, Fisher SK, Uhler MD, eds), pp. 637-670. Lippicot-Raven Publisher, New York

Cornell-Bell AH, Finkbeiner SM, Cooper MS, Smith SJ (1989) Glutamate induces calcium waves in cultured astrocytes: long-range glial signaling. *Nature* 247: 470-473

Coyle P (1975) Arterial patterns of the rat rhinencephalon and related structures. *Exp Neurol* 49: 671-690

Coyle P, Jokelainen PT (1982) Dorsal cerebral arterial collaterals of the rat. *Anat Rec* 203: 397-404

Cruz F, Cerdan S (1999) Quantitative $^{13}C$ NMR studies of metabolic compartmentation in the adult mammalian brain. *NMR Biomed* 12: 451-462

Daikhin Y, Yudkoff M (2000) Compartmentation of brain glutamate metabolism in neurons and glia. *J Nutr* 130 (4S Suppl): 1026S-1031S

Davis D, Ulatowski J, Eleff S, Izuta M, Mori S, Shungu D, van Zijl PCM (1994) Rapid monitoring of changes in water diffusion coefficients during reversible ischemia in cat and rat brain. *Magn Reson Med* 31: 454-460

Davis SM, Lees KR, Albers GW, Diener HC, Markabi S, Karlsson G, Norris J, for the ASSIST Investigators (2000) Selfotel in acute ischemic stroke. Possible neurotoxic effects of an NMDA antagonist. *Stoke* 31: 347-354

Dawson LA, Djali S, Gonzales C, Vinegra MA, Zaleska MM (2000) Characterization of transient focal ischemia-induced increase in extracellular glutamate and aspartate in spontaneously hypertensive rats. *Brain Res Bull* 53: 767-776

DeGraba TJ, Pettigrew LC (2000) Why do neuroprotective drugs work in animals but not humans? *Neurologic Clin* 18: 475-493

Dermietzel R, Spray DC (1993) Gap junctions in the brain: Where, what type, how many and why. *Trends Neurosci* 16: 186-192

Deutch AY, Roth RH (1999) Neurotransmitters. In: *Fundamental Neuroscience* (Zigmond MJ, Bloom FE, Landis SC, Roberts JL, Squire LR, eds.), pp. 193-234. Academic Press, San Diego

Diamond SM, Henrich WL (1987) Acetate dialysate versus bicarbonate dialysate: a continuing controversy. *Am J Kid Dis* 9: 3-11

Dingledine R, McBain CJ (1999) Glutamate and aspartate. In: *Basic Neurochemistry*, Sixth edition (Siegel GJ, Agranoff BW, Albers RW, Fisher SK, Uhler MD, eds), pp 315-333. Lippicot-Raven Publisher, New York

Driscoll BF, Deibler GE, Law MJ, Crane AM (1993) Damage to neurons in culture following medium change: role of glutamine and extracellular generation of glutamate. *J Neurochem* 61: 1795-1800

Drejer J, Benveniste H, Diemer NH, Schousboe A (1985) Cellular origin of ischemia-induced glutamate release from brain tissue in vivo and in vitro. *J Neurochem* 45: 145-151

Duckrow RB, Bryan RM Jr (1987) Regional cerebral glucose utilization during hyperglycemia. *J Neurochem* 48: 989-993

Ellekjær H, Holmen J, Indredavik B, Terent A (1997) Epidemiology of stroke in Innherred, Norway, 1994 to 1996. Incidence and 30-day fatality rate. *Stroke* 28: 2180-2184

Erecinska M (1987) The neurotransmitter amino acid transport systems. A fresh outlook on an old problem. *Biochem Pharmacol* 36: 3547- 3555

Erecinska M, Nelson D, Daikhin Y, Yudkoff M (1996) Regulation of GABA level in rat brain synaptosomes: fluxes through enzymes of the GABA shunt and effects of glutamate, calcium and ketone bodies. *J Neurochem* 67: 2325-2334

European Ad Hoc Consensus Group (1998) Neuroprotection as initial therapy in acute stroke. Third report of an ad hoc consensus meeting. *Cerebrovasc Dis* 8: 59-72

Fan TW-M (1996) Metabolite profiling by one- and two-dimensional NMR analysis of complex mixtures. *Prog Nucl Mag Res Spec* 28:161-219

Farinelli SE, Nicklas WJ (1992) Glutamate metabolism in rat cortical astrocyte cultures. *J Neurochem* 58: 1905- 1915

Fiskum G (2000) Mitochondrial participation in ischemic and traumatic neuronal cell death. *J Neurotrauma* 17: 843-855

Fitzpatrick SM, Hetherington HP, Behar KL, Shulman RG (1990) The flux from glucose to glutamate in the rat brain in vivo as determined by $^{1}$H-observed, $^{13}$C edited NMR spectroscopy. *J Cereb Blood Flow Metab* 19: 170-179

Fredholm BB, Dunwiddie TV (1988) How does adenosine inhibit transmitter release? *TIPS* 9: 130-134

Fredholm BB, Wallman-Johansson A (1996) Effects of ethanol and acetate on adenosine production in rat hippocampal slices. *Pharmacol Toxicol* 79: 120-123

Friebolin H (1998) Basic one- and two-dimensional NMR spectroscopy. Third revised edition. Wiley-VCH Verlag GnbH, Weinheim

Gaitonde MK, Dahl DR, Elliott KAC (1965) Entry of glucose into amino acids of rat brain and liver in vivo after injection of uniformly $^{14}$C-labeled glucose. *Biochem J* 94: 345-352

Garcia JH, Liu K-F, Ho K-L (1995) Neuronal necrosis after middle cerebral artery occlusion in Wistar rats progress at different time intervals in the caudoputamen and the cortex. *Stroke* 26: 636-643

Gerhart DZ, Enerson BE, Zhdankina OY, Leino R, Drewes LR (1997) Expression of the monocarboxylate transporter MCT1 by brain endothelium and glia in adult and suckling rats. *Am J Physiol* 273: E207-213

Giaume C, McCarthy KD (1996) Control of junctional communication in astrocytic networks. *Trens Neurosci* 19: 319-325

Gill R, Lodge D (1994) The neuroprotective effects of the decahydroisoquinoline, LY 215490; a novel AMPA antagonist in focal ischaemia. *Neuropharmacol* 33: 1529-1536

Ginsberg MD, Busto R (1998) Combating hyperthermia in acute stroke: a significant clinical concern. *Stroke* 29: 529-534

Ginsberg MD, Prado R, Dietrich WD, Busto R, Watson BD (1987) Hyperglycemia reduces the extent of cerebral infraction in rats. *Stroke* 18: 570-574

Ginsberg MD, Pulsinelli WA (1994) The ischemic penumbra, injury thresholds and the therapeutic window for acute stroke. *Ann Neurol* 362: 553-554

Goldberg MP, Monyer H, Choi DW (1988) Hypoxic neuronal in vitro injury depends on extracellular glutamine. *Neurosci Lett* 94: 52-57

Gorini A, D'Angelo A, Villa RF (1999) Energy metabolism of synaptosomal subpopulations from different neuronal systems of rat hippocampus: effect of L-acetylcarnitine administration in vivo. *Neurochem Res* 24: 617-624

Graefe U, Milutinovich J, Follette WC, Vizzo JE, Babb AL, Scribner BH (1978) Less dialysis-induced morbidity and vascular instability with bicarbonate dialysate. *Ann Intern Med* 88: 332-336

Gruetter R, Novotny EJ, Boulware SD, Mason GF, Rothman DL, Prichard JW, Shulman RG (1994) Localized $^{13}$C NMR spectroscopy in the human brain of amino acid labeling from $^{13}$C glucose. *J Neurochem* 63: 1377-1385

Gruetter R, Seaquist ER, Kim S, Ugurbil K (1998) Localized in vivo $^{13}$C-NMR of glutamate metabolism in the human brain: initial results at 4 tesla. *Dev Neurosci* 20: 380-388

Hajat C, Hajat S, Sharma P (2000) Effects of poststroke pyrexia on stroke outcome. A meta-analysis of studies in patients. *Stroke* 31: 410-414

Harada M, Okuda C, Sawa T, Murakami T (1992) Cerebral extracellular glucose and lactate concentration during and after moderate hypoxia in glucose- and saline-infused rats. *Anesthesiol* 77: 728-734

Harada H, Kelly PJ, Cole DJ, Drummond JC, Patel PM (1999) Isoflurane reduces N-methyl-D-aspartate toxicity in the rat cerebral cortex. *Aesth Analg* 89: 1442-1447

Hassel B, Bråthe A (2000) Cerebral metabolism of lactate in vivo: evidence for neuronal pyruvate carboxylation. *J Cerb Blood Flow Metab* 20: 327-336

Hassel B, Sonnewald U (1995) Glial formation of pyruvate and lactate from TCA cycle intermediates: implications for the inactivation of transmitter amino acids. *J Neurochem* 65: 2227-2234

Hassel B, Sonnewald U, Fonnum F (1995a) Glial-neuronal interactions as studied by cerebral metabolism of [2-$^{13}$C]acetate and [1-$^{13}$C]glucose: An ex vivo $^{13}$C NMR spectroscopic study. *J Neurochem* 64: 2773- 2782

Hassel B, Westergaard N, Schousboe A, Fonnum F (1995b) Metabolic differences between primary cultures of astrocytes and neurons from cerebellum and cerebral cortex. Effects of fluorocitrate. *Neurochem Res* 20: 413-420

Hassel B, Johannessen CU, Sonnewald U, Fonnum F (1998) Quantification of the GABA shunt and the importance of the GABA shunt versus the 2-oxoglutarate dehydrogenase pathway in GABAergic neurons. *J Neurochem* 71: 1511-1518

Hawkins RA, Mans AM, Davis DW, Vina JR, Hibbard LS (1985) Cerebral glucose use measured with [$^{14}$C] glucose labeled in the 1,2 or 6 position. *Am J Physiol* 248: C170-C176

He Z, Yamawaki T, Yang S, Day AL, Simpkins JW, Naritomi H (1999) Experimental model of small deep infarcts involving the hypothalamus in rats. Changes in body temperature and postural reflex. *Stroke* 30: 2743-2751

Heiss WD,Graf R, Weinhard K, Lottgren D, Saito R, Fujita T, Rosner G, Wagner R (1994) Dynamic penumbra demonstrated by sequential multi-tracer PET after middle cerebral artery occlusion in cats. *J Cereb Blood Flow Metab* 14: 892-902

Heiss W-D, Kracht L, Grond M, Rudolf J, Bauer B, Wienhard K, Pawlik G (2000) Early [$^{11}$C]Flumazenil/$H_2O$ positron emission tomography predicts irreversible ischemic cortical damage in stroke patients receiving acute thrombolytic therapy. *Stroke* 31: 366-369

Hertz L (1979) Functional interactions between neurons and astrocytes I. Turnover and metabolism of putative amino acid transmitters. *Prog Neurobiol* 13: 277- 323

Hertz L, Schousboe A (1987) Primary cultures of GABAergic and glutamatergic neurons as model systems to study neurotransmitter functions. I. Differentiated cells. In: *Model systems of development and aging of the nervous system* (Vernadakis A Privat A, Lauder JM, Timiras PS and Giacobini E eds.), pp. 19-31. Martinus Nijhoff Publishing, Boston

Hertz L, Peng L, Westergaard N, Yudkoff M, Schousboe A (1992) Neuronal-astrocytic interactions in metabolism of transmitter amino acids of the glutamate family. In: *Drug Research Related to Neuroactive Amino Acids*, Alfred Benzon Symposium 32 (Schousboe A, Diemer NH and Kofod H, eds.) pp. 30-48. Munksgaard, Copenhagen

Hertz L, Dringen R, Schousboe A, Robinson SR (1999) Astrocytes: glutamate producers for neurons. *J Neurosci Res* 57: 417-428

Hoehn-Berlage M (1995) Diffusion-weighted NMR imaging: application to experimental focal cerebral ischemia. *NMR Biomed* 8: 345-358

Hoffman WE, Edelman G, Kochs E, Werner C, Segil L, Albrecht RF (1991) Cerebral autoregulation in awake versus isoflurane-anesthetized rats. *Anesth Analg* 73: 753- 757

Hogstad S, Svenneby G, Torgner IAa, Kvamme E, Hertz L, Schousboe A (1988) Glutaminase in neurons and astrocyte cultured from mouse brain: Kinetic properties and effects of phosphate, glutamate and ammonia. *Neurochem Res* 13: 383-388

Hollmann M, Heinemann S (1994) Cloned glutamate receptors. *Annu Rev Neurosci* 17: 31-108

Holz RW, Fisher SK (1999) Synaptic transmission and cellular signaling: An overview. In: *Basic Neurochemistry*, Sixth edition (Siegel GJ, Agranoff BW, Albers RW, Fisher SK, Uhler MD, eds), pp. 191-212. Lippicot-Raven Publisher, New York

Horn J, Limburg M (2001) Calcium antagonists for acute ischemic stroke. Cochrane Database of Systematic Reviews. Issue 1

Hossmann KA (1994) Viability thresholds and the penumbra of focal ischemia. *Ann Neurol* 362: 557-565

Hsu CC, Thomas C, Chen W, Davis KM, Foos T, Chen JL, Wu E, Floor E, Schloss JV, Wu JY (1999) Role of synaptic vesicle proton gradient and protein phosphorylation in ATP-mediated activation of membrane-associated brain glutamate decarboxylase. *J Biol Chem* 274: 24366-24371

Hume RI, Dingledine R, Heinemann SF (1991) Identification of a site in glutamate receptor subunits that controls calcium permeability. *Science* 253: 1028-1032

Janzer RC, Raff MC (1987) Astrocytes induce blood-brain barrier properties in endothelial cells. *Nature* 325: 253-256

Jones TH, Morawetz RB, Crowell RM, Marcoux FW, FitzGibbon SJ, DeGirolami U, Ojemann RG (1981) Thresholds of focal cerebral ischemia in awake monkeys. *J Neurosurg* 54: 773-782

Kapus G, Szekely JI, Durand J, Ruiz A, Tarnawa I (2000) AMPA receptor antagonists, GYKI 52466 and NBQX, do not block the induction of long-term potentiation at therapeutically relevant concentrations. *Brain Res Bull* 56: 511-517

Katz J, Rognstad R (1976) Futile cycles in the metabolism of glucose. *Curr Topics Cell Regulation* 10: 237- 289

Kaufman DL, Houser CR, Tobin AJ (1991) Two forms of the gamma-aminobutyric acid synthetic enzyme glutamate decarboxylase have distinct intraneuronal distribution and cofactor interactions. *J Neurochem* 56: 720-723

Kauppinen RA, McMahon HT, Nicholls DG (1988) $Ca^{2+}$-dependent and $Ca^{2+}$-independent glutamate release, energy status and cytosolic free $Ca^{2+}$

concentration in isolated nerve terminals following metabolic inhibition: possible relevance to hypoglycaemia and anoxia. *Neurosci* 27: 175-182

Kawamura S, Li YP, Shirasawa M, Yasui N, Fukasawa H (1994) Reversible middle cerebral artery occlusion in rats using an intraluminal thread technique. *Surg Neurol* 41: 368-373

Kawasaki-Yatsugi S, Yatsugi S, Takahashi M, Toya T, Ichiki C, Shimizu-Sasamata M, Yamaguchi T, Minematsu K (1998) A novel AMPA receptor antagonist, YM872, reduces infarct size after middle cerebral artery occlusion in rats. *Brain Res* 793: 39-46

Kimmelberg HK, Goderie S, Higman S, Pang S, Waniewski RA (1990) Swelling-induced release of glutamate, aspartate and taurine from astrocyte cultures. *J Neurosci* 10: 1583-1591

Kirkendol PL, Devia JC, Bower JD, Holbert RD (1977) A comparison of the cardiovascular effects of sodium acetate, sodium bicarbonate and other potential sources of fixed base in hemodialysate solutions. *Trans Am Soc Atrif Intern Organs* 23: 399-404

Kitagawa H, Hayashi T, Mitsumoto Y, Koga N, Itoyama Y, Abe K (1998) Reduction of ischemic brain injury by topical application of glial cell line-derived neurotrophic factor after permanent middle cerebral artery occlusion in rats. *Stroke* 29: 1417-1422

Klatzo I (1967) Neuropathological aspects of brain edema. *J Neuropathol Exp Neurol* 26: 1-14

Knight RA, Dereski MO, Helpern JA, Ordidge RJ, Chopp M, (1994) Magnetic resonance imaging assessment of evolving focal cerebral ischemia. Comparison with histopathology in rats. *Stroke* 25: 1252-1262

Kobayashi T, Mori Y (1998) $Ca^{2+}$-channel antagonists and neuroprotection from cerebral ischemia. *Eur J Pharmacol* 363: 1-15

Kohno K, Hoehn-Berlage M, Mies G, Back T, Hossmann K-A (1995) Relationship between diffusion-weighted MR images, cerebral blood flow, and energy state in experimental brain infarction. *Mag Res Imag* 13:73-80

Koizumi J, Yoshida Y, Nakazawa T, Ooneda G (1986) Experimental studies of ischemic brain edema. I. A new experimental model of cerebral embolism in rats in which recirculation can be introduced in the ischemic area. *Jpn J Stroke* 8: 1-8

Kristián T, Siesjö BK (1998) Calcium in ischemic cell death. *Stroke* 29: 705-718

Künneck B, Ceredan S, Seelig J (1993) Cerebral metabolism of [1,2-$^{13}C_2$]glucose and [U-$^{13}C_4$]3-hydroxybutyrate in rat brain as detected by $^{13}C$ NMR spectroscopy. *NMR in Biomed* 6: 264-277

Kvamme E, Roberg B, Torgner IA (2000) Phosphate-activated glutaminase and mitochondrial glutamine transport in the brain. *Neurochem Res* 25: 1497-1519

Laake JH, Slyngstad TA, Haug FM, Ottersen OP (1995) Glutamine from glial cells is essential for the maintenance of the nerve terminal pool of glutamate: Immunogold evidence from hippocampal slice cultures. *J Neurochem* 65: 871-881

Laake JH, Takumi Y, Eidet J, Torgner IA, Roberg B, Kvamme E, Ottersen OP (1999) Postembedding immunogold labelling reveals subcellular localization and

pathway-specific enrichment of phosphate activated glutaminase in rat cerebellum. *Neurosci* 88: 1137-1151

Lajtha A, Berl S, Waelsch H (1959) Amino acid and protein metabolism of the brain-IV. The metabolism of glutamic acid. *J Neurochem* 3:322-332

Lansberg MG, Thijs VN, O'Brien MW, Ali JO, de Crespigny AJ, Tong DC, Moseley ME, Albers GW (2001) Evolution of apparent diffusion coefficient, diffusion-weighted, and T2-weighted signal intensity of acute stroke. *AJNR* 22: 637-644

Lapidot A, Gopher A (1994) Cerebral metabolic compartmentation. Estimation of glucose flux via pyruvate carboxylase/pyruvate dehydrogenase by $^{13}C$ NMR isotopomere analysis of D-[U-$^{13}C$]glucose metabolites. *J Biol Chem* 269: 27198-27208

Lee J-M, Zipfel GJ, Choi DW (1999) The changing landscape of ischeamic brain injury mechanisms. *Nature* 399: A7-A14

Lee W-NP, Edmond J, Bassilian S, Morrow JW (1996) Mass isotopomer study of glutamine oxidation and synthesis in primary culture of astrocytes. *Dev Neurosci* 18: 469-477

Lees KR (1999) Cerestate and other NMDA antagonists in ischemic stroke. *Neurol* 49 (5 Suppl 4):S66-69

Lenz C, Rebel A, van Ackern K, Kuschinsky W, Waschke KF (1998) Local cerebral blood flow, local cerebral glucose utilization, and flow-metabolism coupling during sevoflurane versus isoflurane anesthesia in rats. *Anesthesiology* 89: 1480-1488

Li F, Han S, Tatlisumak T, Carano RAD, Irie K, Sotak CH, Fisher M (1998) A new method to improve in-bore middle cerebral artery occlusion in rats: demonstrated by diffusion- and perfusion-weighted imaging. *Stroke* 29: 1715-1720

Li F, Omae T, Fisher M (1999) Spontaneous hyperthermia and its mechanism in the intraluminal suture middle cerebral artery occlusion model of rats. *Stroke* 30: 2464-2471

Li F, Liu K-F, Garcia JH, Silva MD, Omae T, Sotak CH, Fenstermacher JD, Fisher M (2000) Transient and permanent resolution of ischemic lesions on diffusion-weighted imaging after brief periods of focal ischemia in rats. Correlations with histopathology. *Stroke* 31: 946-954

Liesi P, Risteli L (1989) Glial cells of mammalian brain produce a variant form of laminin. *Exp Neurol* 105: 86-92

Lin L-HF, Doherty DH, Lile JD, Bektesh S, Collins F (1993) GDNF: a glial cell line-derived neurotrophic factor for midbrain dopaminergic neurons. *Science* 260: 1130-1132

Linden JM (1999) Purinergic systems. In: *Basic Neurochemistry*, Sixth edition (Siegel GJ, Agranoff BW, Albers RW, Fisher SK, Uhler MD, eds), pp. 347-362. Lippicot-Raven Publisher, New York

Løberg EM, Hassel B, Fonnum F, Torvik A (1994) Early entry of plasma proteins into damaged neurons in brain infarcts. *APMIS* 102: 771-776

Longa EZ, Weinstein PR, Cummins R (1989) Reversible middle cerebral artery occlusion without craniectomy in rats. *Stroke* 20: 84- 91

Louw DF, Masada T, Sutherland GR (1998) Ischemic neuronal injury is ameliorated by astrocyte activation. *Can J Neurol Sci* 25: 102-107

Lund-Andersen H (1979) Transport of glucose from blood to brain. *Physiol Rev* 59: 305-352

Magistretti PJ, Pellerin L, Rothman DL, Shulman RG (1999a) Energy on demand. *Science* 283: 496-497

Magistretti PJ (1999b) Brain energy metabolism. In: *Fundamental Neuroscience* (Zigmond MJ, Bloom FE, Landis SC, Roberts JL, Squire LR, eds.), pp. 389-413. Academic Press, San Diego

Maher F, Vannucci SJ, Simpson IA (1994) Glucose transporter proteins in the brain. *FASEB J* 8: 1003-1011

Maiese K (1998) From the bench to the bedside: the molecular management of cerebral ischemia. *Clin Neuropharmacol* 21:1-17

Mancuso A, Karibe H, Rooney WD, Zarow GJ, Graham SH (1995) Correlation of early reduction in the apparent diffusion coefficient of water with blood flow reduction during middle cerebral artery occlusion in rats. *Magn Reson Med* 34: 368-377

Martin DL, Rimvall K (1993) Regulation of gamma-butyric acid synthesis in the brain. *J Neurochem* 60: 395-407

Matsuoka Y, Hossmann K-A (1982a) Brain tissue osmolality after middle cerebral artery occlusion in cats. *Exp Neurol* 77: 599-611

Matsuoka Y, Hossmann K-A (1982b) Cortical impedance and extracellular volume changes following middle cerebral artery occlusion in cats. *J Cereb Blood Flow Metab* 2: 466-474

Mattson MP, Culmsee C, Yu ZF (2000) Apoptotic and antiapoptotic mechanisms in stroke. *Cell Tissue Res* 301: 173-187

McDonald JW, Bhattacharyya T, Sensi SL, Lobner D, Ying HS, Canzoniero LM, Choi DW (1998) Extracellular acidity potentiates AMPA receptor mediated cortical neuronal death. *J Neurosci* 18: 6290-6299

McLean MA, Badar-Goffer RS, Bachelard HS, Morris PG (1993) Simultaneous measurement of neuronal and glial metabolism via $^{13}$C-MRS isotopomer analysis. (Abstr.) New York, 12th meeting of SMRM, p. 511

McKenna MC, Tildon JT, Stevenson JH, Huang X (1996) New insights into the compartmentation of glutamate and glutamine in cultured rat brain astrocytes. *Dev Neurosci* 18: 380-390

Meldrum BS (2000) Glutamate as transmitter in the brain: review of physiology and pathology. *J Nutr* 130 (4S Suppl): 1007S-1015S

Memezawa H, Minamisawa H, Smith M-L, Siesjö BK (1992a) Ischemic penumbra in a model of reversible middle cerebral artery occlusion in the rat. *Exp Brain Res* 89: 67-78

Memezawa H, smith M-L, Siesjö BK (1992b) Penumbra tissue salvage by reperfusion following middle cerebral artery occlusion in rats. *Stroke* 23: 552-559

Mies G, Ishimaru S, Xie Y, Seo K, Hossmann K-A (1991) Ischemic thresholds of cerebral protein synthesis and energy state following middle cerebral artery occlusion of rat. *J Cereb Blodd Flow Metab* 11: 753-761

Minematsu K, Li L, Fisher M, Sotak CH, Davis MA (1992) Diffusion weighted magnetic resonance imaging: rapid and quantitative detection of focal brain ischemia. *Neurology* 42: 235-240

Mintorovitch J, Moseley ME, Chileuitt L, Shimizu H, Cohen Y, Weinstein PR (1991) Comparison of diffusion and $T_2$-weighted MRI for the early detection of cerebral ischemia and reperfusion in rats. *Magn Reson Med* 18:39-50

Mitani A, Andou Y, Metsuda S, Arai T, Sakanaka M, Kataoka K (1994) Origin of ischemia-induced glutamate efflux in the CA 1 field of the gerbil hippocampus: an in vivo brain microdialysis study. *J Neurochem* 63: 2152-2164

Morawetz RB, DeGirolami U, Ojemann RG, Marcoux FW, Crowell RM (1978) Cerebral blood flow determined by hydrogen clearance during middle cerebral artery occlusion in unanesthetized monkeys. *Stroke* 9: 143-149

Morley P, Hogan MJ, Hakim AM (1994) Calcium-mediated mechanisms of ischemic injury and protection. *Brain Pathol* 4: 37-47

Morris PG, Bachelard HS, Cox DWG, Cooper JC (1986) $^{13}C$ nuclear magnetic resonance studies of glucose metabolism in guinea-pig brain slices. *Biochem Soc Trans* 14: 1720-1721

Moseley ME, Cohen Y, Mintorovitch J, Chileuitt I, Shimizu H, Kucharczyk J, Wendland MF, Weinstein PR (1990a) Early detection of regional cerebral ischemia in cats: comparison of diffusion and T2-weighted MRI and spectroscopy. *Magn Reson Med* 14: 330-346

Moseley ME, Kucharczyk J, Mintorovitch J, Cohen Y, Kurhanewicz J, Derugin N, Asgari H, Norman D (1990b) Diffusion-weighted MR imaging of acute stroke: correlation with T2-weighted and magnetic susceptibility-enhanced MR imaging in cats. *Am J Neuroradiol* 11: 423-429

Müller TB, Haraldseth O, Unsgård G (1994) Characterization of microcirculation during ischemia and reperfusion in the penumbra of a rat model of temporary middle cerebral artery occlusion: A laser Doppler flowmerty study. *Int J Microcirc Clin Exp* 14: 289- 295

Müller TB, Haraldseth O, Jones R, Sebastiani G, Godtliebsen F, Lindboe CF, Unsgård G (1995) Combined perfusion and diffusion-weighted magnetic resonance imaging in a rat model of reversible middle cerebral artery occlusion. *Stroke* 26: 451-458

Nawashiro H, Brenner M, Fukui S, Shima K, Hallenbeck JM (2000) High susceptibility to cerebral ischemia in GFAP-null mice *J Cereb Blood Flow Metab* 20: 1040-1044

Nedergaard M, Diemer NH (1987) Focal cerebral ischemia in the rat, with special reference to the influence of plasma glucose concentration. *Acta Neuropathol* 73: 131-137

Nedergaard M, Jakobsen J, Diemer NH (1988) Autoradiographic determination of cerebral glucose content, blood flow, and glucose utilization in focal ischemia in the rat brain: influence of the plasma glucose concentration. *J Cereb Blood Flow Metab* 8: 100-108

Nemoto EM, Hoff JT, Severinghaus JW (1974) Lactate uptake and metabolism by brain during hyperlactemia and hypoglycemia. *Stroke* 5: 81-84

Nicholls DG, Budd SL (1998) Neuronal excitotoxicity: the role of mitochondria. *Biofactors* 8: 287-299

Norenberg MD, Martinez-Hernandez A (1979) Fine structural localization of glutamine synthetase in astrocytes of rat brain. *Brain Res* 161: 303-310

Norris DG, Niendorf, T, Leibfritz D (1994) Healthy and infarcted brain tissues studied at short diffusion times: origin of apparent restriction and the reduction in apparent diffusion coefficient. *NMR Biomed* 7: 304-310

Nowicki J-P, Assumel-Lurdin C, MacKenzie ET (1988) Temporal evolution of regional energy metabolism following focal cerebral ischemia in the rat. J *Cereb Blood Flow Metab* 8: 462-473

Obrenovitch TP (1996) Origins of glutamate release in ischaemia. *Acta Neurochir [Suppl]* 66: 50-55

Ogata T, Nakamura Y, Shibata T, Kataoka K (1992) Release of excitatory amino acid from cultured hippocampal astrocytes induced by a hypoxic-hypoglycemic stimulation. *J Neurochem* 58: 1957-1959

Oldendorf WH (1973) Carrier-mediated blood-brain barrier transport of short-chain monocarboxylic organic acids. John Wiely, New York

Olney JW (1994) Neurotoxicity of NMDA receptor antagonists: an overview. *Psycopharmacol Bull* 30: 533-540

Olsson Y, Crowell RM, Klatzo I (1971) The blood brain barrier to protein tracers in focal cerebral ischemia and infarction caused by occlusion of the middle cerebral artery. *Acta Neuropathol (Berlin)* 18: 89-102

Ottersen OP (1989) Quantitative electron microscopic immunocytochemistry of neuroactive amino acids. *Anat Embryol* 180: 1-15

Ottersen OP, Zhang N, Walberg F (1992) Metabolic compartmentation of glutamate and glutamine: morphological evidence obtained by quantitative immunocytochemistry in rat cerebellum. *Neurosci* 46: 519-534

Ottersen OP, Laake JH, Reichelt W, Haug FM, Torp R (1996) Ischemic disruption of glutamate homeostasis in brain: quantitative immunocytochemical analyses. *J Chem Neuroanat* 12:1-14

Pardridge WM (1983) Brain metabolism: a perspective from the blood-brain barrier. *Physiol Rev* 63: 1481-1535

Pascual JM, Carceller F, Roda JM, Cerdán S (1998) Glutamate, glutamine, and GABA as substrates for the neuronal and glial compartments after focal cerebral ischemia in rats. *Stroke* 29: 1048-1057

Patel MS (1974) The relative significance of $CO_2$-fixing enzymes in the metabolism of rat brain. *J Neurochem* 22: 717-724

Patel PM, Drummond JC, Cole DJ, Goskowicz (1995) Isoflurane reduces ischemia-induced glutamate release in rats subjected to forebrain ischemia. *Anesthesiol* 82: 996-1003

Paulsen RE, Odden E, Fonnum F (1988) Importance of glutamine for γ-aminobutyric acid synthesis in rat neostriatum in vivo. *J Neurochem* 51: 1294-1299

Pellegrini-Giampietro DE, Zukin RS, Bennett MV, Cho S, Pulsinelli WA (1992) Switch in glutamate receptor subunit gene expression in CA1 subfield of hippocampus following global ischemia in rat. *Proc Natl Acad Sci USA* 89: 10499-10503

Pellegrini-Giampietro DE, Gorter JA, Bennet MV, Zukin RS (1997) The GluR2 (GluR-B) hypothesis: $Ca^{2+}$ permeable AMPA receptors in neurological disorders. *Trends Neurosci* 20: 464-470

Pellerin L, Magisteretti PJ (1994) Glutamate uptake into astrocytes stimulates aerobic glycolysis: a mechanism coupling neuronal activity to glucose utilization. *Proc Natl Acad Sci USA* 91: 10625-10629

Peng L, Schousboe A, Hertz L (1991) Utilization of alpha-ketoglutarate as a precursor for transmitter glutamate in cultured cerebellar granule cells. *Neurochem Res* 16: 29-34

Perry TL, Hansen S, Gandham SS (1981) Postmortem changes of amino compounds in human and rat brain. *J Neurochem* 36: 406-412

Phillis JW, Ren J, O'Regan MH (2000) Transporter reversal as a mechanism of glutamate release from the ischemic rat cerebral cortex: studies with DL-threo-beta-benzyloxyaspartate. *Brain Res* 868: 105-112

Pizzi M, Boroni F, Bianchetti KM, Memo M, Spano P (1999) Reversal of glutamate excitotoxicity by activation of PKC-associated metabotropic glutamate receptors in cerebellar granule cells relies on NR2C subunit expression. *Eur J Neurosci* 11: 2489-2496

Pontén U, Ratcheson RA, Salford LG, Siesjö BK (1973) Optimal freezing conditions for cerebral metabolites in rat. *J Neurochem* 21: 1127-1138

Prado R, Ginsberg MD, Dietrich WD, Watson BD, Busto R (1988) Hyperglycemia increases infarct size in collaterally but not end-arterial vascular territories. *J Cereb Blood Flow Metab* 8: 186-192

Preece NE, Cerdan S (1996) Metabolic precursors and compartmentation of cerebral GABA in Vigabatrin-treated rats. *J Neurochem* 67: 1718-1725

Randle PJ, England PJ, Denton RM (1970) Control of the tricarboxylate cycle and its interactions with glycolysis during acetate utilization in the rat heart. *Biochem J* 117: 677-695

Rao VL, Dogan A, Todd KG, Bowen KK, Kim BT, Rothstein JD, Dempsey RJ (2001) Antisense knockdown of the glial glutamate transporter GLT-1, but not the neuronal glutamate transporter EAAC1, exacerbates transient focal cerebral ischemia-induced neuronal damage in rat brain. *J Neurosci* 21: 1876-1883

Raub TJ, Kuentzel S, Sawada GA (1992) Permeability of bovine brain microvessel endothelial cells in vitro: Barrier tightening by a factor released from astroglioma cells. *Exp Cell Res* 199: 330-340

Reier PJ, Stenasaas LJ, Guth L (1983) The astrocytic scar as an impediment to regeneration in the central nervous system. In: *Spinal Cord Regeneration* (Kao CC, Bunge RP, Reier PJ, eds), pp. 163-195. Raven Press, New York

Richter C, Gogvadze V, Laffranchi R, Schlapbach R, Schweizer M, Suter M, Walter P, Yaffee M (1995) Oxidants in mitochondria: from physiology to diseases. *Biochim Biophys Acta* 1271: 67-74

Ridet JL, Malhotra SK, Privat A, Gage FH (1997) Reactive astrocytes: cellular and molecular clues to biological function. *Trends Neurosci* 20: 570-577

Rosenberg PA (1991) Accumulation of extracellular glutamate and neuronal death in astrocyte-poor cortical cultures exposed to glutamine. *Glia* 4: 91-100

Rosenberg PA, Aizenman E (1989) Hundred-fold increase in neuronal vulnerability to glutamate toxicity in astrocyte-poor cultures of rat cerebral cortex. *Neurosci Lett* 103: 162-168

Rossi DJ, Oshima T, Attwell D (2000) Glutamate release in severe brain ischaemia is mainly by reversed uptake. *Nature* 403: 316-321

Rothman DL, Behar KL, Hetherington HP, den Hollander JA, Bendall MR, Petroff CA, Shulman RG (1985) $^{1}$H-observed/$^{13}$C-decouple spectroscopic measurements of lactate and glutamate in the rat brain in vivo. *Proc Natl Acad Sci USA* 82: 1633-1637

Rothman DL, Sibson NR, Hyder F, Shen J, Behar KL, Shulman RG (1999) In vivo nuclear magnetic resonance spectroscopy studies of the relationship between the glutamate-glutamine neurotransmitter cycle and functional neuroenergetics. *Phil Trans R Soc Lond* 354: 1165-1177

Rothman S, Olney J (1986) Glutamate and the pathophysiology of hypoxic-ischemic brain damage. *Ann Neurol* 19: 105-111

Rudolphi KA, Schubert P, Parkinson FE, Fredholm BB (1992) Adenosine and brain ischemia. *Cerebrovasc Brain Metab Rev* 4: 346-369

Sanchez-Pietro J, Gonzalez P (1988) Occurrence of a large $Ca^{2+}$-independent release of glutamate during anoxia in isolated nerve terminals (synaptosomes). *J Neurochem* 50: 1322-1324

Scatton B (1994) Excitatory amino acid receptor antagonists: a novel treatment for ischemic cerebrovascular diseases. *Life Sci* 55: 2115- 2124

Schousboe A (2000) Pharmacological and functional characterization of astrocytic GABA transport: a short review. *Neurochem Res* 25: 1241-1244

Schousboe A, Divac I (1979) Differences in glutamate uptake in astrocytes cultured from different brain regions. *Brain Res* 16: 407-409

Schuier FJ, Hossmann K-A (1980) Experimental brain infarcts in cats. II. Ischemic brain edema. *Stroke* 11: 593-601

Schwab S, Schwarz S, Spranger M, Keller E, Bertram M, Hacke W (1998) Moderate hypothermia in the treatment of patients with severe middle cerebral artery infarction. *Stroke* 29: 2461-2466

Shank RP, Aprison MH (1971) Postmortem changes in the content and specific radioactivity of several amino acids in four areas of the rat brain. *J Neurobiol* 2: 145-151

Shank RP, Bennett GS, Freytag SO, Campell GL (1985) Pyruvate carboxylase: an astrocyte-specific enzyme implicated in the replenishment of amino acid neurotransmitter pools. *Brain Res* 329: 364- 367

Shank RP, Leo GC, Zielke HR (1993) Cerebral metabolic compartmentation as revealed by nuclear magnetic resonance analysis of D-[1-$^{13}$C]glucose metabolism. *J Neurochem* 61: 315-323

Shimada N, Graf R, Rosner G, Wakayama A, George CP, Heiss WD (1989) Ischemic flow threshold for extracellular glutamate increase in cat cortex. *J Cereb Blood Flow Metab* 9: 603-606

Shiraishi K, Sharp FR, Simon RP (1989) Sequential metabolic changes in rat brain following middle cerebral artery occlusion: a 2-deoxyglucose study. *J Cereb Blood Flow Metab* 9: 765-773

Siesjö BK (1992) Pathophysiology and treatment of focal cerebral ischemia. Part II: Mechanisms of damage and treatment. *J Neurosurg* 77: 337-354

Siesjö BK, Bengtsson F (1989) Calcium fluxes, calcium antagonists, and calcium-related pathology in brain ischemia, hypoglycemia, and spreading depression: a unifying hypothesis. *J Cereb Blood Flow Metab* 9: 127-140

Simantov R (1989) Glutamate neurotoxicity in culture depends on the presence of glutamine: implications for the role, of glial cells in normal and pathological brain development. *J Neurochem* 52: 1694-1699

Sloviter RS, Dichter MA, Rachinsky TL, Dean E, Goodman JH, Sollas AL, Martin DL (1996) Basal expression and induction of glutamate decarboxylase and GABA in excitatory granule cells of the rat and monkey hippocampal dentate gyrus. *J Comp Neurol* 373: 593-618

Sokoloff L, Reivich M, Kennedy C, Des Rosiers MH, Patlak CS, Pettigrew KD, Sakurada O, Shinohara M (1977) The [$^{14}$C]deoxyglucose method for the measurement of local cerebral glucose utilization: Theory, procedure, and normal values in the conscious and anesthetized albino rat. *J Neurochem* 28: 897-916

Sonnewald U, Westergaard N, Hassel B, Müller TB, Unsgård G, Fonnum F, Hertz L, Schousboe A, Petersen SB (1993a) NMR spectroscopic studies of $^{13}$C acetate and $^{13}$C glucose metabolism in neocortical astrocytes: evidence for mitochondrial heterogeneity. *Dev Neurosci* 15: 351-358

Sonnewald U, Westergaard N, Petersen SB, Unsgård G, Schousboe A (1993b) Metabolism of [U-$^{13}$C]glutamate in astrocytes studied by $^{13}$C NMR spectroscopy: Incorporation of more label into lactate than into glutamine demonstrates the importance of the TCA cycle. *J Neurochem* 61: 1179-1182

Sonnewald U, Müller TB, Westergaard N, Unsgård G, Petersen SB, Schousboe A (1994a) NMR spectroscopic study of cell cultures of astrocytes and neurons exposed to hypoxia: Compartmentation of astrocyte metabolism. *Neurochem Int* 24: 473-483

Sonnewald U, Müller TB, Westergaard N, Svendsen JS, Unsgård G, Schousboe A (1994b) Neuroanl-glial interactions in glutamate and GABA homeostasis: Effects of hypoxia. In: *Pharmacology of Cerebral Ischemia* (Oberpichler-Schwenk H, ed.), pp 177-190. Wissenschaftliche Verlagsgesellschaft mbH, Stuttgart

Sonnewald U, Westergaard N, Jones P, Taylor A, Bachelard HS (1996a) Metabolism of [U-$^{13}C_5$]glutamine in cultured astrocytes studied by NMR spectroscopy: First evidence of astrocytic pyruvate recycling. *J Neurochem* 67: 2566-2572

Sonnewald U, Therrien G, Butterworth RF (1996b) Portocaval anastomosis results in altered neuro-astrocytic metabolic trafficking of amino acids: Evidence from $^{13}$C NMR studies. *J Neurochem* 67: 1711-1717

Sonnewald U, Hertz L, Schousboe A (1998) Mitochondrial heterogeneity in the brain at the cellular level. *J Cerb Blood Flow Metab* 18: 231-237

Sorensen AG, Buonanno FS, Gonzalez RG, Schwamm LH, Lev MH, Huang-Hellinger FR, Reese TG, Weisskoff RM, Davis TL, Suwanwela N, Can U, Moreira JA, Copen WA, Look RB, Finklestein SP, Rosen BR, Koroshetz WJ (1996) Hyperacute stroke: evaluation with combined multisection diffusion-weighted

and hemodynamically weighted echo-planar MR imaging. *Radiology* 199: 391-401

Swanson RA (1992) Astrocyte glutamate uptake during chemical hypoxia in vitro. *Neurosci Lett* 147: 143-146

Symon L, Pasztor E, Branston NM (1974) The distribution and density of reduced blood flow following acute middle cerebral artery occlusion: an experimental study by the technique of hydrogen clearance in baboons. *Stroke* 5: 355-364

Szatkowski M, Barbour B, Attwell D (1990) Non-vesicular release of glutamate from glial cells by reversed electrogenic glutamate uptake. *Nature* 348: 443-446

Szerb JC, O'Regan PA (1985) Effect of glutamine on glutamate release from hippocampal slices induced by high $K^+$ or by electrical stimulation: interactions with different $Ca^{2+}$ concentrations. *J Neurochem* 44: 1724-1731

Takagi K, Ginsberg MD, Globus MY-T, Dietrich WD, Martinez E, Kraydieh S, Busto R (1993) Changes in amino acid neurotransmitters and cerebral blood flow in the ischemic penumbral region following middle cerebral artery occlusion in the rat: Correlation with histopathology. *J Cereb Blood Flow Metab* 13: 575-585

Tanaka K (2000) Functions of glutamate transporters in the brain. *Neurosci Res* 37: 15-19

Tansey FA, Farooq M, Cammer W (1991) Glutamine synthetase in oligodendrocytes and astrocytes: new biochemical and immunocytochemical evidence. *J Neurochem* 56: 266-272

Taylor A, McLean M, Morris P, Bachelard H (1996) Approaches to studies on neuronal/glial relationships by $^{13}$C-MRS analysis. *Dev Neurosci* 18: 434-442

Thanki CM, Sugden D, Thomas AJ, Bradford HF (1983) In vivo release from cerebral cortex of [$^{14}$C]glutamate synthesized from [$^{14}$C]glutamine. *J Neurochem* 41: 611- 617

Tholey G, Ledig M (1990) Plastisite neuronal et astrocytaire: aspects metaboliques. *Ann Med Intern* 141: 3-18

Thommessen B, Laake K, Bautz-Holter E (1997) Rehabilitering av eldre slag pasienter i en geriatrisk avdeling. Forløp og prognose. *Tidsskr Nor Laegeforen*117: 3834-3837

Torp R, Andiné P, Hagberg H, Karagülle T, Blackstad TW, Ottersen OP (1991) Cellular and subcellular redistribution of glutamate-, glutamine- and taurine-like immunoreactivities during forebrain ischemia: A semiquantitative electron microscopic study in rat hippocampus. *Neurosci* 41: 443-447

Torp R, Arvin B,Le Peillet E, Chapman AG, Ottesen OP, Meldreum BS (1993) Effect of ischemia and reperfusion on the extra- and intracellular distribution of glutamamte, glutamine, aspartayte and GABA in the rat hippocampus, with a note on the effect on sodium blocker BW1003C87. *Exp Brain Res* 96: 365-376

Touzani O, Young AR, Derlon JM, Beaudouin V, Marchal G, Rioux P, Mézenze F, Baron JC, MacKenzie ET (1995) Sequential studies of severely hypometabolic tissue volumes after permanent middle cerebral artery occlusion: a positron emission tomographic investigation in anesthetized in baboons. *Stroke* 26: 2112-2119

Turský T (1970) Inhibition of brain glutamate decarboxylase by adenosine triphosphate. *Eur J Biochem* 12: 544-549

Uchiyama-Tsuyuki Y, Araki H, Otomo S (1994) Changes in the extracellular concentrations of amino acids in the rat striatum during transient focal cerebral ischemia. *J Neurochem* 62: 1074-1078

Van den Berg CJ (1973) A model of compartmentation in the mouse brain based on glucose and acetate metabolism. In: *Metabolic Compartmentation in the Brain* (Balazs R and Cremer JE, eds), pp. 137-166. Maxmillian Press, London

Van den Berg CJ, Ronda G (1976) The incorporation of doubled-labeled acetate into glutamate and related amino acids from adult mouse brains: compartmentation of amino acid metabolism in the brain. *J Neurochem* 27: 1443-1448

Varoqui H, Zhu H, Yao D, Ming H, Erickson JD (2000) Cloning and functional identification of a neuronal glutamine transporter. *J Biol Chem* 275: 4049-4054

Verkhratsky A, Steinhauser C (2000) Ion channels in glial cells. *Brain Res Review* 32: 380-412

Vrba R (1962) Glucose metabolism in rat brain in vivo. *Nature* 195: 663-665

Waagepetersen HS, Sonnewald U, Larsson OM, Schousboe A (1999a) Synthesis of vesicular GABA from glutamine involves TCA cycle metabolism in neocortical neurons. *J Neurosci Res* 57: 342-349

Waagepetersen HS, Bakke IJ, Larsson OM, Sonnewald U, Schousboe A (1999b) Metabolism of lactate in cultured GABAergic neurons studied by $^{13}C$ NMR spectroscopy. *J Cereb Blood Flow Metab* 18: 109-117

Waagepetersen HS, Sonnewald U, Larsson OM, Schousboe A (2000) Compartmentation of the TCA cycle metabolism in cultured neocortical neurons revealed by $^{13}C$ MR spectroscopy. *Neurochem Int* 36: 349-358

Wahl F, Obrenovitch TP, Hardy AM, Plotkine M, Boulu R, Symon L (1994) Extracellular glutamate during focal cerebral ischemia in rats: Time course and calcium dependency. *J Neurochem* 63: 1003-1011

Waltz W (2000) Role of astrocytes in the clearance of excess extracellular potassium. *Neurochem Int* 36: 291-300

Waniewski RA, Martin DL (1998) Preferential utilization of acetate by astrocytes is attributable to transport. *J Neurosci* 18: 5225-5233

Warach S, Chien D, Li W, Ronthal M, Edlman RR (1992) Fast magnetic resonance diffusion-weighted imaging of acute human stroke. *Neurology* 42: 1717-1723

Warach S, Wielopolski P, Edelman RR (1993) Identification and characterization of the ischemic penumbra of acute human stroke using echoplanar diffusion and perfusion imaging (Abstr), New York, 12th meeting of SMRM, p. 263

Ward HK, Thanki CM, Bradford HF (1983) Glutamine and glucose as precursors of transmitter amino acids: ex vivo studies. *J Neurochem* 40: 855- 864

Westbrook C, Kaut C (1993) MRI in practice. Blackwell Science Ltd, Oxford

Westergaard N, Sonnewald U, Schousboe A (1994) Release of α-ketoglutarate, malate and succinate from cultured astrocytes: Possible role in neurotransmitter homeostasis. *Neurosci Lett* 176: 105-109

Westergaard N, Sonnewald U, Schousboe A (1995a) Metabolic trafficking between neurons and astrocytes: the glutamate/glutamine cycle revisited. *Dev Neurosci* 17: 203- 211

Westergaard N, Sonnewald U, Petersen SB, Schousboe A (1995b) Glutamate and glutamine metabolism in cultured GABAergic neurons studied by $^{13}C$ NMR

spectroscopy may indicate compartmentation and mitochondrial heterogeneity. *Neurosci Lett* 185: 24-28

Westergaard N, Drejer J, Schousboe A, Sonnewald U (1996) Evaluation of the importance of transamination versus deamination in astrocytic metabolism of [U-$^{13}$C]glutamate. *Glia* 17: 160-168

Wollmuth LP, Kuner T, Seeberg PH, Sakmann B (1996) Differential contribution of the $NMDA_1$- and $NMDA_2A$-subunits to the selectivity filter of recombinant NMDA receptor channels. *J Physiol (Lond.)* 491: 779-797

Yu ACH, Drejer J, Hertz L, Schousboe A (1983) Pyruvate carboxylase activity in primary cultures of astrocytes and neurons. *J Neurochem* 41: 1484-1487

Yudkoff M (1997) Brain metabolism of branched-chained amino acids. *Glia* 21: 92-98

Yudkoff M, Nissim I, Hummeler K, Medow M, Pleasure D (1986) Utilization of [$^{15}$N]glutamate by cultured astrocytes. *Biochem J* 234: 185- 192

Yudkoff M, Nissim I, Hertz L, Pleasure D, Erecinska M (1992) Nitrogen metabolism: Neuronal-astroglial relationships. *Brain Res* 94: 213-224

Zhao G and Flavin MP (2000) Differential sensitivity of rat hippocampal and cortical astrocytes to oxygen-glucose deprivation injury. *Neurosci Lett* 285: 177-180

Zhao H, Asai S, Kohno T, Ishikawa K (1998) Effects of brain temperature on CBF thresholds for extracellular glutamate release and reuptake in the striatum in a rat model of graded global ischemia. *NeuroReport* 9: 3183-3188

Zhao Q, Memezawa H, Smith ML, Siesjö BK (1994) Hyperthermia complicates middle cerebral artery occlusion induced by an intraluminal filament. *Brain Res* 649: 253-259

Zhao W, Belayev L, Ginsberg MD (1997) Transient middle cerebral artery occlusion by intraluminal suture: II. Neurological deficits, and pixel-based correlation of histopathology with local blood flow and glucose utilization. *J Cereb Blood Flow Metab* 17: 1281-1290

Zipfel GJ, Babcock DJ, Lee JM, Choi DW (2000) Neuronal apoptosis after CNS injury: the roles of glutamate and calcium. *J Neurotrauma* 17: 857-869

Papers I- IV

Are not included due to copyright

# Paper V

# Differences in Neurotransmitter Synthesis and Intermediary Metabolism between Glutamatergic and GABAergic Neurons during 4 Hours of MCAO in the Rat. The Role of Astrocytes in Neuronal Survival.

Asta Håberg [1,2,3], Hong Qu[1,4,6], Oddbjørn Sæther[5], Geirmund Unsgård[3], Olav Haraldseth[2,6], Ursula Sonnewald[1]

1. Department of Clinical Neuroscience, 2. Department of Anesthesia and Medical Imaging, 3. Department of Neurosurgery, 4. Department of Physics, 5. Department of Biophysics, Norwegian University of Science and Technology (NTNU), 7489 Trondheim, 6. MR-Center, SINTEF UNIMED, 7006 Trondheim, Norway.

Address for correspondence and reprint requests:

Ursula Sonnewald, PhD

Department of Neuroscience, Medical Faculty, NTNU,

N-7489 Trondheim, Norway.

Telephone: + 47-73-590492, fax: + 47-73-598655,

e-mail: usula.sonnewald@medisin.ntnu.no

Abbreviations used: DWI, diffusion weighted imaging; GABA, γ-aminobutyric acid; GABA-T, γ-aminobutyric acid transaminase; GS, glutamine synthetase; MCAO, middle cerebral artery occlusion; MRS, magnetic resonance spectroscopy; PAG, phosphate activated glutaminase; PC, pyruvate carboxylase; PDH, pyruvate dehydrogenase; TCA, tricarboxylic acid.

**Abstract**

Astrocytes are intimately involved in both glutamate and GABA synthesis thus ischemia induced disruption of normal neuro-astrocytic interactions may have important implications for neuronal survival. The effects of middle cerebral artery occlusion (MCAO) on neuronal and astrocytic intermediary metabolism were studied in rats 30, 60, 120 and 240 min after MCAO using *in vivo* injection of [1-$^{13}$C]glucose and [1,2-$^{13}$C]acetate combined with *ex vivo* $^{13}$C MR spectroscopy and HPLC analysis of the ischemic core (lateral caudoputamen and lower parietal cortex) and penumbra (upper frontoparietal cortex). In the ischemic core both neuronal and astrocytic metabolism were impaired from 30 min of MCAO. In glutamatergic neurons there was a continuos loss of glutamate which was not replaced as neuronal glucose metabolism and utilization of astrocytic precursors gradually declined. In GABAergic neurons astrocytic precursors were not used in GABA synthesis at any time after MCAO, and neuronal glucose metabolism and GABA-shunt activity declined with time. At 240 min of MCAO no flux through the tricarboxylic acid cycle was found in GABAergic neurons indicating neuronal death. In the penumbra the neurotransmitter pool of glutamate coming from astrocytic glutamine was preserved while neuronal metabolism progressively declined implying that glutamine contributed significantly to glutamate excitotoxicity. In GABAergic neurons astrocytic precursors were used to a limited extent during the initial 120 min, and tricarboxylic acid cycle activity was continued for 240 min. The present study demonstrated the paradoxical role astrocytes play in neuronal survival in ischemia as changes in the use of astrocytic precursors appeared to contribute significantly to neuronal death, although through different mechanisms in glutamatergic and GABAergic neurons.

Key words: MCAO, glutamate, glutamine, GABA, astrocytes, $^{13}$C MRS

Running title: Neuronal and astrocytic metabolism in MCAO

## Introduction

Astrocytes are intimately involved in both glutamate and γ-aminobutyric acid (GABA) synthesis, and changes in trafficking of metabolites between astrocytes and glutamatergic and GABAergic neurons during ischemia *in vivo* may have important implications for neuronal survival. In a previous paper on middle cerebral artery occlusion (MCAO) we showed that astrocytic and neuronal intermediary metabolism as well as trafficking of metabolites between these two cellular compartments can be analyzed in great detail by combining *in vivo* injection of $^{13}C$ labeled acetate and glucose with *ex vivo* $^{13}C$ magnetic resonance spectroscopy (MRS) of deproteinized brain extracts (Håberg et al., 1998a). In the present work this method was used to identify changes in glutamate and GABA synthesis, and also in astrocytic metabolism during the first four hours of MCAO. In cerebral ischemia glutamate excitotoxicity is considered an important mediator of neuronal death (Choi, 1992; Meldrum, 2000). GABA, on the other hand, is recognized as an endogenous neuroprotectant in the mature brain (Schwartz-Bloom and Sah, 2001).

The lateral caudoputamen and lower parietal cortex, and the upper frontoparietal cortex ipsilateral to the MCAO were analyzed separately to gain insight into regionally specific alterations in the metabolic activity of glutamatergic and GABAergic neurons as well as astrocytes. In MCAO induced with the intraluminal filament technique, the ipsilateral lateral caudoputamen and lower parietal cortex are rendered severely ischemic, whereas the upper frontoparietal cortex represents moderately ischemic tissue. The former is often referred to as the ischemic core, and thelatter as the penumbra (Memezawa et al., 1992a; Back, 1998). Inherent to the definition of the penumbra is the possibility of reversing the neuronal failure, but with time the penumbra is incorporated into the ischemic core (Back, 1998). In the present study neuronal and astrocytic tricarboxylic acid (TCA) cycle activity and utilization of astrocytic intermediates for neurotransmitter synthesis in the two regions were followed

closely during the initial 240 min of MCAO in order to identify changes influencing neuronal survival.

## Materials and Method

*Animal experiments*

All animal procedures were conducted following an institutionally approved protocol in accordance with the guidelines set by the Norwegian Committee for Animal Research.

Male Wistar rats (Møllegaard Breeding Center, Copenhagen, Denmark), weighing 320-340 g, were fasted over night. Anesthesia was induced with 3.5% isoflurane in 70/30% $N_2/O_2$. During surgery the animals were spontaneously breathing 2% isoflurane in 70/30% $N_2/O_2$ delivered through a face mask. Body temperature was maintained using a feedback-controlled heating blanket connected to a rectal temperature probe. A catheter was introduced into the right femoral vein, externalized at the tail radix and taped in place. MCAO was induced with the intraluminal filament technique (Longa et al., 1989; Memezawa et al., 1992a). All incisions were sprayed with lidocaine (10 mg/doses) before closure. The rats subjected to MCAO were assigned to four different groups with MCAO lasting 30 (n=7), 60 (n=7), 120 (n=7) or 240 min (n=7). Ten rats were sham operated and allowed to recover for either 30 (n=3) or 240 min (n=7). Isoflurane was turned off at time of MCAO except in rats assigned to MCAO for 120 and 240 min which underwent diffusion weighted MR imaging (DWI) directly after surgery. DWI was performed 18 min after MCAO on a 2.35 T Bruker Biospec (Bruker AG, Fällanden, Switzerland) with a single b value of 1468 $mm^2/s$, TE/TR 32/1500 and NEX two in eighth transaxial slices with slice thickness 1.5 mm covering the entire hemisphere. Isoflurane was maintained at 2% during MR imaging. Rats assigned to either 30 or 60 min of MCAO did not undergo DWI in order to avoid unwanted effects of anesthesia on the cerebral metabolism. The rats were returned to individual cages and allowed to recover directly after surgery or MR imaging. An intravenous injection (1 mL/100g rat) of 0.3 mmol/L [1-$^{13}$C]

glucose and [1,2-$^{13}$C]acetate (Cambridge Isotopes Laboratories, Woburn, MA, USA) in sterile water was given over 2 min starting 15 min before decapitation. The rats were decapitated into liquid $N_2$ 30, 60, 120 or 240 min after MCAO or sham operation. Blood was collected from the severed neck vessels of rats subjected to 240 min of MCAO. From the frozen brains a 5 mm coronal slice extending from chiasma opticum and caudally was cut using a brain matrix (RBM-40000, Activational Systems, Warren, MI, USA), and the right lateral caudoputamen and lower parietal cortex, and upper frontoparietal cortex were sampled. The brain and plasma samples were extracted as described previously (Håberg et al., 1998a).

*$^{13}$C MRS*

Proton decoupled 125.5 MHz $^{13}$C MR spectra were obtained on a Bruker DRX-500 spectrometer (Bruker AG, Fällanden, Switzerland) using a 35° pulse angel, 25 kHz spectral width and 64 K data points. The acquisition time was 1.3 s per scan, plus 2.5 s for relaxation delay. The number of scans was typically 8 000 for brain samples. To avoid nuclear Overhauser effects, some spectra were broadband decoupled during acquisition only. The respective correction factors were then applied to the spectra obtained.

*$^{1}$H MRS*

500 MHz $^{1}$H MR spectra of the plasma extracts were obtained on a Bruker DRX-500 spectrometer using a 90° pulse angle, 7.5 kHz spectral width and 16 K data points. The acquisition time was 1.1 s per scan and an additional 15.0 s relaxation delay was used. The number of scans was typically 200.

*HPLC analysis*

After $^{13}$C MRS total amino acid concentrations were determined with HPLC (Specta System Gradient Pump, Freemont, CA, USA), and fluorescence detection (Shimadzu RF 530, Tokyo, Japan) after derivatization with σ-phthaldialdehyde (Sigma Chemical Co., St. Louise, MO, USA) using L-amino-butyric acid as an internal standard.

*Analysis of $^{13}C$ and $^{1}H$ MR spectra and rationale behind data interpretation*

Relevant peaks in the $^{13}C$ and $^{1}H$ MR spectra were identified, and the total amount of $^{13}C$ or $^{1}H$ in the resonance of a particular metabolite was quantified from the integral of the peak area, using ethyleneglycol as an internal standard. The total amount of $^{13}C$ includes the naturally abundant $^{13}C$ (1.1% of all carbon atoms). Data anlysis is described in detail in Håberg et al. (1998a).

The neuronal and the astrocytic compartment can be analyzed simultaneously by concomitant administration of [1-$^{13}$C]glucose and [1,2-$^{13}$C]acetate (Badar-Goffer et al., 1990; McLean et al, 1993; Sonnewald et al., 1996; Håberg et al., 1998a) due to uneven distribution of enzymes and transporter proteins between neurons and astrocytes.

The astrocytic compartment is recognized by its ability to use acetate as a substrate for the TCA cycle (Van den Berg, 1973) owing to the presence of a specific acetate uptake mechanism (Waniewski and Martin, 1998). In the astroctes [1,2-$^{13}$C]acetate is metabolized by acetyl CoA synthetase (EC 6.2.1.1) to acetyl CoA which enters the TCA cycle and finally gives rise to [4,5-$^{13}$C]glutamate. [4,5-$^{13}$C]Glutamate is rapidly converted to [4,5-$^{13}$C]glutamine by the glia specific enzyme glutamine synthetase (GS, EC 6.3.1.2; Norenberg and Martinez-Hernandez, 1979). Glutamate is present only in low concentrations in astrocytes (Ottersen, 1989). [4,5-$^{13}$C]Glutamine is released from astrocytes and taken up by high affinity glutamine transporter present on neurons (Varoqui et al., 2000). In the neurons glutamate is regenerated from glutamine by phosphate activated glutaminase (PAG, EC 3.4.1.2; Kvamme et al., 2000), which converts [4,5-$^{13}$C]glutamine to [4,5-$^{13}$C]glutamate. In GABAergic neurons GABA is synthesized from glutamate by glutamate decarboxylase (GAD; EC 4.1.1.15), and direct conversion of [4,5-$^{13}$C]glutamate results in [1,2-$^{13}$C]GABA. GABA synthesis only takes place in neurons (Sze, 1979; Sloviter et al., 1996). [4,5-$^{13}$C]glutamate/glutamin and [1,2-

$^{13}$C]GABA can be reintroduced into the TCA cycle. In the secomd turn of the TCA cycle, label originally in [4,5-$^{13}$C]glutamate/glutamine will be equally distributed into [1,2-$^{13}$C]- and [3-$^{13}$C]glutamate/glutamine due to the symmetrical succinate step. Likewise, label in [1,2-$^{13}$C] GABA is distributed equally into [3-$^{13}$C]- and [4-$^{13}$C]GABA in the second turn.

Astrocytes can also metabolize glucose, but to a lesser extent than neurons. However, in these cells glucose can enter the TCA cycle via the astrocyte specific anaplerotic enzyme pyruvate carboxylase (PC, EC 6.4.1.1; Yu et al., 1983) which is the brain's principal anaplerotic enzyme (Patel, 1974). In astrocytes, [1-$^{13}$C]glucose metabolized via PC activity gives rise to [2-$^{13}$C]glutamine formation. In the neurons [2-$^{13}$C]glutamine is converted to [2-$^{13}$C]glutamate and in GABAergic neurons to [4-$^{13}$C]GABA.

Neurons metabolize primarily glucose (Van den Berg, 1973; Künnecke et al., 1993). [1-$^{13}$C]Glucose enters the neuronal TCA cycle as acetyl CoA solely via pyruvate dehydrogenase (PDH; EC 1.2.4.1), and finally results in [4-$^{13}$C]glutamate formation. However, glutamate *de novo* synthesis is considered not to take place in neurons, but in astrocytes (Hertz et al., 1999). The majority of glutamate is found in glutamatergic neurons (Ottersen, 1989). Synaptically released glutamate is predominantly taken up by high affinity glutamate transporters located on astrocytes (Erecinska, 1987; Tanaka, 2000). In the astrocyte [4-$^{13}$C]glutamate is either converted directly to [4-$^{13}$C]glutamine, or reintroduced into the TCA cycle (Farinelli and Nicklas, 1992). The exchange of glutamate and glutamine between astrocytes and neurons is termed the glutamate-glutamine cycle (Westergaard et al., 1995; Daikhin and Yudkoff, 2000). After one turn in the astrocytic TCA cycle label from [4-$^{13}$C]glutamate will be recovered in [3-$^{13}$C]- and [2-$^{13}$C]glutamine. In GABAergic neurons [4-$^{13}$C]glutamate is rapidly converted to [2-$^{13}$C]GABA, and very little glutamate is present in these neurons (Ottersen, 1989). After

one turn in the TCA cycle label originally in [2-$^{13}$C]GABA will be distributed equally into [3-$^{13}$C]- and [4-$^{13}$C]GABA.

Neurons depend on transfer of metabolites from astrocytes because of their inability of glutamate *de novo* synthesis and lack of anaplerotic activity combined with the continuous drain of metabolic intermediates from the neuronal TCA cycle caused by neurotransmitter production and release (Hertz, 1979; Kaufmann and Driscoll, 1993; Hertz et al., 1999). The contribution from astrocytic precursors to neuronal glutamate and GABA formation can be derived from the PC versus PDH activity ratio, which is an estimate of the anaplerotic (astrocytic) compared to the oxidative (neuronal) pathway in glutamate, glutamine and GABA formation (Taylor et al., 1996). Furthermore, the acetate versus glucose utilization ratio gives an approximation for the relative contribution from precursors for the astrocytic TCA cycle compared to precursors for the neuronal TCA in glutamate, glutamine and GABA formation (Taylor et al., 1996).

All values are mean ± SD. Statistical comparisons between the groups subjected to MCAO of varying duration and the sham operated rats recovering for 240 min before decapitation were performed with ANOVA followed by LSD post hoc test for multiple comparisons. Unpaired two-way Student's T-test was used to compare the sham operated rats recovering for 30 and 240 min after termination of anesthesia. $p<0.05$ was considered significant.

## Results

### Diffusion weighted MR imaging

The total volume of ischemic tissue 18 min after MCAO as estimated by DWI was 125.5 ± 52.15 mm$^3$ (n=14). The volume of ischemia for each separate slice from caudal to rostral was 2.2 ± 4.8 mm$^3$, 18.9 ± 12.1 mm$^3$, 31.1 ± 16.2 mm$^3$, 38.5 ± 10.5 mm$^3$, 22.2 ± 10.9 mm$^3$, 8.1 ± 10.0 mm$^3$, 8.3 ± 2.1 mm$^3$ and 1.3 ± 4.2 mm$^3$. The 5 mm slice cut after decapitation to sample

brain tissue for further analysis with $^{13}C$ MR spectroscopy was aimed to be located between slice three and five in which the largest areas of ischemic tissue were found.

**Analysis of plasma extracts**

In rats subjected to 240 min of MCAO the total glucose concentration in plasma was 16.1 ± 1.1 mM estimated from the $^{1}H$ MR spectra, and only glucose enriched in the C-1 position was detected in significant amounts. The concentration of [1,2-$^{13}C$]acetate was 1.7 ± 0.8 mM. The total amount of lactate was 2.1 ± 0.5 mM and hydroxybutyrate 1.2 ± 0.4 mM. There was no significant $^{13}C$ enrichment in lactate or hydroxybutyrate. The observed amino acid labeling thus originated from cerebral [1-$^{13}C$]glucose and [1,2-$^{13}C$]acetate metabolism. Furthermore, neither the duration of fasting nor the stress of cerebral ischemia influenced the plasma composition as similar amounts of $^{13}C$ labeled substrates were present in plasma at 90 min of MCAO (Håberg et al., 1998a).

**Effects of MCAO on total amino acid content**

*Lateral caudoputamen and lower parietal cortex.* In this region rendered severely ischemic the total glutamate content was significantly decreased already 30 min after MCAO, and continued to decline for the next 240 min (Fig.1A). The glutamine content was at control levels until 240 min when it was significantly decreased only compared to 60 min of MCAO (Fig.1A). The total GABA content was more than doubled at 240 min of MCAO (Fig.1C). The alanine levels started to rise markedly from 60 min of MCAO, and at 240 min it had doubled (Fig.1E). The total amount of aspartate on the other hand, fell from 60 min of MCAO, and was about half the amount found in sham operated rats at 240 min of MCAO (Fig.1E).

*Upper frontoparietal cortex.* In the region subjected to moderate ischemia glutamate was at control levels during the 240 min of MCAO (Fig.1B), but the glutamine content increased significantly from 60 min of MCAO and was nearly doubled at 240 min (Fig.1B). Also the

GABA content was significantly increased from 60 min of MCAO and onward (Fig.1D). The alanine levels were not markedly elevated before 120 min (Fig.1F). The aspartate concentration was at control levels during 240 min of MCAO (Fig.1F).

**$^{13}$C MRS of brain extracts**

**Effects of MCAO on cerebral metabolism**

*[1-$^{13}$C]GLUCOSE AND [1,2-$^{13}$C]ACETATE*

*Lateral caudoputamen and lower parietal cortex.* The [1-$^{13}$C]glucose content was significantly increased, to a similar level, at all time points following MCAO (Fig.2A). Unmetabolized [1,2-$^{13}$C]acetate was present at all times after MCAO (Fig.2A).

*Frontoparietal cortex.* The [1-$^{13}$C]glucose content increased steadily and significantly from 60 to 240 min of MCAO (Fig.2B). [1,2-$^{13}$C]Acetate was present at 30 min of MCAO, but not at 60 min, then again at 120 min. At 240 min the [1,2-$^{13}$C]acetate content was significantly elevated compared to all previous time points (Fig.2B).

*GLUTAMATE AND GLUTAMINE*

*Lateral caudoputamen and lower parietal cortex.* The total amount of $^{13}$C in [4-$^{13}$C]glutamate and [4-$^{13}$C]glutamine fell rapidly during the first 60 min of MCAO, then leveled out before being further reduced 240 min after MCAO (Fig.3A). The fall was most notable in [4-$^{13}$C]glutamate. The total amount of label in [4,5-$^{13}$C]glutamate was also significantly reduced from 30 min of MCAO (Fig.3C), still the use of acetate compared to glucose as precursor for glutamate was markedly increased throughout the 240 min of MCAO (Tbl.1). In glutamine the total amount of label in [4,5-$^{13}$C]glutamine was slightly reduced during the initial 120 min, then declined steeply at 240 min of MCAO (Fig.3C). The acetate/glucose utilization ratio was significantly elevated for 120 min of MCAO, but was returned to control levels at 240 min (Tbl.1). In [3-$^{13}$C]glutamate the total amount of $^{13}$C fell markedly and was in the same range

as the total amount of label in [3-$^{13}$C]glutamine from 60 min of MCAO (Fig. 3E). PC activity in glutamate was present at all times after MCAO, but from 120 min of MCAO it was significantly reduced (Tbl.1). In glutamine the PC/PDH activity ratio was markedly increased at 60 min of MCAO, then at 240 min no PC activity was detectable (Tbl.1).

*Upper frontoparietal cortex.* The total amount of label in [4-$^{13}$C]glutamate was significantly reduced to about the same level the initial 120 min of MCAO, and then declined further at 240 min of MCAO (Fig.3B). In [4-$^{13}$C]glutamine the total amount of $^{13}$C was markedly reduced to the same extent at all times after MCAO (Fig. 3B). In [4,5-$^{13}$C]glutamate the total amount of label was reduced to the same level from 30 to 240 min of MCAO (Fig.3D). However, from 60 min of MCAO acetate became increasingly important as precursor in glutamate formation indicated by the significantly elevated acetate/glucose utilization ratio in glutamate which was almost doubled at 240 min (Tbl.1). There was no decline in the total amount of $^{13}$C in [4,5-$^{13}$C]glutamine for 240 min of MCAO (Fig.3D), and the acetate/glucose utilization ratio was elevated from 30 min of MCAO and continued to increase with time (Tbl.1). The total amount of $^{13}$C in [3-$^{13}$C]glutamate declined rapidly and was in the same range as the total amount of $^{13}$C in [3-$^{13}$C]glutamine from 60 min of MCAO (Fig. 3F). In glutamate the PC/PDH activity ratio was significantly lower from 120 min of MCAO, whereas in glutamine the PC/PDH activity was markedly lowered first at 60 min and then at 240 min of MCAO (Tbl.1).

*GABA*

*Lateral caudoputamen and lower parietal cortex.* The total amount of label in [2-$^{13}$C]GABA was significantly reduced at all times after MCAO (Fig.3G). In [3-$^{13}$C]GABA the total amount of $^{13}$C fell significantly after MCAO, but between 120 and 240 min of MCAO the amount of label in [3-$^{13}$C]- and [4-$^{13}$C]GABA (data not shown) increased markedly (Fig. 3G). At 240 min of MCAO the total amount of $^{13}$C was similar in [2-$^{13}$C]-, [3-$^{13}$C]- and [4-

$^{13}$C]GABA (Fig.3G). This implied cessation of GABAergic TCA cycle activity, as the amount of label in [2-$^{13}$C]GABA must exceed the amount of label found in the subsequent turns using the present infusion scheme. The stop in GABAergic TCA cycle activity was verified by the lack of incorporation of $^{13}$C above the natural abundance level of 1.1% in the GABA isotopomers at 240 min of MCAO. [1,2-$^{13}$C]GABA was not detected at any time after MCAO, indicating that there was no direct utilization of [4,5-$^{13}$C]glutamine in GABA synthesis after MCAO (Fig.3G). Furthermore, there was no detectable PC activity in GABA (Tbl.1).

*Upper frontoparietal cortex*. The total amount of label in [2-$^{13}$C]GABA fell rapidly during the initial 60 min of MCAO and then leveled out during the remainder of the experimental period (Fig.3H). Also the total amount of label in [3-$^{13}$C]- and [4-$^{13}$C]GABA (data nor shown) was significantly decreased at all times after MCAO, but not as markedly as for [2-$^{13}$C]GABA (Fig.3H). [1,2-$^{13}$C]GABA was not detected at any time after MCAO, but PC activity was present from 30 to 120 min of MCAO (Tbl.1).

*ASPARTATE AND ALANINE*

*Lateral caudoputamen and lower parietal cortex*. The total amount of $^{13}$C in [3-$^{13}$C]aspartate was about halved at 30 min of MCAO and continued to decline for 240 min (Fig.3I). The total amount of $^{13}$C in [3-$^{13}$C]alanine, on the other hand, was significantly increased at 60 and 120 min of MCAO, but at 240 min it was down to a level similar to that in sham operated (Fig.3I).

*Upper frontoparietal cortex*. The total amount of amount of $^{13}$C in [3-$^{13}$C]aspartate was significantly reduced to the same level at 30 to 120 min of MCAO, then there was a further marked reduction at 240 min of MCAO (Fig.3J). In [3-$^{13}$C]alanine the total amount of label increased steadily and significantly throughout 240 min of MCAO (Fig.3J).

**Effects of isoflurane on cerebral metabolism**

*Lateral caudoputamen and lower parietal cortex*. In sham operated rats recovering for 30 min after termination of anesthesia the total amount of label in [3-$^{13}$C]aspartate, [2-$^{13}$C]GABA, [4-$^{13}$C]glutamate and [4-$^{13}$C]glutamine was significantly lower compared to in sham operated rats recovering for 240 min (Tbl.2). Moreover, [1,2-$^{13}$C]acetate (4.1 ± 1.7 $10^{-8}$ mol/g) was detected in all samples from the 30 min sham group, but was not found in the 240 min group.

*Frontoparietal cortex*. In the sham operated group recovering for 30 min after anesthesia, the total amount of label was significantly decreased in [2-$^{13}$C]GABA and [4-$^{13}$C]glutamate compared to the 240 min sham group (Tbl.2). [1,2-$^{13}$C]Acetate (4.5 ± 1.7 $10^{-8}$ mol/g) was present in the former, but not in the latter sham group.

These results clearly show that isoflurane exerted prolonged effects on neuronal and to some extent also astrocytic metabolism. Thirty min after termination of isoflurane administration, the anesthetic agent still affected incorporation of label from [1-$^{13}$C]glucose into some amino acids via PDH. Previously reduced incorporation of label into amino acids from glucose, but not acetate has been shown during pentobarbital anesthesia (Cremer and Lucas, 1971; Shank et al., 1993). The reduction in glucose metabolism was more prominent in the lateral caudoputamen and the lower parietal cortex than in the upper frontoparietal cortex, agreeing with isoflurane affecting subcortical structures more than cortical structures (Hansen et al., 1988; Hoffman et al., 1991). Furthermore, the marked reduction of label in [4-$^{13}$C]glutamine in this region, which is mostly derived from [4-$^{13}$C]glutamate, implied that isoflurane specifically reduced neuronal glutamate release there. Together these results showed that isoflurane predominantly affected neuronal metabolism and activity. However, astrocytic metabolism was also reduced demonstrated by the presence of unmetabolized [1,2-$^{13}$C]acetate in the 30 min sham group, but not in the 240 min group. Thus, the presence of unmetabolized [1,2-$^{13}$C]acetate in the upper frontoparietal cortex 30 min after MCAO was most likely an

isoflurane artifact since [1,2-$^{13}$C]acetate was not detected at 60 min of MCAO in the same region. Although isoflurane reduced cerebral metabolism 30 min after it had been turned off, it was evident that MCAO exerted its own distinct effects on the cerebral metabolism already 30 min after induction, illustrated for instance by the significant reduction in label incorporation from [1,2-$^{13}$C]acetate into amino acids.

## Discussion

The present study clearly demonstrates that MCAO rapidly induces profound changes in neuronal and astrocytic metabolism, and in the trafficking of metabolites between these two cellular compartments. The changes depended on both the duration of ischemia as well as degree of ischemia. There were both similarities and distinct differences in the metabolic response to MCAO in severely ischemic tissue in the lateral caudoputamen and lower parietal cortex, and in moderately ischemic tissue in the upper frontoparietal cortex.

Label incorporation into amino acid from [1-$^{13}$C]glucose via PDH and the TCA cycle was depressed almost to the same extent in the two ischemic regions, demonstrating how sensitive neuronal metabolism was to CBF reductions. However, decreased neuronal glucose metabolism in MCAO does in itself not indicate irreversible neuronal damage, as reperfusion within 30 min salvages substantial tissue volumes from infarction in the lateral caudoputamen, and the upper frontoparietal cortex can be saved with reperfusion within 90 -- 120 min (Memezawa et al., 1992b; Müller et al., 1995; Garcia et al., 1995). Thus, the development of metabolic insufficiency in neurons appeared to arise from a combination of metabolic disturbances, including alterations in the use of astrocytic precursor.

The most obvious difference between the severely and moderately ischemic tissue was found in the acetate metabolism. Reduced astrocytic metabolism as indicated by reduced formation of [4,5-$^{13}$C]glutamine and/or the presence of unmetabolized [1,2-$^{13}$C]acetate, was detected at 30 min in severely ischemic tissue, and at 120 min of MCAO in moderately ischemic tissue.

These time-points coincide with the time-windows for successful reperfusion of the lateral caudoputamen and lower parietal cortex, and the upper frontoparietal cortex respectively, suggesting that reduced metabolism in astrocytes may be an indicator of irreversible tissue injury.

*MCAO induced changes in the glutamate-glutamine cycle*

*Lateral caudoputamen and lower parietal cortex.* In this region rendered severely ischemic profound changes in the glutamate metabolism were revealed. The normal equilibrium between glutamate and glutamine content and thus the glutamate-glutamine cycle were disturbed from 30 min of MCAO. There was a rapid decline in glutamate synthesis from glucose derived acetyl CoA, representing neuronal derived glutamate synthesis. At the same time a reduction was seen in utilization of glutamine in glutamate formation. This reduction may result from reduced activity in astrocytic or neuronal glutamine transporters in ischemia, and/or reduced PAG activity as both ammonia accumulation and acidosis, which are present in ischemia, inhibit PAG (Benjamin, 1981; Kvamme et al., 1982; Hogstad et al., 1988). Still, at all times after MCAO astrocytic glutamine was a more important precursor for glutamate than precursors derived from neuronal TCA cycle activity, suggesting that astrocytic glutamine contributed significantly to excitotoxicity *in vivo*. This observation concurs with previous studies using cell cultures (Goldberg et al., 1988; Rosenberg, 1991; Huang and Hertz, 1994). The reduced glutamate synthesis present from 30 min of MCAO cannot fully explain the reduced glutamate content detected in the same region. The decreased glutamate levels were most likely connected to increased glutamate utilization, including oxidation, and/or loss of glutamate into systemic circulation and CSF during MCAO. Astrocytic glutamate uptake and subsequent conversion to glutamine was demonstrated by the better preservation of label in [4-$^{13}$C]glutamine than in [4-$^{13}$C]glutamate throughout the 240 min of MCAO, in agreement with earlier studies (Aas et al., 1993; Takagi et al., 1993; Swanson,

1992; Torp et al., 1993; Ottersen et al., 1996). In the astrocytes increased entry of glutamate into the TCA cycle was suggested by the better preservation of the total amount of label in [3-$^{13}$C]glutamine than in [3-$^{13}$C]glutamate at 60 min of MCAO and onward. Previous *in vitro* and *in vivo* data have demonstrated increased glutamate metabolism via the TCA cycle when extracellular glutamate concentrations were elevated and during ischemia (McKenna et al., 1996; Håberg et al., 1998a; Pascual et al., 1998). Glutamate may also be consumed in GABA and glutamine synthesis, and increased alanine synthesis may, via transamination, reduce glutamate content. In addition, glutamate may be lost into the systemic circulation and CSF. Elevated glutamate levels have been demonstrated in CSF in rats subjected to focal ischemia (Cataltepe et al., 1996), and in both plasma and CSF in patients with acute ischemic stroke (Castillo et al., 1996). Loss of glutamate from the brain parenchyma gives an indication of the mismatch between glutamate synthesis and consumption, as well as glutamate release and uptake during MCAO, illustrating the serious metabolic insufficiency in this region. Despite this continuos loss of metabolites, glutamatergic neurons maintained a low level of glutamate synthesis throughout the 240 min of MCAO.

*Upper frontoparietal cortex*. Glutamate metabolism was also affected in moderately ischemic tissue, but the changes in the glutamate/glutamine cycle were in some respect quite distinctive for this region. Like in the severely ischemic tissue, glutamate synthesis was reduced from both neuronal and astrocytic precursors at 30 min of MCAO and onward, but in moderately ischemic tissue the contribution from astrocytic precursors compared to neuronal precursors did not increase significantly before 60 min of MCAO. The fact that neuronal glutamine utilization in glutamate formation was reduced despite the presence of normal [4,5-$^{13}$C]glutamine levels, and that the total amount of [4,5-$^{13}$C]glutamate was at the same level at all times after MCAO indicates some functional inhibition of either glutamine transporters and/or PAG activity independent of the duration of ischemia. PAG activity may for instance

be reduced by the presence of normal glutamate concentrations (Hogstad et al., 1988). From 60 min of MCAO glutamine became increasingly important in glutamate synthesis while the neuronal TCA cycle activity gradually declined. It has been shown that glutamine principally replenishes the neurotransmitter pool of glutamate (Laake et al., 1995), from which glutamate release is considered to originate in moderately ischemic tissue (Takagi et al., 1993; Obrenovitch, 1996). The constellation of gradually declining neuronal metabolic activity and continued replenishment of the neurotransmitter pool of glutamate will render the neurons extremely susceptible to glutamate excitotoxicity. There is increasing evidence for a delayed component in glutamate-mediated neuronal damage in cerebral ischemia, and based on the present data it appears to be connected to the continued astrocytic glutamine production and the subsequent neuronal utilization of glutamine in glutamate neurotransmitter synthesis. The current finding of persistent glutamate synthesis from glutamine and to some extent also from the neuronal TCA cycle precursors for 240 min of MCAO implies that administration of glutamate receptor antagonists has to be continued for a prolonged period. In line with this observation is the finding that AMPA receptor antagonist administration lasting 4 h after MCAO does not reduce final infarct volume, whereas administration lasting 24 h salvages the upper frontoparietal cortex (Håberg et al., 1998b). Furthermore, inhibiting GS activity and thereby reducing glutamine synthesis, has been shown to reduce infarct size in cortex in rats subjected to MCAO (Swanson et al., 1990). Finally, elevated glutamine concentrations detected from 60 min of MCAO, may in itself have deleterious effects, since increased extracellular glutamine concentrations stimulate neuronal glutamate release (Szerb and O'Regan, 1985).

It should be noted that the results from the sham operated rats showed that astrocytic glutamine was a more important precursor for glutamate in the upper frontoparietal cortex than in the lateral caudoputamen and lower parietal cortex, which is in agreement with PAG

density and activity being higher in cortex than in caudate-putamen/striatum (Aoki et al., 1991; Wallace and Dawson, 1993).

*MCAO induced changes in GABA metabolism*

MCAO completely changed GABA metabolism in severely ischemic tissue in the lateral caudoputamen and lower parietal cortex, and also in moderately ischemic tissue in the upper frontoparietal cortex. [1,2-$^{13}$C]GABA was not detectable in either region demonstrating a dramatic reduction in the conversion of astrocytic glutamine to GABA after MCAO. In severely ischemic tissue PC activity was undetectable at all times after MCAO thereby suggesting complete cessation of the use of astrocytic precursors for GABA formation. In the moderately ischemic tissue PC activity was present in GABA from 30 to 120 min of MCAO, indicating that astrocytic precursors participated to some extent in GABA synthesis. This reduction in glutamine utilization in GABA formation was at great variance from the increased use of glutamine in glutamate synthesis during MCAO. However, like in glutamatergic neurons GABA synthesis from neuronal precursors was markedly lowered after MCAO.

GABA build-up, which can proceed in the absence of functioning mitochondria, was present from 60 min of MCAO in moderately ischemic tissue, and at 240 min in severely ischemic tissue. Cerebral ischemia is known to stimulated GABA synthesis via GAD (Sze, 1979; Erecinska et al., 1996) and at the same time inhibit GABA break-down by GABA transaminase (GABA-T; E.C.2.6.1.19) (Schousboe et al., 1973) consequently increasing the GABA content (Erecinska et al., 1984). Decreased GABA-T activity will impede the re-entry of carbon-atoms from GABA into the TCA cycle, thereby decreasing the activity of the GABA-shunt (Balazs, 1970), resulting in loss of TCA cycle intermediates and subsequently also of aspartate (see below). However, in severely ischemic tissue additional mechanisms causing GABA build-up may be operating. The substantial increase in unlabeled GABA from

120 to 240 min of MCAO which was accompanied by a corresponding decline in glutamate levels may arise from direct conversion of unlabeled glutamate to GABA taking place either intracellularely or extracellularly. A substantial increase in GABA levels have been demonstrated both in the in the cells (Torp et al., 1993) as well as in the extracellular compartment (Matsumoto et al., 1993) during cerebral ischemia. The increased extracellular GABA levels is considered to be due to reversal of GABA transporters, but based on the present results the possibility that GAD leaking into the extracellular space, leading to extracellular production of GABA from extracellular glutamate cannot be excluded.

In the GABAergic neurons, MCAO compromised the flux through the TCA cycle in three ways: 1. Significant fall and/or complete stop in the use of astrocytic glutamine; 2. Rapid and marked reduction in utilization of neuronal precursors; 3. Progressive decrease in GABA-shunt activity. At 240 min of MCAO no TCA cycle flux was detected in the region rendered severely ischemic in the lateral caudoputamen and lower parietal cortex, demonstrating death of GABAergic neurons. Selective death of GABAergic neurons in the striatum has previously been shown in rats following transient forebrain ischemia (Francis and Pulsinelli, 1982). However, GABAergic neurons in the hippocampus and cortex have been found to be particularly resistant to ischemia and NMDA excitotoxicity (Tecoma and Choi, 1989; Gonzales et al., 1992; Johansen and Diemer, 1991). These differences in ischemia susceptibility between different populations of GABAergic neurons may reside in the fact that GABAergic neurons are quite diverse in size and function. Based on the present data GABAergic neurons in the lateral caudoputamen and lower parietal cortex were found to be more sensitive to ischemia that glutamatergic neurons in the same region. However, the properties which lead to the increased sensitivity of GABAergic neurons in the lateral caudoputamen and lower parietal cortex to focal ischemia are presently uncertain. The current findings imply that the complete interruption in the utilization of glutamine in GABA

synthesis in this region may contribute substantially to the death of GABAergic neurons as the reduction in glucose utilization and GABA-shunt activity were at least as noticeable in the region with moderate ischemia during the initial 120 min of MCAO.

The MCAO induced changes in aspartate labeling and content were most likely connected to the changes in GABA metabolism since aspartate is found mainly in GABAergic neurons (Ottersen and Storm-Mathisen, 1985). The significant reduction in aspartate synthesis in both ischemic regions present from 30 min of MCAO could be connected to the reduced glutamine utilization in GABAergic neurons as *in vitro* data suggest that aspartate is predominantly synthesized from glutamine in GABAergic neurons (McKenna et al., 2000). The rapid decline in aspartate labeling found between 120 and 240 min of MCAO in the upper frontoparietal cortex coincided with the complete stop in the use of astrocytic precursors lending further support to the notion that glutamine is important in aspartate synthesis. In addition, aspartate consumption has been shown to be increased by reduced GABA-T activity (Hassel et al., 1998), which was also found presently. In summary, aspartate consumption was increased probably due to decreased GABA shunt activity, whereas aspartate synthesis fell as a result of reduced glutamine utilization.

*MCAO induced changes in astrocyte metabolism*

*Lateral caudoputamen and lower parietal cortex.* In this region of severe ischemia astrocytic metabolism was reduced at 30 min, but was not severely impaired before 240 min of MCAO. The first sign of declining astrocytic metabolism was reduced acetate metabolism, both oxidative and for use in amino acid synthesis. Still, acetyl CoA synthetase, PC and GS which are all ATP dependent enzymes, were operating throughout the experimental period. All appeared to maintain a slightly lower level of activity during the initial 120 min of MCAO, but at 240 min dramatically reduced activity was detected in the label incorporation via these enzymes. No PC activity was detected in glutamine and only a low level of PC activity was

present in glutamate, furthermore the acetate/glucose utilization ratio was at control levels in glutamine, but increased in glutamate at 240 min of MCAO. These findings suggested that glutamate metabolism in astrocytes was compartmentalized and that the compartment synthesizing glutamate for glutamine production was more susceptible to ischemia. Alternatively, ischemia reduced the transport of glutamate produced in the astrocytic mitochondria over the mitochondrial membrane into the cytosol where GS is located. Previously, mitochondrial glutamate accumulation has been demonstrated in astrocytes in global ischemia (Torp et al., 1993). Also alanine synthesis may be considered a marker for astrocytic metabolism since it is preferentially synthesized in astrocytes *in vitro* (Westergaard et al., 1993). Furthermore, alanine synthesis is considered to increase specifically in astrocytes in cerebral ischemia (Bachelard, 1998). In the severely ischemic tissue alanine synthesis was significantly increased between 60 and 120 min of MCAO, but declined from 120 to 240 min of MCAO, giving further evidence of rapidly declining astrocyte metabolism at the end of the experimental period.

*Ischemic frontoparietal cortex.* In moderately ischemic tissue astrocytic metabolism appeared relatively unaffected by MCAO until 120 min of MCAO when unmetabolized [1,2-$^{13}$C]acetate appeared. Previously [1,2-$^{13}$C]acetate has been detected in this region after 90 min of MCAO (Håberg et al., 1998a). PC activity showed early signs of reduced activity at 60 min of MCAO, but was notably reduced first at 240 min of MCAO. Both acetyl CoA synthetase and GS activity appeared unaffected by MCAO. In addition the increasing alanine synthesis present throughout the 240 min of MCAO, gave yet another indication of better preservation of metabolism in astrocyte in moderately ischemic tissue.

## Conclusion

The present study demonstrated the paradoxical role astrocytes play in neuronal survival in ischemia. On one hand, the presence of normal astrocytic metabolism appeared to be critical

for neuronal survival. On the other hand, it was evident that alterations in the use of astrocytic precursors contributed significantly to neuronal death, although via different mechanisms in glutamatergic and GABAergic neurons. In glutamatergic neurons astrocytic precursors sustained the neurotransmitter pool of glutamate despite clear indications of failing neuronal metabolism. This was especially notable in the upper frontoparietal cortex, often referred to as the penumbra, thus demonstrating the importance of glutamine in glutamate excitotoxicity. In GABAergic neurons the complete stop in the use of glutamine in GABA formation in the ischemic core in the lateral caudoputamen and lower parietal cortex, may have contribute significantly to the death of these neurons at 240 min of MCAO. Thus, neuronal survival during focal cerebral ischemia depends both on astrocytic metabolism and on neuronal utilization of astrocytic precursors.

*Acknowledgment*

The authors thank Kristin Antonsen and Torild Krogstad for performing the HPLC analysis at the Institute of Biotechnology, NTNU.

This study was supported by the Norwegian Council on Cardiovascular disease, the Norwegian Research Council, the SINTEF foundation and Inger R. Haldorsen's Grant.

## References

Aas J-E, Berg-Johnsen J, Hegstad E, Laake JH, Langmoen IA, Ottersen OP (1993) Redistribution of glutamate and glutamine in slices of human neocortex exposed to combined hypoxia and glucose deprivation in vitro. *J Cereb Blood Flow Metab* 13:503-515

Aoki C, Kaneko T, Starr A, Pickel VM (1991) Identification of mitochondrial and non-mitochondrial glutaminase within select neurons and glia of rat forebrain by electron microscopic immunocytochemistry. *J Neurosci Res* 28:531-548

Bachelard H (1998) Landmarks in the application of $^{13}$C-magnetic resonance spectroscopy to studies of neuronal/glial relationships. *Dev Neurosci* 20:277-288

Back T (1998) Pathophysiology of the ischemic penumbra - revision of a concept. *Cell Molec Neurobiol* 18:621-638

Badar-Goffer RS, Bachelard HS, Morris PG (1990) Cerebral metabolism of acetate and glucose studied by $^{13}$C NMR spectroscopy. A technique for investigating metabolic compartmentation in the brain. *Biochem J* 266:133-139

Balazs R, Machiyama Y, Hammond BJ, Julian T, Richter D (1970) The operation of the γ-aminobutyrate bypath of the tricarboxylic acid cycle in brain tissue in vitro. *Biochem J* 116:445-467

Benjamin AM (1981) Control of glutaminase activity in rat brain cortex in vitro: influence of glutamate, phosphate, ammonia, calcium and hydrogen ions. *Brain Res* 2:363-377

Castillo J, Dávalos A, Naveiro J, Noya M (1996) Neuroexcitatory amino acids and their relation to infarct size and neurological deficit in ischemic stroke. *Stroke* 27:1060-1065

Cataltepe O, Towfighi J, Vannucci RC (1996) Cerebrospinal fluid concentrations of glutamate and GABA during perinatal cerebral hypoxia-ischemia and seizures. *Brain Res* 709:326-330

Choi DW (1992) Excitotoxic cell death. *J Neurobiol* 23:1261-1276

Cremer JE, Lucas HM (1971) Sodium pentobarbitone and metabolic compartments in rat brain. *Brain Res* 35:619-621

Daikhin Y, Yudkoff M (2000) Compartmentation of brain glutamate metabolism in neurons and glia. *J Nutr* 130(4S Suppl):1026S-1031S

Erecinska M, Nelson D, Wilson DF, Silver IA (1984) Neurotransmitter amino acids in the CNS. I. Regional changes in amino acid levels in rat brain during ischemia and reperfusion. *Brain Res* 304:9-22

Erecinska M (1987) The neurotransmitter amino acid transport systems. A fresh outlook on an old problem. *Biochem Pharmacol* 36:3547-3555

Erecinska M, Nelson D, Daikhin Y, Yudkoff M (1996) Regulation of GABA level in rat brain synaptosomes: fluxes through enzymes of the GABA shunt and effects of glutamate, calcium, and ketone bodies. *J Neurochem* 67:2325-2334

Farinelli SE, Nicklas WJ (1992) Glutamate metabolism in rat cortical astrocyte cultures. *J Neurochem* 58:1905-1915

Francis A, Pulsinelli W (1982) The response of GABAergic and cholinergic neurons to transient cerebral ischemia. *Brain Res* 243:271-278

Garcia JH, Liu K-F, Ho K-L (1995) Neuronal necrosis after middle cerebral artery occlusion in Wistar rats progress at different time intervals in the caudoputamen and the cortex. *Stroke* 26:636-643

Goldberg MP, Monyer H, Choi DW (1988) Hypoxic neuronal in vitro injury depends on extracellular glutamine. *Neurosci Lett* 94:52-57

Gonzales C, Lin RC, Chesselet MF (1992) Relative sparing of GABAergic interneurons in the striatum of gerbils with ischemia induced lesions. *Neurosci Lett* 135:53-58

Håberg A, Qu H, Haraldseth O, Unsgård G, Sonnewald U (1998a) In vivo injection of [1-$^{13}$C]glucose and [1,2-$^{13}$C]acetate combined with ex vivo $^{13}$C NMR spectroscopy: A novel approach to the study of MCA occlusion in rat. *J Cereb Blood Flow Metab* 18:1223-1232

Håberg A, Takahashi M, Yamaguchi T, Hjelstuen M, Haraldseth O (1998b) Neuroprotective effect of the novel glutamate AMPA receptor antagonist YM872 assessed with in vivo MR imaging of rat MCA occlusion. *Brain Res* 811:63-70

Hansen TD, Warner DS, Todd MM, Vust LJ, Trawick BS (1988) Distribution of cerebral blood flow during halothane versus isoflurane anesthesia in rats. *Anesthesiol* 69:332-337

Hassel B, Johannessen CU, Sonnewald U, Fonnum F (1998) Quantification of the GABA shunt and the importance of the GABA shunt versus the 2-oxoglutarate dehydrogenase pathway in GABAergic neurons. *J Neurochem* 71:1511-1518

Hertz L (1979) Functional interactions between neurons and astrocytes. I. Turnover and metabolism of putative amino acid transmitters. *Prog Neurobiol* 13:277-323

Hertz L, Dringen R, Schoousboe A, Robinson SR (1999) Astrocytes: glutamate producers for neurons. *J Neurosci Res* 57:417-428

Hoffman WE, Edelman G, Kochs E, Werner C, Segil L, Albrecht RF (1991) Cerebral autoregulation in awake versus isoflurane-anesthetized rats. *Anesth Analg* 73:753-757

Hogstad S, Svenneby G, Torgner IAa, Kvamme E, Hertz L, Schousboe A (1988) Glutaminase in neurons and astrocyte cultured from mouse brain: Kinetic properties and effects of phosphate, glutamate and ammonia. *Neurochem Res* 13:383-388

Huang R, Hertz L (1994) Effect of anoxia on glutamate formation from glutamine in cultured neurons: dependence on neuronal subtypes. *Brain Res* 660:129-137

Johansen FF, Diemer NH (1991) Enhancement of GABA neurotransmission after cerebral ischemia in the rat reduces loss of hippocampal CA1 pyramidal cells. *Acta Neurol Scand* 84:1-6

Kaufman EE, Driscoll BF (1993) Evidence for cooperativity between neurons and astroglia in the regulation of $CO_2$ fixation in vitro. *Dev Neurosci* 15:299-305

Künneck B, Ceredan S, Seelig J (1993) Cerebral metabolism of [1,2-$^{13}C_2$]glucose and [U-$^{13}C_4$]3-hydroxybutyrate in rat brain as detected by $^{13}C$ NMR spectroscopy. *NMR in Biomed* 6:264-277

Kvamme E, Svenneby G, Hertz L, Schousboe A (1982) Properties of phosphate activated glutaminase in astrocytes cultured from mouse brain. *Nerochem Res* 6:761-770

Kvamme E, Roberg B, Torgner IA (2000) Phosphate-activated glutaminase and mitochondrial glutamine transport in the brain. *Neurochem Res* 25:1407-1419

Laake JH, Slyngstad TA, Haug F-MS, Ottersen OP (1995) Glutamine from glial cells is essential for the maintenance of the nerve terminal pool of glutamate: Immunogold evidence from hippocampal slice cultures. *J Neurochem* 65:871-881

Longa EZ, Weinstein PR, Cummins R (1989) Reversible middle cerebral artery occlusion without craniectomy in rats. *Stroke* 20:84-91

Matsumoto K, Graf R, Rosner G, Taguchi J, Heiss W-D (1993) Elevation of neuroactive substances in the cortex of cats during prolonged focal ischemia. *J Cereb Blood Flow Metab* 13:586-594

McKenna MC, Sonnewald U, Huang X, Stevenson J, Zielke HR (1996) Exogenous glutamate concentration regulates the metabolic fate of glutamate in astrocytes. *J Neurochem* 66:386-393

McKenna MC, Stevenson JH, Huang X, Hopkins IB (2000) Distribution of the enzymes glutamate dehydrogenase and aspartate aminotransferase in cortical synaptic mitochondria contributes to metabolic compartmentation in cortical synaptic terminals. *Neurochem Int* 37:229-241

McLean MA, Badar-Goffer RS, Bachelard HS, Morris PG (1993) Simultaneous measurement of neuronal and glial metabolism via $^{13}$C-MRS isotopomer analysis (Abstr.) New York, 12$^{th}$ meeting of SMRM, p. 511

Meldrum BS (2000) Glutamate as transmitter in the brain: review of physiology and pathology. *J Nutr* 130(4S Suppl):1007S-1015S

Memezawa H, Minamisawa H, Smith M-L, Siesjö BK (1992a) Ischemic penumbra in a model of reversible middle cerebral artery occlusion in the rat. *Exp Brain Res* 89:67-78

Memezawa H, Smith ML, Siesjö BK (1992b) Penumbral tissues salvaged by reperfusion following middle cerebral artery occlusion in rats. *Stroke* 23:552-560

Müller TB, Haraldseth O, Jones RA, Sebastiani G, Lindboe CF, Øksendal AN, Unsgård G (1995) Combined perfusion and diffusion weighted MR imaging in a rat model of reversible middle cerebral artery occlusion. *Stroke* 26:451-458

Norenberg MD, Martinez-Hernandez A (1979) Fine structural localization of glutamine synthetase in astrocytes of rat brain. *Brain Res* 161:303-310

Obrenovitch TP (1996) Origins of glutamate release in ischaemia. *Acta Neurochir [suppl]* 66:50-55

Ottersen OP (1989) Quantitative electron microscopic immunocytochemistry of neuroactive amino acids. *Anat Embryol* 180:1-15

Ottersen OP, Storm-Matisen J (1985) Different neuronal localization of aspertate-like and glutamate-like immunoreactivities in the hippocampus of rat, guinea-pig and Senegalese baboon (Papio papio), with a note on the distribution γ-aminobutyrate. *Neurosci* 6:589-606

Ottersen OP, Laake JH, Reichelt W, Haug FM, Torp R (1996) Ischemic disruption of glutamate homeostasis in brain: quantitative immunocytochemical analyses. *J Chem Neuroanat* 12:1-14

Pascual JM, Carceller F, Roda JM, Cerdán S (1998) Glutamate, glutamine, and GABA as substrates for the neuronal and glial compartments after focal cerebral ischemia in rats. *Stroke* 29:1048-1057

Patel MS (1974) The relative significance of $CO_2$-fixing enzymes in the metabolism of rat brain. *J Neurochem* 22:717-724

Rosenberg PA (1991) Accumulation of extracellular glutamate and neuronal death in astrocyte-poor cortical cultures exposed to glutamine. *Glia* 4:91-100

Schousboe A, Yu J-Y, Roberts E (1973) Purification and characterization of the 4-aminobyturtate-2-ketoglutatate transaminase from mouse brain. *Biochem* 12:2868-2873

Schwartz-Bloom RD, Sah R (2001) γ-Aminobutyric $acid_A$ neurotransmission and cerebral ischemia. *J Neurochem* 77:353-371

Shank RP, Leo GC, Zielke HR (1993) Cerebral metabolic compartmentation as revealed by nuclear magnetic resonance analysis of D-[1-$^{13}$C] glucose metabolism. *J Neurochem* 61:315-323

Sloviter RS, Dichter MA, Rachinsky TL, Dean E, Goodman JH, Sollas AL, Martin DL (1996) Basal expression and induction of glutamate decarboxylase and GABA in excitatory granule cells of the rat and monkey hippocampal dentate gyrus. *J Comp Neurol* 373:593-618

Sonnewald U, Håberg A, Haraldseth O, Müller TB, Unsgård G (1996) Glial/neuronal interactions studied by MRS of rat brain after MCAO. In: *Pharmacology of Cerebral Ischemia.* (Kriegelstein J, ed). Stuttgart, Medpharm, pp. 285-290

Swanson RA, Shiraishi K, Morton MT, Sharp FR (1990) Methionine sulfoximine reduces cortical infarct size in rats after middle cerebral artery occlusion. *Stroke* 21:322-327

Swanson RA (1992) Astrocyte glutamate uptake during chemical hypoxia in vitro. *Neurosci Lett* 147:143-146

Sze PY (1979) L-Glutamate decarboxylase. *Adv Exp Med Biol* 123:59-78

Szerb JC, O'Regan PA (1985) Effect of glutamine on glutamate release from hippocampal slices induced by high $K^+$ or by electrical stimulation: interactions with different $Ca^{2+}$ concentrations. *J Neurochem* 44:1724-1731

Takagi K, Ginsberg MD, Globus MY-T, Dietrich WD, Martinez E, Kraydieh S, Busto R (1993) Changes in amino acid neurotransmitters and cerebral blood flow in the ischemic penumbral region following middle cerebral artery occlusion in the rat: Correlation with histopathology. *J Cereb Blood Flow Metab* 13:575-585

Tanaka K (2000) Functions of glutamate transporters in the brain. *Neurosci Res* 37:15-19

Taylor A, McLean M, Morris P, Bachelard H (1996) Approaches to studies on neuronal/glial relationships by $^{13}C$-MRS analysis. *Dev Neurosci* 18:434-442

Tecoma ES, Choi DW (1989) GABAergic neocortical neurons are resistant to NMDA receptor-mediated injury. *Neurology* 39:676-682

Torp R, Arvin B, Le Peillet E, Chapman AG, Ottersen OP, Meldrum BS (1993) Effect of ischemia and reperfusion on the extra- and intracellular distribution of glutamate, glutamine, aspartate and GABA in the rat hippocampus, with a note on the effect of the sodium channel blocker BW1003C87. *Exp Brain Res* 96:365-376

Van den Berg CJ (1973) A model of compartmentation in the mouse brain based on glucose and acetate metabolism. In: *Metabolic Compartmentation in the Brain* (Balazs R and Cremer JE, eds). London, Maxmillian Press, pp. 137-166

Varoqui H, Zhu H, Yao D, Ming H, Erickson JD (2000) Cloning and functional identification of a neuronal glutamine transporter. *J Biol Chem* 275:4049-4054

Wallace DR, Dawson R Jr. (1993) Regional differences in glutaminase activation by phosphate and calcium in rat brain: impairment in aged rats and implications for regional glutaminase isoenzymes. *Neurochem Res* 12:1271-1279

Waniewski RA and Martin DL (1998) Preferential utilization of acetate by astrocytes is attributable to transport. *J Neurosci* 18:5225-5233

Westergaard N, Varming T, Peng L, Sonnewald U, Hertz L, Schousboe A (1993) Uptake, release and metabolism of alanine in neurons and astrocytes in primary cultures. *J Neurosci Res* 35:540-545

Westergaard N, Sonnewald U, Schousboe A (1995) Metabolic trafficking between neurons and astrocytes: the glutamine/glutamate cycle revisited. *Dev Neurosci* 17:203-211

Yu ACH, Drejer J, Hertz L, Schousboe A (1983) Pyruvate carboxylase activity in primary cultures of astrocytes and neurons. *J Neurochem* 41:1484-1487

**Figure legends**

**Figure 1.** Effect of MCAO on total amino acid content.

Time zero represents sham operated rats allowed to recover for 240 min before sacrifice.

The amino acid content was analyzed with HPLC, see Materials and Methods.

The lateral caudoputamen and lower parietal cortex (A,C and E) represent severely ischemic tissue. The upper frontoparietal cortex (B,D and F) represents moderately ischemic tissue.

All values are mean ± SD. n = 7 in each group.

Statistical comparisons were performed with ANOVA followed by post hoc test for multiple comparisons.

[a] Significantly different from sham operated, $p<0.05$, [aa] $p<0.01$, [aaa] $p<0.001$

[b] Significantly different from group subjected to 30 min of MCAO, $p<0.05$, [bb] $p<0.01$, [bbb] $p<0.001$

[c] Significantly different from group subjected to 60 min of MCAO, $p<0.05$,

[ccc] $p<0.001$

[d] Significantly different from group subjected to 120 min of MCAO, $p<0.05$,

[ddd] 0.001

**Figure 2.** The total amount of [1-$^{13}$C]glucose and [1,2-$^{13}$C]acetate in ischemic tissue after MCAO.

Time zero represents sham operated rats allowed to recover for 240 min before sacrifice.

The total amount of $^{13}$C ($10^{-8}$mol/g tissue) was analyzed with $^{13}$C MRS as described in Materials and Methods, and was not corrected for naturally abundant $^{13}$C (1.1%).

The lateral caudoputamen and lower parietal cortex (A) represent severely ischemic tissue. The upper frontoparietal cortex (B) represents moderately ischemic tissue.

All values are mean ± SD. n = 7 in each group.

Statistical comparisons were performed with ANOVA followed by post hoc test for multiple comparisons.

[a] Significantly different from sham operated rats, $p<0.05$, [aa] $p<0.01$, [aaa] $p<0.001$

[b] Significantly different from group subjected to 30 min of MCAO, $p<0.05$, [bb] $p<0.01$, [bbb] $p<0.001$

[c] Significantly different from group subjected to 60 min of MCAO, $p<0.05$, [cc] $p<0.01$

[d] Significantly different from group subjected to 120 min of MCAO, $p<0.05$, [dd] $p<0.01$

**Figure 3.** Effect of MCAO on incorporation of label from [1-$^{13}$C]glucose and [1,2-$^{13}$C]acetate in amino acids.

Time zero represents sham operated rats allowed to recover for 240 min before sacrifice.

The total amount of $^{13}$C ($10^{-8}$mol/g tissue) was analyzed with $^{13}$C MRS as described in Materials and Methods, and was not corrected for naturally abundant $^{13}$C (1.1%).

All values are mean ± SD. n = 7 in each group.

The lateral caudoputamen and lower parietal cortex (A,C,E,G and I) represent severely ischemic tissue. The upper frontoparietal cortex (B,D,F,H and J) represents moderately ischemic tissue.

Statistical comparisons were performed with ANOVA followed by post hoc test for multiple comparisons.

[a] Significantly different from sham operated, $p<0.05$, [aa] $p<0.01$, [aaa] $p<0.001$

[b] Significantly different from group subjected to 30 min of MCAO, $p<0.05$, [bb] $p<0.01$, [bbb] $p<0.001$

[c] Significantly different from group subjected to 60 min of MCAO, $p<0.05$,

[ccc] $p<0.001$

[d] Significantly different from group subjected to 120 min of MCAO, $p<0.05$,

[dd] $p<0.01$, [ddd] 0.001

**Table 1.** Effects of MCAO on the use of precursors derived from astrocytic metabolism compared to neuronal metabolism in glutamate, glutamine and GABA formation.

| | **Acetate/glucose utilization ratio** | | | | | |
|---|---|---|---|---|---|---|
| | Lateral caudoputamen and lower parietal cortex | | | Upper frontoparietal cortex | | |
| | Glutamate | Glutamine | GABA | Glutamate | Glutamine | GABA |
| Sham operated | 0.20 ± 0.01 | 1.30 ± 0.15 | 0.20 ± 0.04 | 0.24 ± 0.02 | 1.34 ± 0.13 | 0.21 ± 0.02 |
| 30 min of MCAO | 0.26 ± 0.04 [a] | 1.79 ± 0.28 [a] | NQ | 0.26 ± 0.03 | 2.22 ± 0.09 [aa] | NQ |
| 60 min of MCAO | 0.27 ± 0.08 [a] | 2.30 ± 0.52 [aaa,b] | NQ | 0.32 ± 0.04 [aa,b] | 3.71 ± 0.53 [aaa,bbb] | NQ |
| 120 min of MCAO | 0.34 ± 0.04 [aaa, b, c] | 2.17 ± 0.42 [aaa] | NQ | 0.30 ± 0.06 [a] | 2.77 ± 0.60 [aaa,c] | NQ |
| 240 min of MCAO | 0.31 ± 0.11 [aa] | 1.75 ± 0.51 | NQ | 0.43 ± 0.07 [aaa,bbb,cc,ddd] | 3.27 ± 0.78 [aaa,bb] | NQ |
| | **PC/PDH activity ratio** | | | | | |
| | Lateral caudoputamen and lower parietal cortex | | | Upper frontoparietal cortex | | |
| | Glutamate | Glutamine | GABA | Glutamate | Glutamine | GABA |
| Sham operated | 0.20 ± 0.02 | 0.45 ± 0.09 | 0.06 ± 0.03 | 0.17 ± 0.05 | 0.76 ± 0.07 | 0.06 ± 0.02 |
| 30 min of MCAO | 0.16 ± 0.06 | 0.36 ± 0.15 | ND | 0.10 ± 0.02 | 0.73 ± 0.18 | 0.07 ± 0.03 |
| 60 min of MCAO | 0.18 ± 0.05 | 0.76 ± 0.08 [aaa, bbb] | ND | 0.11 ± 0.08 | 0.68 ± 0.46 [aaa,bbb] | 0.06 ± 0.05 |
| 120 min of MCAO | 0.11 ± 0.05 [aa, c] | 0.37 ± 0.18 [ccc] | ND | 0.03 ± 0.01 [aa] | 0.77 ± 0.13 [ccc] | 0.04 ± 0.02 |
| 240 min of MCAO | 0.07 ± 0.04 [aaa, b, cc] | ND | ND | 0.05 ± 0.02 [a] | 0.20 ± 0.13 [aa,bb,c,dd] | ND |

All values are mean ± SD. ND, not detectable. NQ, not quantifiable as [1,2-$^{13}$C]GABA was not detected.

Ratios for PC/PDH activity and acetate/glucose utilization were calculated as described in Materials and Methods.

Statistical comparisons between groups were performed with ANOVA followed by post hoc test for multiple comparisons.

[a] Significantly different from sham operated, $p<0.05$, [aa] $p<0.01$, [aaa] $p<0.001$

[b] Significantly different from group subjected to 30 min of MCAO, $p<0.05$, [bb] $p<0.01$, [bbb] $p<0.001$

[c] Significantly different from group subjected to 60 min of MCAO, $p<0.05$, [cc] $p<0.01$, [ccc] $p<0.001$

[dd] Significantly different from group subjected to 120 min of MCAO, $p<0.01$, [ddd] $p<0.001$

**Table 2**. Delayed effects of isoflurane on cerebral metabolism in sham operated rats.

| Amino Acid Isotopomer | Lateral caudoputamen and lower parietal cortex | | Upper frontoparietal cortex | |
|---|---|---|---|---|
| | sham 30 min (n=3) | sham 240 min (n=7) | sham 30 min (n=3) | sham 240 min (n=7) |
| [3-$^{13}$C]Alanine | 7.1 ± 1.4 | 7.3 ± 1.6 | 7.0 ± 0.5 | 6.0 ± 0.8 |
| [3-$^{13}$C]Aspartate | 7.3 ± 0.9 | 12.1 ± 1.3*** | 12.2 ± 4.5 | 12.3 ± 1.5 |
| [2-$^{13}$C]GABA | 14.1 ± 2.0 | 18.6 ± 2.0* | 11.0 ± 0.4 | 14.8 ± 1.9** |
| [1,2-$^{13}$C]GABA | 3.7 ± 0.3 | 3.5 ± 0.5 | 3.2 ± 0.5 | 3.5 ± 0.8 |
| [4-$^{13}$C]Glutamine | 15.9 ± 2.3 | 24.6 ± 1.9*** | 20.7 ± 4.8 | 25.3 ± 3.9 |
| [4,5-$^{13}$C]Glutamine | 30.4 ± 0.2 | 31.7 ± 3.8 | 33.9 ± 7.8 | 32.2 ± 3.5 |
| [4-$^{13}$C]Glutamate | 67.6 ± 8.4 | 100.9 ± 5.9*** | 84.7 ± 3.0 | 108.9 ± 8.1** |
| [4,5-$^{13}$C]Glutamate | 18.0 ± 1.6 | 19.1 ± 0.6 | 23.8 ± 0.9 | 28.4 ± 5.4 |

The sham operated rats were allowed to recover for 30 or 240 min after termination of anesthesia before sacrifice. All values are total amount of $^{13}$C ($10^{-8}$ mol/g tissue) and was calculated with $^{13}$C MRS as described in Materials and Methods. The total amount of $^{13}$C was not corrected for naturally abundant $^{13}$C (1.1%). The values are given as mean ± SD.

Two-way unpaired Student's T-test was used to determined statistical differences.

* Significantly different from sham operated rats allowed to recover for 240 min, $p<0.05$,

** p

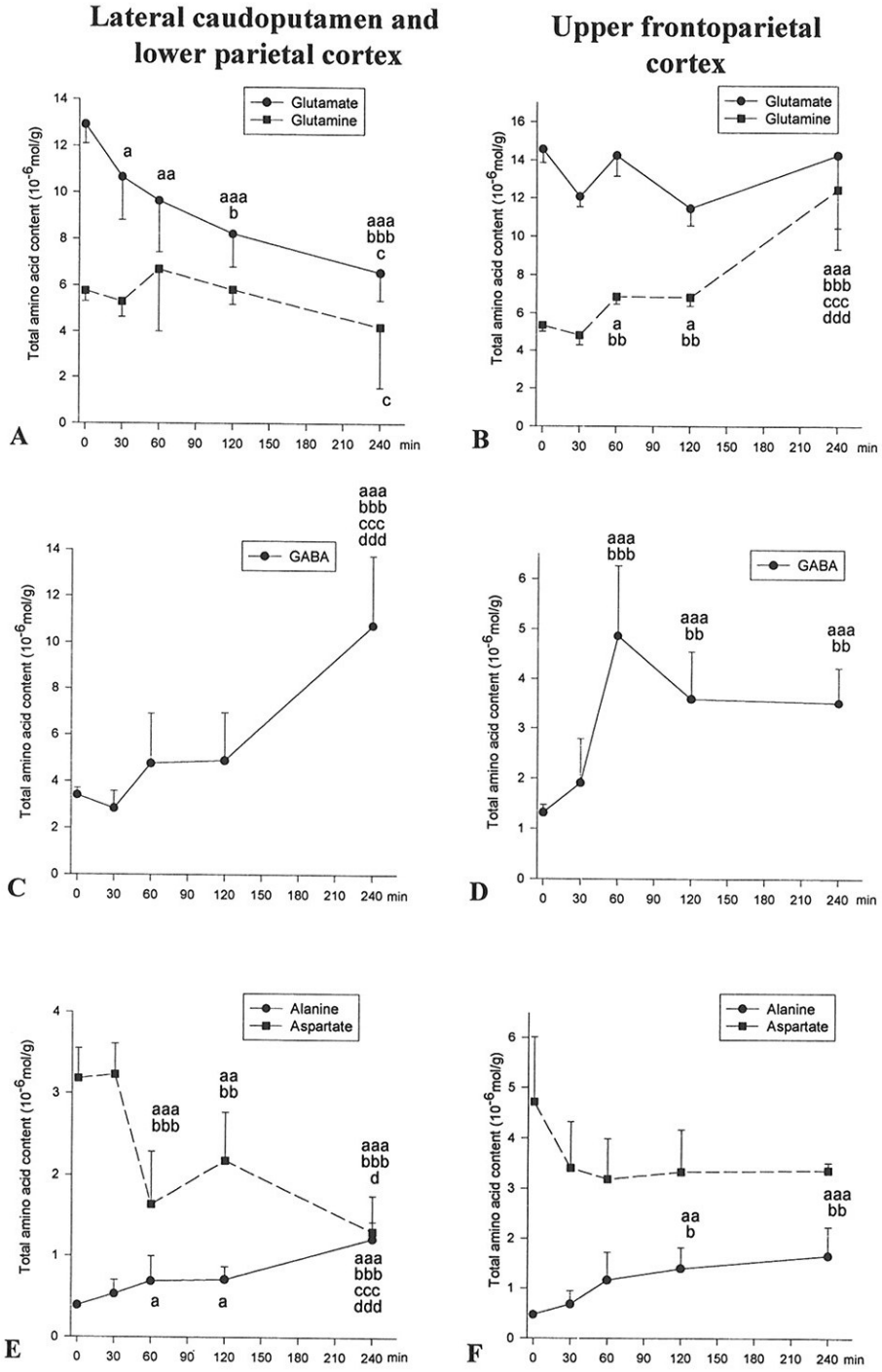
Lateral caudoputamen and lower parietal cortex
Upper frontoparietal cortex
Glutamate
Glutamine
GABA
Alanine
Aspartate
Total amino acid content ($10^{-6}$mol/g)
min
A
B
C
D
E
F

**Lateral caudoputamen and lower parietal cortex**

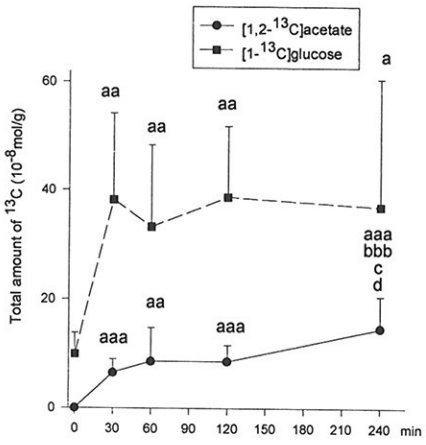


A

**Upper frontoparietal cortex**

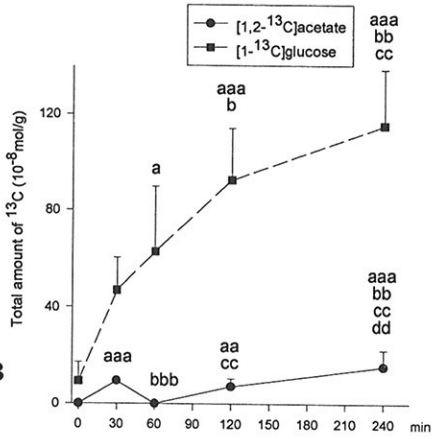


B

**Lateral caudoputamen and lower parietal cortex**

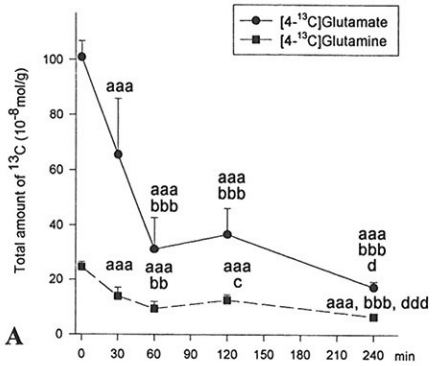


A

**Upper frontoparietal cortex**

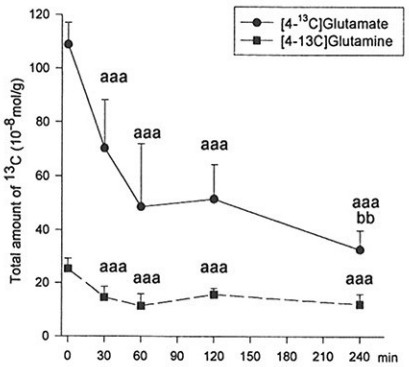


B

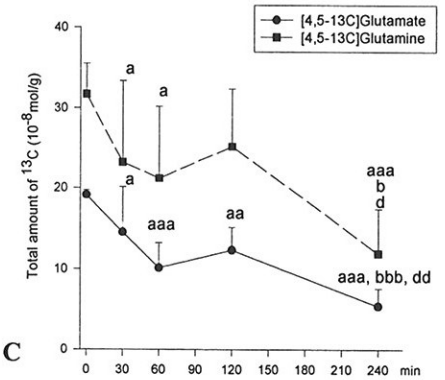


C

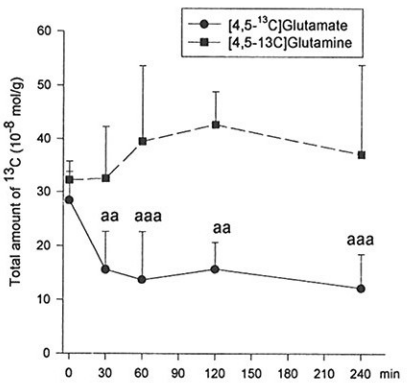


D

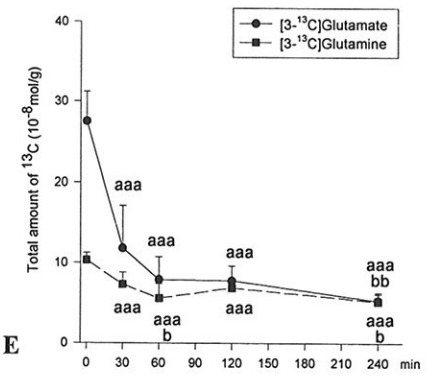


E

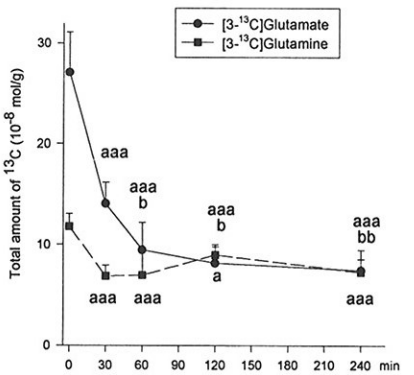


F

## Lateral caudoputamen and lower parietal cortex

## Upper frontoparietal cortex

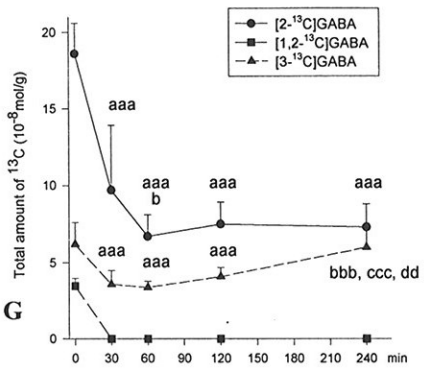


G

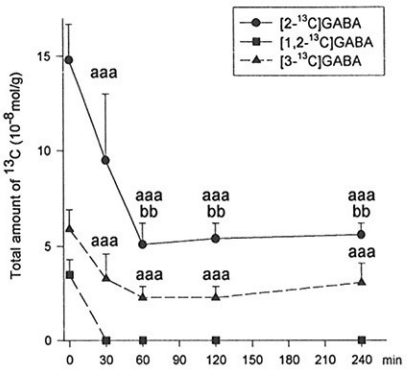


H

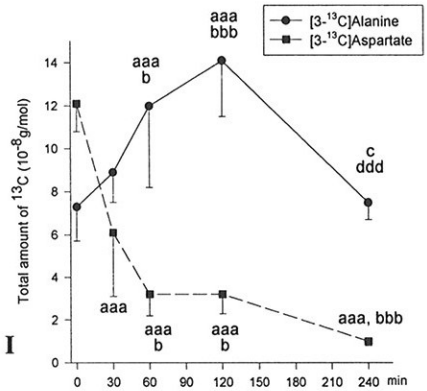


I

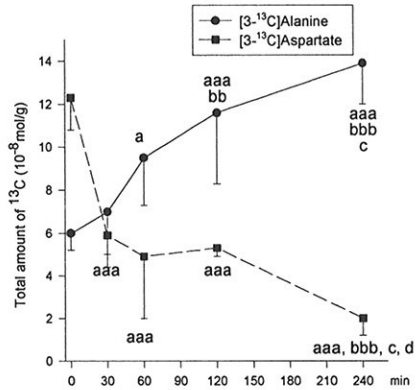


J

# Paper VI

ELSEVIER

Brain Research 811 (1998) 63–70

BRAIN RESEARCH

Research report

# Neuroprotective effect of the novel glutamate AMPA receptor antagonist YM872 assessed with in vivo MR imaging of rat MCA occlusion

Asta Håberg [a], Masayasu Takahashi [b], Tokio Yamaguchi [b], Mari Hjelstuen [c], Olav Haraldseth [a,c,*]

[a] *MR-Center, University Hospital, RIT, N-7006, Trondheim, Norway*
[b] *Neuroscience Research, Yamanouchi Pharmaceutical, Tsukuba, Ibaraki, Japan*
[c] *SINTEF UNIMED, Trondheim, Norway*

Accepted 8 September 1998

**Abstract**

The neuroprotective effect of post-ischemic treatment with the novel, highly water-soluble, glutamate AMPA receptor antagonist YM872 was evaluated by using MR imaging and histopathology of rats subjected to permanent MCA occlusion. Two treatment groups with continuous i.v. infusion of 20 mg $kg^{-1}$ $h^{-1}$ YM872 during either the first 4 h or first 24 h after MCA occlusion, called 4 h YM872 treatment group ($n = 9$) and 24 h YM872 treatment group ($n = 8$) respectively, were compared to a control group ($n = 8$). The main end-point was T2 weighted MR imaging and histopathology 24 h after MCA occlusion. Also the time evolution of the ischemic tissue damage was studied by diffusion weighted MR imaging $4\frac{1}{2}$ and 24 h after MCA occlusion. The volume of ischemic tissue damage as assessed by diffusion weighted MR imaging $4\frac{1}{2}$ h after MCA occlusion was significantly smaller in both YM872 treatment groups ($99 \pm 52$ $mm^3$ and $102 \pm 44$ $mm^3$ compared to $186 \pm 72$ $mm^3$ in the control group, ±S.D. and $p = 0.008$). The infarct volume as assessed by T2 weighted MR imaging 24 h after MCA occlusion was significantly smaller only in the 24 h YM872 treatment group ($262 \pm 57$ $mm^3$ compared to $366 \pm 49$ $mm^3$ in the control group, ±S.D. and $p = 0.01$) while the infarct volume in the 4 h YM872 treatment group ($357 \pm 88$ $mm^3$) was similar to the control group. YM872 treatment significantly reduced the infarct volume 24 h after MCA occlusion when the drug was administered as continuous infusion during the 24-h observation period. 

*Keywords:* Cerebral ischemia; Neuroprotective; AMPA; MR imaging; Experimental stroke

## 1. Introduction

Synaptic release of glutamate and activation of post synaptic glutamate receptors are considered to be important mediators of ischemia induced neuronal damage in stroke. Antagonists of both the NMDA (*N*-methyl-D-aspartate) and AMPA (α-amino-3-hydroxy-5-methyl-4-isoxasole propionate) subtype of glutamate receptors have been shown to have neuroprotective effects in animal studies of cerebral ischemia. The usefulness of NMDA antagonists as therapeutic agents may, however, be limited by their association with adverse effects, including psychomimetic effects [15], cognitive impairment [23], and neurotoxicity [28,29]. AMPA antagonists seem not to share these unfavourable properties of NMDA antagonists [8], and in animal models of focal cerebral ischemia significant reduction of infarct volume has been found after treatment with the AMPA antagonists NBQX [2,5,8,19,37], GYKI 52466 [2,32,37], LY-293558 [3] and YM90K [38,39]. However, investigations in clinical trials have been limited because first generation compounds such as NBQX had the major drawback of being poorly soluble in water and thus nephrotoxic [6,8,37].

In the present study we assessed the neuroprotective effects of the promising novel AMPA receptor antagonist YM872 ([2,3-dioxo-7-(1*H*-imidazol-1-yl)-6-nitro-1,2,3,4-tetrahydro-1-quinoxalinyl]-acetic acid monohydrate), which is a highly water-soluble agent keeping the selectivity and potency for AMPA receptors [16]. YM872 has, in three recent studies, been shown to provide significant neuroprotection in experimental models of focal cerebral ischemia

* Corresponding author. Fax: +47-7399-7708; E-mail: olav.haraldseth@unimed.sintef.no

0006-8993/98/$ - see front matter 
PII: S0006-8993(98)00957-3

in cat [33] and rat [12,34]. In the present study, T2 weighted MR imaging and histopathology 24 h after MCA occlusion in rats were used as the main end-points for evaluation of neuroprotection, and diffusion weighted MR imaging $4\frac{1}{2}$ h and 24 h after MCA occlusion was used to study the temporal evolution of the ischemic tissue damage. T2 weighted MR imaging is sensitive to the vasogenic edema [10], and well defined changes in the images may not be observed until 6–8 h after onset of experimental focal cerebral ischemia [14,22,35]. However, diffusion weighted MR imaging is sensitive to ischemic tissue damage during the first hour of acute ischemia [4,7,11,17,24,31]. This offers a possibility to study the evolution of the tissue damage during drug treatment in the critical acute phase [21,25], and it has been shown that in the case of early reperfusion the diffusion weighted MR imaging changes were reversed to indicate brain cell recovery [9,11,24].

## 2. Materials and methods

All surgical procedures and animal handling were approved by the Norwegian Committee for Animal Experiments. Permanent unilateral MCA (middle cerebral artery) occlusion was induced in male Wistar rats weighing approximately 340 g, using the intraluminal filament technique [20,24,26]. The rats were fasted overnight with free access to water. During surgery the spontaneously breathing rats were anaesthetized with 2% isoflurane in 70/30% $N_2/O_2$, and the rectal temperature was maintained at 37°C with a heating blanket coupled to a feedback circuit. For continuous intravenous infusions a catheter was inserted into the femoral vein, externalized at the tail radix, and covered with tape along the surface of the tail until the tip. A nylon filament with a diameter of 0.27 mm and a rounded tip was introduced through the external carotid artery and advanced 19 to 20 mm, thus blocking the origin of the MCA, and isoflurane was turned off immediately after induction of the MCA occlusion. After surgery the tip of the tail was fastened to a freely rotating device in the roof of a spacious cage. This was considered to be close to freely moving conditions as the rats could move in all directions, including rotation around the axis of the tail.

Prior to surgery the rats were randomly distributed into three experimental groups:

1. Control group ($n = 8$),
2. 4 h YM872 treatment group ($n = 9$),
3. 24 h YM872 treatment group ($n = 8$).

YM872 was dissolved in isotonic saline with a few drops of 1 M sodium hydroxide (NaOH) to adjust pH to approximately 7.4. The two treatment groups received a continuous infusion via the femoral vein of 20 mg YM872 $kg^{-1}$ $h^{-1}$ in a volume of 3 ml $kg^{-1}$ $h^{-1}$ lasting 4 h or 24 h, respectively. The control group received an identical volume of saline, as did the 4 h treatment group after termination of drug administration, in order to achieve the same total volume load in all rats. The infusions were started 10 min after induction of MCA occlusion in all three groups. In both the 4 h and the 24 h YM872 treatment group the drug infusion was turned off 30 min prior to MR imaging to avoid interactions with the isoflurane anaesthesia necessary for MR imaging.

Four and a half hours after MCA occlusion, the spontaneously breathing rats were reanaesthetized with 1.5% isoflurane in 70/30% $N_2/O_2$ for 20 min to allow diffusion weighted MR imaging. During the 6 min MR acquisition period isoflurane was increased to 3.5% to obtain deep anaesthesia as even the smallest head movement induced by the onset of noise linked to MR imaging cause major artifacts in diffusion weighted images. Rectal temperature was measured at the start of anaesthesia and regulated during the imaging.

Twenty-four hours after MCA occlusion the rats were intubated, connected to a respirator, and reanaesthetized with 1% isoflurane in 70/30% $N_2/O_2$ for 40 min to allow T2 weighted and diffusion weighted MR imaging. The rats received an i.m. injection of 2 mg $kg^{-1}$ pancuronium bromide for muscle relaxation. Rectal temperature was measured at the start of anaesthesia and regulated during the imaging. An arterial blood sample for analysis of blood gas, electrolytes and glucose was withdrawn 10 min after intubation. Immediately after end of imaging the rats were perfusion fixed with 4% formaldehyde and decapitated. The heads were stored for at least 24 h in 4% formaldehyde before brain dissection.

The MR imaging was performed on a 2.35T Bruker Biospec with a specially designed rat head coil. Both T2 weighted and diffusion weighted MR imaging were performed in eight transaxial slices through the rat head with a slice thickness of 1.5 mm and an interslice gap of 0.3 mm, covering the whole brain between the olfactory bulb and the cerebellum. The head coil was designed to lock the rat head into the same position for each MR imaging session, and the slices were positioned according to several anatomical landmarks to obtain the best possible co-registration of images between rats and between the two MR imaging sessions in each rat. The acquisition matrix was $128 \times 128$ and the Field of View was 45 mm giving an in-plane spatial resolution of approximately 0.35 mm $\times$ 0.35 mm, and a voxel size of approximately 0.185 $mm^3$.

The T2 weighted images were acquired with a multi echo spin echo sequence with four different T2 weighting with echo times (TE) of 40, 80, 120 and 160 ms, respectively. With repetition time (TR) 1500 ms and number of excitations (NEX) 4 the total acquisition time was approximately 14 min.

The diffusion weighted images were acquired with a spin echo sequence with TE 32 ms and TR 1500 ms and with $z$ direction (axial direction) diffusion gradients placed symmetrically about the 180° pulse to achieve a '$b$' value of approximately 1468 s $mm^{-2}$.

Table 1
Measured rat physiology from the three experimental groups

| | Control group ($n=8$) | YM872 4 h ($n=9$) | YM872 24 h ($n=8$) |
|---|---|---|---|
| 24 h MCAO Arterial blood: | | | |
| pH | 7.43±0.05 | 7.45±0.04 | 7.46±0.05 |
| $pCO_2$ (kPa) | 4.8±0.8 | 4.5±0.9 | 4.7±0.8 |
| $pO_2$ (kPa) | 25.2±3.4 | 23.3±2.7 | 21.6±4.7 |
| Base excess | −0.5±1.8 | −0.7±3.0 | +1.1±1.9 |
| Glucose (mmol $l^{-1}$) | 7.6±1.3 | 6.8±1.6 | 9.9±2.1* |
| Hemoglobin (g $dl^{-1}$) | 14.0±1.2 | 14.6±0.6 | 14.4±0.8 |
| Hematocrite (%) | 0.43±0.04 | 0.45±0.02 | 0.44±0.02 |
| $Na^+$ (mmol $l^{-1}$) | 142±2 | 140±2 | 143±2 |
| $K^+$ (mmol $l^{-1}$) | 4.4±0.4 | 4.5±0.2 | 4.6±0.5 |
| $Ca^{2+}$ (mmol $l^{-1}$) | 1.17±0.05 | 1.18±0.07 | 1.19±0.03 |
| Rectal temperature | | | |
| 4 1/2 h MCAO (°C) | 39.0±0.7 | 38.4±1.0 | 38.7±0.7 |
| 24 h MCAO (°C) | 38.0±0.7 | 37.8±0.8 | 37.9±1.1 |

All values are mean±S.D. MCAO = MCA occlusion.
*: Significantly different from control group ($p < 0.05$).

Based on the MR imaging information the area of infarct 24 h after MCA occlusion was measured for each slice and rat by a blinded observer in two separate ways: (1) in each T2 weighted image of TE 120 ms as the number of pixels with signal intensity increase of more than 25% compared to a measured mean value in cortical gray matter in the contralateral hemisphere; (2) in each diffusion weighted image as the number of pixels with signal hyperintensity based on observer dependent adjustment of the threshold for signal hyperintensity.

In both cases the infarct volume was calculated in $mm^3$ by multiplying the number of pixels with the voxel size of approximately 0.185 $mm^3$.

The main statistical comparison between the groups both 4 1/2 and 24 h after MCA occlusion was based on the total infarct volume calculated from the sum of the eight imaged slices. The area of tissue damage in each separate slice was also compared between the three groups. For the data based on diffusion weighted imaging the increase in infarct volume between $4\frac{1}{2}$ and 24 h after MCA occlusion was calculated for each slice and rat separately and compared between the groups.

For the histopathological evaluation eight coronal sections were cut for each brain, aiming at representing the middle of each of the eight imaged slices. The sections were stained with hematoxylin and eosin. Neuronal damage was defined on the basis of the following morphological characteristics: microvacuolation, shrinkage of the neuropil, and presence of dark neurons and eosinophilic neurons. Delineation of infarct area in the eight coronal slices was carried out by an observer unaware of the drug treatment for each rat. The infarct area was calculated with a computer-aided image analyzer system (Luzex III, Nireco, Tokyo, Japan). The infarct volume in each brain was evaluated by integrating these areas. The endpoints for integration were interaural 13.3 mm and interaural 0.7 mm according to Paxinos and Watson [30].

All statistical comparisons between the experimental groups were performed with an ANOVA analysis of variance and subsequent Fisher PLSD. Differences between the groups were considered to be statistically significant only with $p < 0.05$ in the $F$-test based on the analysis of the variance table. Regression analysis was performed to compare the different end-point assessments at 24 h after

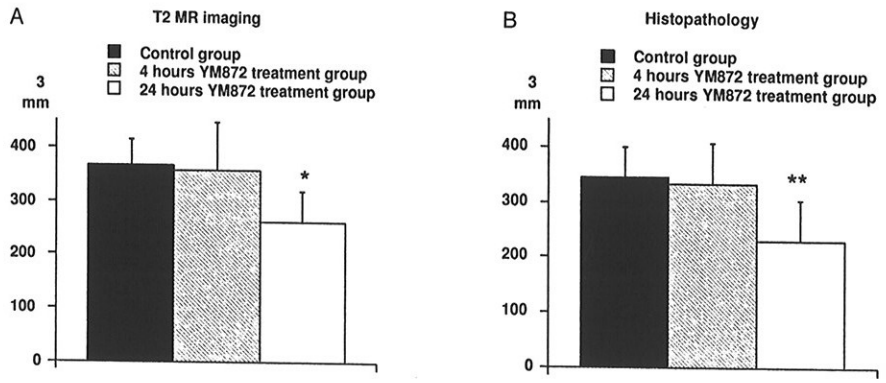


Fig. 1. Total infarct volume 24 h after MCA occlusion as assessed by T2 weighted MR imaging (A) and histopathology (B), presented as mean of each experimental group (±S.D.). *: Significantly different from both control group and 4 h YM872 treated group ($p = 0.01$). **: Significantly different from both control group and 4 h YM872 treated group ($p = 0.005$).

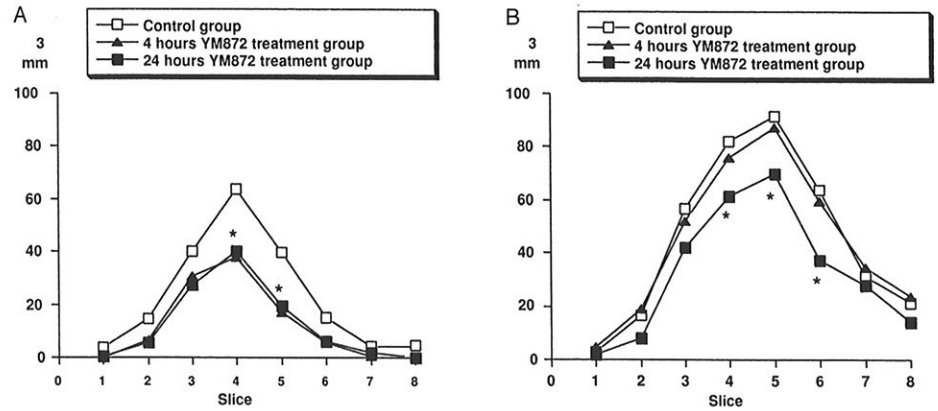


Fig. 2. Infarct volume as assessed by diffusion weighted MR imaging 4 1/2 h after MCA occlusion (A) and T2 weighted MR imaging 24 h after MCA occlusion (B), presented for each slice separately (mean of each group). Slice 1 is at the cranial end and slice 8 at the caudal end of the brain. *: Significant difference between control group and 24 h YM872 treatment group ($p < 0.05$).

MCA occlusion and to compare the results at $4\frac{1}{2}$ and 24 h after MCA occlusion. All values are given as mean ± S.D.

## 3. Results

The physiological variables for the three experimental groups are shown in Table 1. Except for a significantly higher blood glucose in the 24 h YM872 treatment group ($9.9 \pm 2.1$ mmol $l^{-1}$ compared to $7.6 \pm 1.3$ mmol $l^{-1}$ in the control group) there were no statistical differences between the groups for any of the measured parameters. The treatment was performed under freely moving conditions, and in this dosing regimen of YM872, no abnormal behaviour such as stereotyped behaviour, ataxia, hyperactivity, catalepsy or agitation was observed during the infusion period.

Infarct volume as assessed by T2 weighted MR imaging 24 h after MCA occlusion is presented in Fig. 1a, and for each slice separately in Fig. 2b. The total infarct volume was significantly smaller in the 24 h YM872 treatment group ($262 \pm 57$ mm$^3$) compared to both the 4 h YM872 treatment group ($357 \pm 88$ mm$^3$) and the control group ($366 \pm 49$ mm$^3$, $p = 0.01$). Infarct volume as assessed by histopathology 24 h after MCA occlusion is presented in Fig. 1b, and the results were in accordance with the MR imaging. The total infarct volume was significantly smaller in the 24 h YM872 treatment group ($230 \pm 26$ mm$^3$) compared to both the 4 h YM872 treatment group ($332 \pm 74$ mm$^3$) and the control group ($345 \pm 54$ mm$^3$, $p = 0.005$). The correlation between the different end-point assessments is shown in Fig. 3.

The temporal evolution of the ischemic damage based on the diffusion weighted MR imaging 4 1/2 and 24 h after MCA occlusion is presented in Figs. 2, 4 and 5. At 4 1/2 h, the affected volume was significantly smaller in both treatment groups ($99 \pm 52$ mm$^3$ in the 4 h and $102 \pm 44$ mm$^3$ in 24 h YM872 treatment groups, respec-

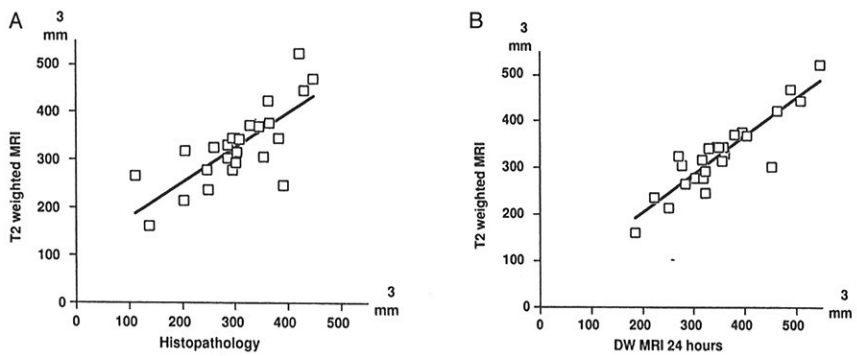


Fig. 3. Scatterplots to show correlation between infarct volume 24 h after MCA occlusion; in (A) as assessed by T2 weighted MR imaging and histopathology ($p = 0.0001$, $R = 0.76$), and in (B) as assessed by T2 weighted and diffusion weighted (DW) MR imaging ($p = 0.0001$, $R = 0.90$).

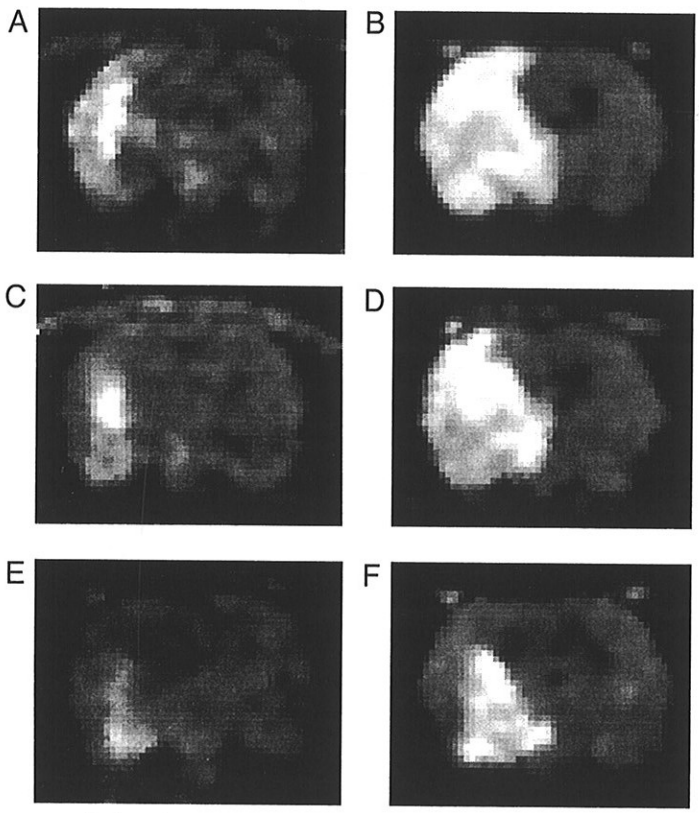


Fig. 4. Diffusion weighted MR images $4\frac{1}{2}$ h (A,C,E) and 24 h (B,D,F) after MCA occlusion of the same central slice (slice 5) of one rat from each group. (A) and (B) are from the control group, (C) and (D) the 4-h YM872 treatment group and (E) and (F) the 24 h YM872 treatment group.

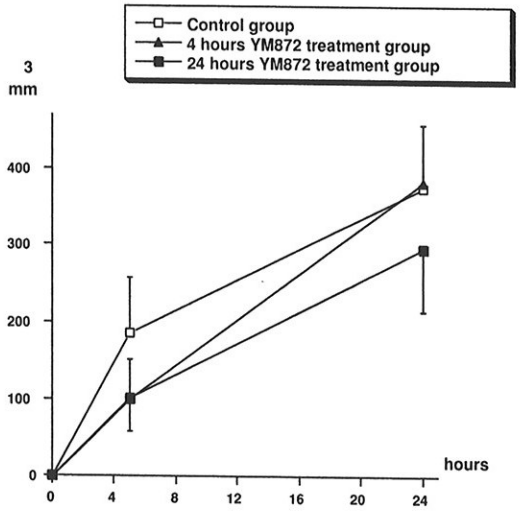


Fig. 5. Time evolution of infarct volume as assessed by diffusion weighted MR imaging 4 1/2 and 24 h after MCA occlusion. Mean of each experimental group (±S.D.).

tively) compared with the control group ($186 \pm 72$ mm$^3$, $p = 0.008$). After 24 h MCA occlusion, however, the volume of ischemic tissue damage in the 4 h YM872 treatment group had reached the same level as the control group. The increase in infarct volume between 4 1/2 and 24 h was larger in the 4 h YM872 treatment group ($284 \pm 102$ mm$^3$) when compared to the control group ($189 \pm 37$ mm$^3$). This difference was close to statistical significance ($p = 0.051$). The infarct volume increase in the 24 h YM872 treated group ($194 \pm 97$ mm$^3$) was similar to the control group.

The correlation between diffusion weighted MR imaging 4 1/2 and 24 h after MCA occlusion is shown in Fig. 6. Regression analysis showed no correlation for the pooled data (Fig. 6a, $p = 0.12$, $R = 0.32$). However, when performed separately for each group (Fig. 6b) there was a statistically significant correlation for the control group ($p = 0.003$, $R = 0.90$) to indicate that in the case of no treatment, diffusion weighted MR imaging at 4 1/2 h after MCA occlusion could predict the final outcome. For both treatment groups there was no correlation. Similar results were obtained when diffusion weighted MR imaging $4\frac{1}{2}$ h

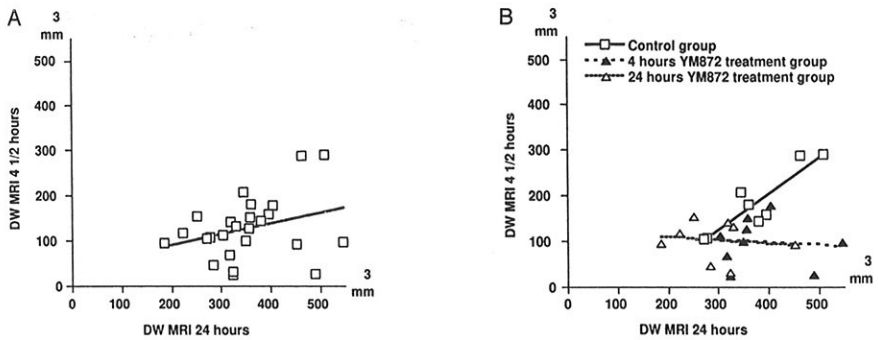


Fig. 6. Scatterplots of volume of ischemic tissue damage $4\frac{1}{2}$ h after MCA occlusion and infarct volume 24 h after MCA occlusion, assessed at both time points by diffusion weighted MR imaging (DW MRI). In (A) all three groups are pooled and there is no correlation ($p = 0.12$, $R = 0.32$). In (B) regression analysis is performed for each group separately, to reveal a statistically significant correlation for the control group ($p = 0.003$, $R = 0.90$).

after MCA occlusion was correlated to the other end-point assessments (data not shown).

## 4. Discussion

Post-ischemic treatment with the glutamate AMPA receptor antagonist YM872 in rat caused a reduction of mean infarct volume 24 h after MCA occlusion by approximately 30% when the drug was administered as continuous intravenous infusion during the 24-h observation period (see Fig. 1). The degree of neuroprotection seemed to be comparable to published results from animal studies of other AMPA receptor antagonists [2,3,5,8,37,39]. Comparison between experimental studies of neuroprotection in different laboratories are complicated by differences in animal model, anaesthesia, drug dose, drug administration and choice of end-point. The present results and the results from three other animal studies of experimental stroke [12,33,34] do, however, indicate that YM872 offers significant neuroprotection, without the potential side effects of nephrotoxicity [12,33,34] described for other glutamate AMPA receptor antagonists [6,8,37]. In preliminary experiments (unpublished data), administration of YM872 at a rate of 20 mg $kg^{-1}$ $h^{-1}$ starting 10 min after occlusion of MCA produced a brain concentration of approximately 100 ng $g^{-1}$ (0.3 μM), a concentration at which the drug has been shown in vitro to selectively block AMPA receptors without blocking NMDA receptors [16]. This indicates that the neuroprotective effect of YM872 in this study was due to its selective AMPA receptor blockade potency.

Already $4\frac{1}{2}$ h after MCA occlusion the volume of ischemic tissue damage was significantly smaller in both the 4 and 24 h YM872 treatment groups. The infarct volume expansion between $4\frac{1}{2}$ and 24 h after MCA occlusion seemed to be similar in the 24 h YM872 treatment group and the control group, while in the 4 h YM872 treatment group the expansion was increased after termination of drug treatment (see Fig. 5). In a recent study by Lo et al. [19] the neuroprotective effect of the AMPA receptor antagonist NBQX was examined after permanent MCA occlusion in rat, and their results indicated that single slice diffusion weighted MR imaging at 3 h after the ischemic onset could predict the final outcome as assessed with TTC staining 24 h after the onset as the single end-point. Our findings, however, suggested that YM872 in a dose of 20 mg $kg^{-1}$ $h^{-1}$ during the first 4 h merely delayed the evolution of the ischemic tissue damage. In the present study diffusion weighted MR imaging with the same protocol at both $4\frac{1}{2}$ and 24 h allowed direct comparison between the two time points, and, in addition, multi slice imaging was performed in order to cover the entire MCA territory (see Fig. 2). Our results showed that the early MR imaging could predict final outcome in the control group, but not in the treatment groups (see Fig. 6b), indicating that the predictive value of early tissue damage assessment is reduced when neuroprotective treatment is given. However, the discrepancy between the present study and the study of Lo et al. [19] may result from differences in the pharmacokinetics of NBQX and YM872. The plasma half-life of YM872 is short (1.5 h, unpublished data), and YM872 did probably disappear from plasma quickly after the end of infusion in the 4 h treatment group. Furthermore, due to the high water solubility, YM872 did most likely not precipitate in the internal organs, as found for NBQX after intraperitoneal administration [2,27]. This eliminates the potential problem of a drug depot which might provide sustained release of drug as seen with NBQX [27], and thus the early NBQX treatment may be compared to the 24 h treatment group in the present study. On the other hand, as the observed neuroprotection in the 24 h treatment group also may reflect a delay of the expansion of tissue damage, a later end-point (e.g., 1 week after the ischemic onset) is necessary to evaluate the long term benefit of the drug in the case of permanent ischemia [34].

In the present study, no effect of YM872 treatment on the measured physiology parameters was observed except

a small, but statistically significant, increase in blood glucose in the 24 h YM872 treatment group (see Table 1). Profound hyperglycemia has been shown to increase the infarct size in animal studies of experimental stroke, but we are not aware of any published study that has investigated the effect of such a small increase in blood glucose from approximately 7.5 to approximately 10 mmol $l^{-1}$. Recent studies have reported localization of AMPA receptor subunits in the pancreatic islets of rat and guinea pig [18,36], and in a perfused rat pancreas preparation glutamate was found to potentiate glucose stimulated secretion of insulin via actions at AMPA type glutamate receptors [1]. If this is the case also in man, blood glucose should be closely monitored in clinical trials with AMPA receptor antagonist treatment of stroke patients.

In this study, rectal hyperthermia was observed in all three groups $4\frac{1}{2}$ h after MCA occlusion. Spontaneous hyperthermia in rats subjected to intraluminal filament MCA occlusion has been observed by other groups [13,40], and is probably caused by ischemic tissue damage extending into hypothalamic centers regulating body temperature [40]. However, in the present study there were no significant differences between the experimental groups, and at the dose used in this study, no hypothermic effect of YM872 was observed.

In conclusion, when using MR imaging and histopathology 24 h after MCA occlusion as main end-points, post ischemic treatment with the glutamate AMPA receptor antagonist YM872 was demonstrated to markedly reduce the infarct volume when administered as continuous i.v. infusion for 24 h after onset of ischemia, but not when the treatment was terminated 4 h after the MCA occlusion. The combination of serial diffusion weighted and T2 weighted MR imaging seemed well suited for in vivo evaluation of infarct size and temporal evolution of brain tissue damage in the study of therapeutic interventions for the treatment of stroke.

## Acknowledgements

The study was partially funded by Yamanouchi Pharmaceutical, Tsukuba, Ibaraki, Japan, and supported by The Norwegian Council on Cardiovascular Disease and The Norwegian Research Council. We also appreciate the scientific contribution from Tomm B. Müller and Trond Singstad.

## References

[1] G. Bertrand, R. Gross, R. Puech, M.M. Loubatières-Mariani, J. Bockaert, Evidence for a glutamate receptor of the AMPA subtype which mediates insulin release from rat perfused pancreas, Br. J. Pharmacol. 106 (1992) 354–359.

[2] A.M. Buchan, H. Lesiuk, K.A. Barnes, L. Hui, Z.-G. Huang, K.E. Smith, D. Xue, AMPA antagonists: do they hold more promise for clinical stroke trials than NMDA antagonists?, Stroke 24 (1993) I148–I152.

[3] R. Bullock, D.I. Graham, S. Swanson, J. McCulloch, Neuroprotective effect of the AMPA receptor antagonist LY-293558 in focal cerebral ischemia in the cat, J. Cereb. Blood Flow Metab. 14 (1994) 466–471.

[4] A.J. de Crespigny, M. Tsuura, M.E. Moseley, J. Kucharczyk, Perfusion and diffusion MR imaging of thromboembolic stroke, J.M.R.I. 3 (1993) 746–754.

[5] R. Gill, L. Nordholm, D. Lodge, The neuroprotective actions of 2,3-dihydroxy-6-nitro-7-sulfamoyl-benzo(*F*)quinoxaline (NBQX) in a rat focal ischaemia model, Brain. Res. 580 (1992) 35–43.

[6] R. Gill, The pharmacology of α-amino-3-hydroxy-5-methyl-4-isoxasole propionate (AMPA)/kainate antagonists and their role in cerebral ischemia, Cerebrovasc. Brain Metab. Rev. 6 (1994) 225–256.

[7] R. Gill, N.R. Sibson, R.H. Hatfield, N.G. Burdett, T.A. Carpenter, L.D. Hall, J.D. Pickard, A comparison of the early development of ischaemic damage following permanent middle cerebral artery occlusion in rats as assessed using magnetic resonance imaging and histology, J. Cereb. Blood Flow Metab. 15 (1995) 1–11.

[8] S.H. Graham, J. Chen, J.Q. Lan, R.P. Simon, A dose–response study of neuroprotection using the AMPA antagonist NBQX in rat focal cerebral ischemia, J. Pharmacol. Exp. Ther. 276 (1996) 1–4.

[9] Y. Hasegawa, M. Fisher, L.L. Latour, B.J. Dardzinski, C.H. Sotak, MRI diffusion mapping of reversible ischemic injury in focal brain ischemia, Neurology 44 (1994) 1484–1490.

[10] K.-A. Hossmann, The pathophysiology of experimental brain edema, Neurosurg. Rev. 12 (1989) 263–280.

[11] Q. Jiang, M. Chopp, Z.G. Zhang, J.A. Helpern, R.J. Ordidge, J. Ewing, P. Jiang, B.A. Marchese, The effect of hypothermia on transient focal ischemia in rat brain evaluated by diffusion- and perfusion-weighted NMR imaging, J. Cereb. Blood Flow Metab. 14 (1994) 732–741.

[12] S. Kawasaki-Yatsugi, S. Yatsugi, M. Takahashi, T. Toya, C. Ichiki, M. Shimizu-Sasamata, T. Yamaguchi, K. Minematsu, A novel AMPA receptor antagonist, YM872, reduces infarct size after middle cerebral artery occlusion in rats, Brain Res. 793 (1998) 39–46.

[13] Y. Kiyota, K. Pahlmark, H. Memezawa, M.-L. Smith, B.K. Siesjö, Free radicals and brain damage due to transient middle cerebral artery occlusion: the effect of dimethylthiourea, Exp. Brain Res. 587 (1993) 66–72.

[14] R.A. Knight, R.J. Ordidge, J.A. Helpern, M. Chopp, L.C. Rodolosi, D. Peck, Temporal evolution of ischemic damage in rat brain measured by proton nuclear magnetic resonance imaging, Stroke 22 (1991) 802–808.

[15] W. Koek, J.H. Woods, G.D. Winger, MK-801, a proposed noncompetitive antagonist of excitatory amino acid neurotransmission, produces phencyclidine-like behavioural effects in pigeons, rats and rhesus monkeys, J. Pharmacol. Exp. Ther. 245 (1988) 969–974.

[16] A. Kohara, M. Okada, R. Tsutsumi, K. Ohno, M. Takahashi, M. Shimizu-Sasamata, J. Shishikura, H. Inami, S. Sakamoto, T. Yamaguchi, In vitro characterization of YM872: a selective, potent and highly water-soluble α-amino-3-hydroxy-5-methylisoxazole-4-propionate (AMPA) receptor antagonist, J. Pharm. Pharmacol., 1998, in press.

[17] K. Kohno, M. Höhn-Berlage, G. Mies, T. Back, K.-A. Hossmann, Relationship between diffusion-weighted MR images, cerebral blood flow, and energy state in experimental brain infarction, Magn. Reson. Imag. 13 (1995) 73–80.

[18] H.-P. Liu, S.S.-W. Tay, S.-K. Leong, Localization of glutamate receptor subunits of the α-amino-3-hydroxy-5-methyl-4-isoxasoleproprionate (AMPA) type in the pancreas of newborn guinea pigs, Pancreas 14 (1997) 360–368.

[19] E.H. Lo, A.R. Pierce, J.B. Mandeville, B.R. Rosen, Neuroprotection with NBQX in rat focal cerebral ischemia. Effects on ADC probabil-

ity distribution functions and diffusion–perfusion relationship, Stroke 28 (1997) 439–447.
[20] H. Memezawa, H. Minamisawa, M.-L. Smith, B.K. Siesjö, Ischemic penumbra in a model of reversible middle cerebral artery occlusion in the rat, Exp. Brain. Res. 89 (1992) 67–78.
[21] K. Minematsu, M. Fisher, L. Li, M.A. Davis, A.G. Knapp, R.E. Cotter, R.N. McBurney, C.H. Sotak, Effects of a novel NMDA antagonist on experimental stroke rapidly and quantitatively assessed by diffusion-weighted MRI, Neurology 43 (1993) 397–403.
[22] J. Mintorovitch, M.E. Moseley, L. Chileuitt, H. Shimizu, Y. Cohen, P.R. Weinstein, Comparison of diffusion- and T2-weighted MRI for the early detection of cerebral ischemia and reperfusion in rats, Magn. Reson. Med. 18 (1991) 39–50.
[23] R.G.M. Morris, E. Anderson, G.S. Lynch, M. Baudry, Selective impairment of learning and blockade of long-term potentiation by *N*-methyl-D-aspartate receptor antagonist, AP5, Nature 319 (1986) 774–776.
[24] T.B. Müller, O. Haraldseth, R.A. Jones, G. Sebastiani, F. Godtliebsen, C.F. Lindboe, G. Unsgård, Combined perfusion and diffusion-weighted magnetic resonance imaging in a rat model of reversible middle cerebral artery occlusion, Stroke 26 (1995) 451–458.
[25] T.B. Müller, O. Haraldseth, R.A. Jones, G. Sebastiani, C.F. Lindboe, G. Unsgård, A.N. Øksendal, Perfusion and diffusion weighted MR imaging for in vivo evaluation of treatment with U73489G in a rat stroke model, Stroke 26 (1995) 1453–1458.
[26] N. Nagasawa, K. Kogure, Correlation between cerebral blood flow and histological changes in a new rat model of middle cerebral artery occlusion, Stroke 20 (1989) 1037–1043.
[27] S. Nurse, D. Corbett, Neuroprotection after several days of mild drug-induced hypothermia, J. Cereb. Blood Flow Metab. 16 (1996) 474–480.
[28] J.W. Olney, J. Labruyere, M.T. Price, Pathological changes induced in cerebrocortical neurones by phencyclidine and related drugs, Science 244 (1989) 1360–1362.
[29] J.W. Olney, J. Labruyere, G. Wang, D.F. Wosniak, M.T. Price, M.A. Sesma, NMDA antagonist neurotoxicity: mechanism and prevention, Science 254 (1991) 1515–1518.
[30] G. Paxinos, C. Watson, The Rat Brain in Stereotaxic Coordinates, 2nd edn., Academic Press, San Diego, 1986, ISBN 0-12-547621-3.
[31] S.A. Roussel, N. van Bruggen, M.D. King, J. Houseman, S.R. Williams, D.G. Gadian, Monitoring the initial expansion of focal ischaemic changes by diffusion-weighted MRI using remote controlled method of occlusion, NMR in Biomed. 7 (1994) 21–28.
[32] S.E. Smith, B.S. Meldrum, Cerebroprotective effect of a non-*N*-methyl-D-aspartate antagonist, GYKI 52466, after focal ischemia in the rat, Stroke 23 (1992) 861–864.
[33] M. Takahashi, J.W. Ni, S. Kawasaki-Yatsugi, T. Toya, S. Yatsugi, M. Shimizu-Sasamata, K. Koshiya, J. Shishikura, S. Sakamoto, T. Yamaguchi, YM872, a novel selective α-amino-3-hydroxy-5 methylisoxazole-4-propionic acid receptor antagonist reduces brain damage after permanent focal cerebral ischemia in cats, J. Pharmacol. Exp. Ther. 284 (1998) 467–473.
[34] M. Takahashi, J.W. Ni, S. Kawasaki-Yatsugi, T. Toya, C. Ichiki, S. Yatsugi, K. Koshiya, M. Shimizu-Sasamata, T. Yamaguchi, Neuroprotective efficacy of YM872, an α-amino-3-hydroxy-5-methylisoxazole-4-propionic acid receptor antagonist, after permanent middle cerebral artery occlusion in rats, J. Pharmacol. Exp. Ther., in press.
[35] H.B. Verheul, J.W. Berkelbach van der Sprenkel, C.A. Tulleken, K.S. Tamminga, K. Nicolay, Temporal evolution of focal cerebral ischemia in the rat assessed by T2-weighted and diffusion-weighted magnetic resonance imaging, Brain Topogr. 5 (1992) 171–176.
[36] C.D. Weaver, T.L. Yao, A.C. Powers, T.A. Verdoorn, Differential expression of glutamate receptor subtypes in rat pancreatic islets, J. Biol. Chem. 271 (1996) 12977–12984.
[37] D. Xue, Z.-G. Huang, K. Barnes, H.J. Lesiuk, K.E. Smith, A.M. Buchan, Delayed treatment with AMPA, but not NMDA, antagonists reduces neocortical infarction, J. Cereb. Blood Flow Metab. 14 (1994) 251–261.
[38] H. Yao, S. Ibayashi, H. Nakane, H. Cai, H. Uchimura, M. Fujishima, AMPA receptor antagonist, YM90K, reduces infarct volume in thrombotic distal middle cerebral artery occlusion in spontaneously hypertensive rats, Brain Res. 753 (1997) 80–85.
[39] S. Yatsugi, M. Takahashi, S. Kawasaki-Yatsugi, K. Koshiya, S. Sakamoto, D. Uematsu, M. Shimizu-Sasamata, Neuroprotective effect of YM90K, a novel AMPA/kainate receptor antagonist, in focal cerebral ischemia in cats, J. Cereb. Blood Flow Metab. 16 (1996) 959–966.
[40] Q. Zhao, H. Memezawa, M.-L. Smith, B.K. Siesjö, Hyperthermia complicates middle cerebral artery occlusion induced by an intraluminal filament, Brain Res. 649 (1994) 253–259.